

The 46th ANNUAL TSDOS



TRANSMISSION AND SUBSTATION DESIGN AND OPERATION SYMPOSIUM

September 11 - 13, 2013

Crowne Plaza Dallas
Near the Galleria

Pre-conference
September 10, 2013

UNIVERSITY OF TEXAS  ARLINGTON

46th ANNUAL

Table of Contents

Abstracts	p. 3
Technical Papers	
Simulating Real World Conditions for Relay Scheme Testing <i>Jason Buneo</i>	p. 20
Sweep Frequency Response Analysis: Failure Mode Analysis <i>Dinesh Chhajer, P.E. and Volney Naranjo</i>	p. 30
345kV Transmission Line Thermal Upgrading Using Connector Shunts <i>Douglas P. Harms, P.E.</i>	p. 63
Baseplate and Flange Weld Inspection of Transmission Tubular Steel Structures <i>Ed Jacobs, Al Clare, Paul Cameron</i>	p. 78
Adventures in Routing: A Case Study From the Big Hill to Kendall 345 KV CREZ Project in Kerrville, TX <i>Nathan Laughlin, P.E. and Curtis D. Symank, P.E.</i>	p. 90
Nip / Tuck Method: A Solution to Providing Additional Conductor-to-Ground Clearances for Transmission Lines <i>Garrett Luszczki, E.I. and Michael Belanger, P.E.</i>	p. 102
AEP 69-kV Oil-Insulated Transmission Line Removal Project <i>Michelle Beckman, Bill Halliburton, Woody McOmber, and C. David Slavin</i>	p. 112
Practical Considerations and Solutions Employed in the Thermal Design and Operation of a Power Transformer <i>John Prunte and David L. Harris</i>	p. 130
Optimization of the Power Transformer Dry-out Process in the Field—Application of Advanced Diagnostic Technologies <i>Diego M. Robalino, Ph.D. and Peter Werelius, Ph.D.</i>	p. 144
Analyzing The Phenomena of Wind-Induced Vibrations on Unloaded Davit Arms <i>Erik A. Ruggeri, P.E.</i>	p. 160
Axial and Lateral Capacity of Tapered Helical Piles for Transmission Pole Structures <i>Mark H. Fairbairn, P.E., Lee Goen, P.E., Jason Herron, P.E., and Gary Seider, P.E.</i>	p. 171
Engineering and Constructing High Quality Drilled Shafts <i>Calvin Stripling, P.E.</i>	p. 184
2013 Conference Sponsors	p. 195

Simulating Real World Conditions for Relay Scheme Testing

Jason Buneo

Megger, 4271 Bronze Way, Dallas, TX 75237

Phone: 214-330-3240

Fax: 214-331-7373

Email: Jason.Buneo@megger.com

Many of today's relay testing methods employ techniques available 50 years ago and have not evolved. These test methods don't fully utilize the capabilities of either the protective relays or the available test equipment. In fact, current standard testing practices for microprocessor-based relays do not even adequately represent real system conditions. Moreover, these methods do not properly utilize the one theory that could help—namely, that of symmetrical components.

This paper looks at four distinct ways of using symmetrical components to more accurately simulate real world conditions, including:

- A current unbalance scenario in a motor protection relay,
- The removal of zero sequence current in a transformer differential relay,
- Operating a phase time overcurrent and a neutral time overcurrent on the same trip output without isolation,

For each of these scenarios listed above, antiquated methods are generally used, or the scenarios are not even tested because of the perceived difficulty of the procedure. In many cases of field-testing relay schemes, the methods employed do not take into consideration symmetrical components in the determination of fault values.

Therefore, a more accurate method for evaluation and testing of protection relays is necessary. In this paper, the method is examined in detail, along with the solutions for the three scenarios, encouraging testers to utilize symmetrical components to more accurately represent the power systems that the relay is protecting. By embracing methods that utilize symmetrical components, the perceived difficulty in testing protective relays will be greatly reduced.

Sweep Frequency Response Analysis: Failure Mode Analysis

Dinesh Chhajer and Volney Naranjo

Dinesh Chhajer dinesh.chhajer@megger.com

Volney Naranjo volney.naranjo@megger.com

This paper will focus on Sweep Frequency Response Analysis (SFRA) diagnostic technique as a tool to identify transformer failure modes. Power transformers during its life cycle are subjected to great amount of electromechanical forces caused by through faults, transportation and catastrophic events like earthquakes. This could result to internal mechanical movements such as winding displacement, core movement, radial and axial deformation and other winding failures. SFRA is a highly accurate and sensitive technique that can diagnose these internal mechanical changes and helps in preventing transformer failures.

The paper will summarize and present the most relevant aspects of IEEE SFRA guide (PC 57.149) that includes SFRA test requirements, measurement methodology, results interpretation and analysis. It will be complemented with recommendations from other SFRA standards (IEC, CIGRE and DL/T 2004) not included in IEEE guide. Failure mode guidelines included in the IEEE and Cigre guide to identify mechanical issues would be reviewed in detail and will be compared with real life cases from field experience. Additionally, it will also provide recommendations on best practices to be considered while performing the SFRA test in field environment. The recommendations will be supported by SFRA case studies collected from utilities that helped in identifying mechanical issues and taking preventive actions to avoid catastrophic failure of power transformers.

Biography

Dinesh Chhajer received his M.S. degree from the University of Texas at Arlington in 2006. Currently, he is working as an applications engineer for Megger. At Megger, his responsibilities include providing engineering consultation and recommendations in relation to the testing of transformers, circuit breakers, batteries and other substation assets. Dinesh has previously worked as a substation maintenance engineer and substation design engineer with POWER Engineers, Inc. He is currently a licensed professional engineer (PE) in the state of Texas.

Volney Naranjo is an applications engineer at Megger for substation applications. He graduated from the University of Valle in Cali, Colombia with a Bachelor of Science in Electrical Engineering and is a member of IEEE. Volney has over ten years of experience working in the power engineering environment including providing professional services for design, testing and commissioning of power systems.

Load Growth in West Texas

Ken Donohoo

The oil boom 2.0 has put the Permian Basin economy in full bloom and is stretching capacity of existing infrastructure. Housing needs have led to the creation of man camps for laborers. Cities, colleges and hospitals patterning for new apartment complexes. Water is being trucked in to facilitate exploration and production. Oil is being trucked to market as inadequate pipeline capacity is expanded. Rail capacity being utilized in lieu of pipeline to reach market. Incessant demand for electricity has created congestion on lines. Oncor is responding with short and long term projects to meet needs.

Planners Perspective on Series Compensated Transmission Lines

Ken Donohoo

Resonance is the tendency of a system to oscillate at a greater amplitude at some frequencies than at others.

Frequencies at which the response is maximized are known as a system's resonant frequencies. At resonant frequencies, even small periodic drivers can produce large amplitude oscillations, because the system stores energy. When a series capacitor is added into a transmission line, it creates a resonant frequency. This is not a problem as long as energy is not injected at the resonant frequency. A generation interconnection which injects power at the resonant frequency can lead to damage to both generation and transmission facilities. ERCOT along with the transmission service providers are experiencing and addressing resonance concerns.

345kV Transmission Line Thermal Upgrading Using Connector Shunts

Douglas P. Harms, P.E.

A CenterPoint Energy 345kV Transmission Line with 2-bundle 795kcm ACSR Drake conductor required upgrading within 24 months to accommodate additional generation. The line was constructed in 1970 and a complete rebuild with structure and conductor replacement would be required unless it could be operated at a higher conductor thermal rating to increase the capacity of the line.

The line had previously been thermally upgraded with minor structure modifications to provide NESC Clearances for an operating temperature of 90OC normal / 120OC emergency. A conductor thermal operating temperature of 120OC normal / 120OC emergency could accommodate the increased generation and avoid the expensive complete rebuild of the line. A 120OC normal operating temperature exceeded the line connectors design limits. The connectors are compliant with ANSI ASC C119.4 – 2011 - Connectors for Use Between Aluminum-to-Aluminum, and Aluminum-to-Copper Conductors Designed for Normal Operation at or Below 93°C and Copper-to-Copper Conductors Designed for Normal Operation at or Below 100°C. Additionally, there was concern regarding the fact that the connectors had been in service for over 42 years.

It was determined that connector shunt devices would provide thermal protection for the connectors and assure their mechanical integrity. It was also determined that the load profile of the line would not exceed 120OC and NESC Clearances previously provided were adequate.

1.CenterPoint Energy performed extensive testing on various types of connectors through the Electric Power Research Institute (EPRI). The testing showed that some connectors have a slight margin of capability of operating at short term emergency above 93OC and some connectors have no margin whatsoever above 93OC.

2.CenterPoint Energy performed extensive testing on various types of connector shunts through the Electric Power Research Institute (EPRI). Connector shunts are devices which can be installed on a line to bridge across a connector to electrically bypass and thermally cool the connector and assure required mechanical strength for the line conductor. The testing showed that the connector shunts were viable devices for the required line upgrading.

What you will learn:

- Overview of the chosen 345kV transmission line thermal upgrading project using connector shunts versus totally rebuilding the line.
- Overview of the connector testing performed at EPRI.
- Overview of the connector shunt testing performed at EPRI.
- Overview of the line connector's condition assessment using SensorLink® Corporations' Radio Ohmstik instrument.
- Presentation of photos and videos of connector shunt installations on the project.

Baseplate and Flange Weld Inspection of Transmission Tubular Steel Structures

Ed Jacobs, Al Clare, Paul Cameron

Thomas & Betts Corporation

8155 T&B Boulevard, 2D-15, Memphis, TN 38125; Ph. (901)-252-5349; Fax (901)-252-1312

Ed Jacobs Director of Quality, R&D, and Solid Modeling

Al Clare NDT Manager

Paul Cameron Plant Quality Manager, CWI

Jon Loveless Quality Engineer

The purpose of this paper is to discuss the shortcomings of the AWS D1.1 weld inspection standards when applied to tubular steel transmission structures, and to inform our industry of the importance of the proper inspection of tubular steel transmission structures and the potential pitfalls that could occur in the process.

The AWS D1.1 standard has been the most widely accepted standard for tubular steel transmission structures and has provided the industry with guidance for many years. However, AWS D1.1, which was originally adopted for building and bridge construction, does not recognize or adequately address the unique characteristics of tubular steel transmission structures. Using AWS D1.1 as a starting point, we can, however, remedy the existing weaknesses and gaps, and develop a more robust inspection process which will validate the structural integrity of the weld.

Our experience indicates that a single structure can be tested by multiple UT (Ultrasonic Testing) Level II personnel, certified in accordance with ASNT (American Society for Nondestructive Testing), with each inspector arriving at conflicting results. Interpretations of the results can also vary. The key to sound inspection practices lies in knowledge of the joints and fabrication methods, consistent equipment and techniques, and an objective basis for the interpretation of results. Properly trained individuals can understand the geometry of a steel pole and interpret any indication found by applying a consistent, repeatable and, most importantly, accurate UT testing methods.

This paper will:

Explain the framework and shortcomings of AWS D1.1 when utilized for UT inspection of tubular steel transmission structures, in particular, T-joints.

Communicate how critical it is to establish a repeatable UT inspection practice to ensure that results are consistent and accurate.

Discuss forensic metallurgical examinations and validations of NDE (Non- Destructive Examinations).

Recommend a “standard” for the inspection and identification of structurally significant defects in tubular steel transmission structures.

CenterPoint Energy Recovery Transformer Project

Jack Heintschel

Author: Reginald W. Comfort, Manager, Substation Projects, CenterPoint Energy Houston

How would a utility respond if a key piece of electrical equipment (such as an auto-transformer), that was essential to the reliable operation of its transmission system were destroyed and removed from service? What would happen if spare equipment, were not readily available? How could the utility restore its power grid to normal operation as soon as possible? CenterPoint Energy teamed with Homeland Security, EPRI and ABB to simulate such a scenario. This scenario would evaluate the electric T&D industry equipment supplier's ability to provide replacement equipment and ship to the utility in a timely manner. The scenario will also evaluate the utilities, readiness and ability to re-install, test and commission this equipment.

Adventures in Routing: A Case Study From the Big Hill to Kendall 345 KV CREZ Project in Kerrville, TX

Curtis D. Symank, P.E., and Nathan Laughlin, P.E.

AUTHORS

Curtis D. Symank, PE, and Nathan Laughlin, PE

ABSTRACT

In designing and constructing its Big Hill to Kendall 345 kV CREZ transmission line project, the Lower Colorado River Authority Transmission Services Corporation (LCRA TSC) encountered many unique challenges. These challenges included a CCN proceeding with over 1,200 intervenors, procuring construction and material resources in a constrained marketplace, designing through rugged terrain and developed areas along an interstate highway, and obtaining the necessary regulatory permits from several agencies, including the U.S. Fish and Wildlife Service (USFWS), the Federal Aviation Administration (FAA), and the Texas Department of Transportation (TxDOT).

A successful coordination process with TxDOT was particularly critical to the success of the project. The route approved by the Public Utility Commission (PUC) paralleled TxDOT roads for approximately 98 of its 139 miles, including 85 miles along Interstate 10, with approximately 35 road crossings. Also, the PUC specifically directed LCRA TSC in its Final Order to “engage in discussions with TxDOT and use its best efforts to reach agreement with the Department to use state ROW along the proposed project where it parallels I-10.” This directive was new to LCRA TSC’s experience, and the two-year permitting process that followed called for a more collaborative approach than is typical with TxDOT.

With the directive from the PUC as a starting point, LCRA TSC engaged TxDOT personnel at both the State and District levels in a series of meetings to identify opportunities for co-location. Out of these meetings, LCRA TSC and TxDOT found about 20 locations where co-location was feasible and mutually acceptable in concept. The accommodations discussed included aerial overhang of conductors, temporary construction access, and in some cases, placing 345 kV pole structures within TxDOT right-of-way. After the conceptual phase, LCRA TSC worked closely with the TxDOT’s San Angelo and San Antonio Districts to implement the co-locations in a manner that was safe for both LCRA TSC’s construction crews and the travelling public, both during the construction phase and the long-term operation of the transmission line. Above all, the success of this process required that good working relationships be developed on all levels of LCRA TSC and TxDOT, including (and especially) the construction crews working with local TxDOT offices.

This paper will provide a case study of how LCRA TSC worked with TxDOT and other parties on a particular design solution that routed the line through the intersection of Interstate 10 and State Highway 16 in Kerrville, Texas. This intersection had numerous design challenges around it, including several homes and businesses near the right-of-way, traffic constraints along the two highways, and a roadside monument with landscaping. Through its collaboration with TxDOT, and negotiations with other parties, LCRA TSC’s design team developed a solution that placed four structures and 4400 feet of the line within TxDOT right-of-way, avoided several homes and businesses in a congested area, preserved the character of the roadside monument, and most importantly, protected the safety of construction crews and the travelling public as the project was constructed. The success of this process illustrates how a well-executed collaborative process and good working relationships between organizations can help resolve complicated design issues where multiple stakeholders are involved.

Pre-Conference Tutorial: Smart Grid for the Bulk Electric System

Dr. Wei-Jen Lee

When the topic of Smart Grid comes up, there is usually a good deal of discussion on Distribution Automation, AMI, Residential Demand management and Distributed Generation. Smart Grid initiatives also have several applications on the Transmission system. This tutorial will provide an in-depth discussion on several transmission system applications.

Topics to be covered include:

- Wide Area Monitoring and Control
- Inter-area oscillation detection and analysis
- Enhanced State estimation
- Dynamic Model validation
- Enhanced Transmission Fault Location Estimation
- Dynamic Thermal Circuit ratings of Transmission lines

Who should attend this tutorial? Engineers involved in transmission line design and operation, system planners and system controllers.

Nip / Tuck Method: A Solution to Providing Additional Conductor-to-Ground Clearances for Transmission Lines

Michael Belanger, P.E. and Garrett Luszczki, E.I.

Since the release of the NERC alert, utilities have sought to ensure their transmission lines meet minimum design clearance criteria. This type of analysis often results in select spans which are noncompliant. With tight utility budgets and the accelerated schedule for the completion of the NERC work, the need for a safe, quick, low cost, and reliable fix has risen to new levels. Often the structures in the field are more than structurally adequate but not tall enough to allow clearance for the entire span. The Nip Tuck Method is an iterative modeling technique for eliminating clearance violations without the need for replacing/raising the more costly structures such as steel lattice towers. The method uses the SAPs module of PLS-CADD to simulating nipping-out a small section of conductor and splicing the cables back together. Removing a section of the conductor reduces the length of the line and raises the conductor elevation. Once the section is spliced back together, insulators can be re-plumbed, and clearances and structural stability rechecked. This method was recently used successfully on a 765kV line.

AEP 69-kV Oil-Insulated Transmission Line Removal Project

Michael Gluek, Woody McOmber, C. David Slavin, Bill Halliburton,
and Michelle Beckman

Authors: Michael Glueck American Electric Power (AEP), Woody McOmber Burns & McDonnell (BMcD) and C. David Slavin/Bill Halliburton/Michelle Beckman Burns & McDonnell (BMcD)

AEP installed two underground oil-insulated 69-kV transmission lines and one spare conduit from its Nueces Bay Substation, under the Corpus Christi Ship Channel, and to the Avery Point Terminal in the 1950s. The length of each transmission line was approximately 1.1 miles. The two transmission lines were taken out of service in the 1990s. To ensure the conduits remained intact and no oil escaped into the ship channel, the lines remained pressurized. Keeping the lines pressurized was a continuing maintenance issue, so AEP decided to remove the lines in 2010. AEP hired BMcD to lead engineering, coordinate the stakeholders, and manage the sub-consultants and subcontractors required for this project.

The portion of the conduits on land were covered with an asbestos-containing somastic coating and encased in concrete. The portion of the conduits under the Ship Channel is coated with an asbestos-containing somastic and cement mixture. The decommissioning and demolition phase of the project (Phase I) consisted of the removal of the conductor cables and insulating fluid from the underground inactive conduits and demolition of surface structures associated with the conduits. The second phase (Phase II) of the project (when conducted) will consist of removing the segment of conduits that cross under the Ship Channel.

In order to drain the mineral oil and remove the copper cables from the conduits, the splice joints had to be located and exposed. The oil, cable, and somastic coating had to be sampled and tested. The oil testing indicated the presence of a high concentration of dissolved hydrogen, which required special handling of the insulating oil when it was removed from the conduits. It was determined that the conductor contained no hazardous materials and it was sold for scrap. The conduits were then thoroughly cleaned using a biodegradable, water-based (non-hazardous) degreasing solvent and swabbed using absorbent pigs, pressure tested for leaks, and stabilized with dry nitrogen. The associated surface structures for this electrical system at the Nueces Bay Substation and Avery Point Terminal were decommissioned and demolished. Any and all suspect ACM waste was disposed in an AEP-approved Texas landfill. Phase I was completed in fall 2012.

As the southernmost portion of the conduit was located along a county road currently under construction, it was essential that the conduit removal be coordinated and phased with ongoing road work to reduce impact to the road expansion project. Furthermore, as a significant portion of the conduit was installed below the Corpus Christi Ship Channel, it was essential to have a specialty contractor with experience in conductor cable removal, cleaning and swabbing of pipelines, and demolition to ensure the success of the project. AEP requested BMcD conduct a feasibility study to better understand the practicability, risks, liability, costs, and technical feasibility associated with the removal of the three AEP conduits crossing the Corpus Christi Ship Channel. Components of this feasibility study included historical document review, summarization of discussions with potential removal contractors, commissioning of a marine survey, summarization of the scope and liabilities, a Limited Risk Assessment using United States Environmental Protection Agency (EPA) Risk Model, and assistance with the draft AEP/POCCA Letter Agreement for Ownership Transfer of 69-kV Conduit Segments.

To complete the removal of the conductor cables, BMcD coordinated with a series of stakeholders including the Port of Corpus Christi Authority (POCCA), United States Corps of Engineers, and AEP as well as a multitude of other government entities such as the City of Corpus Christi, Nueces County, the Texas Commission on Environmental Quality, the Texas Railroad Commission, and other contractors, sub-consultants, and subcontractors utilized to complete the project.

ERCOT Energy Prices and Market Update

Matt Mereness

Review of the following topics to update us on the current state of the ERCOT Nodal Market and how it is responding to power demands in West Texas and other booming areas of the grid.

1. ERCOT Market Operations & Prices for 2012

Slides showing how 2012 compared with 2011

2. Transmission constraint costs and markets

Top 10 constraints and how much paid for in markets

3. Recent Market Design Changes

Rule changes implemented recently

4. Future Market Design Changes

Pilots programs

Future changes/challenges from Brattle report (staged in offer cap to \$9,000)

Practical Considerations and Solutions Employed in the Thermal Design and Operation of a Power Transformer

John Prunte

David L. Harris Customer Technical Executive SPX Transformer Solutions, Inc.

John Prunte Director of Technical Support SPX Transformer Solutions, Inc.

ABSTRACT

Presented is an analysis of the thermal characteristics of oil-filled, core form medium power transformers. The aging effects of heating on the insulation system, resulting from losses and loading, are examined and the cooling system's role in minimizing these effects is shown. How the cooling system operates and how its performance is verified by temperature rise testing will also be explained. Our intent is for this presentation to provide the necessary information and understanding as to why properly designed cooling systems are important to maintain suitable temperatures and maximize the transformer's operational life.

Optimization of the Power Transformer Dry-out Process in the Field—Application of Advanced Diagnostic Technologies

Diego Robalino and Peter Werelius

Diego M. Robalino
Megger North America
4271 Bronze Way, Dallas, TX 75237, USA

Peter Werelius
Megger Sweden
Eldarvägen 4, 187 75
Täby, Sweden

Utilities in North America face the continuous growing demand for power from customers and focus their efforts on providing efficient, secure and reliable energy supply to the entire industrial, commercial and domestic population. Power and distribution transformers—maybe the most important components of the energy system—are affected by the normal and unidirectional aging process. Due to load demand, fewer opportunities arise to take transformers out of service for routine testing and/or maintenance. Therefore, the risk of failure must be minimized by applying technical methods capable to reduce time and materials spent during the testing and maintenance of high voltage apparatus.

Field dry-out of power transformers is nothing new to power system operators; the procedure and the expectations of the different types of processes are well known (as well as the limitations of each specific system). At the beginning of the manufacturing process, strict control over the quality of materials used for the construction and assembly of transformers is implemented. Special attention is given to the solid insulation components in order to minimize exposure to an environment where they might get contaminated (especially with moisture). After assembly completion of the active part of the transformer, the windings and core are subjected to different dry-out processes to remove moisture from the cellulosic material without affecting the life expectancy parameters (defined by the degree of polymerization and tensile strength of the cellulose). Throughout the life of the transformer and due to the normal aging effect, several byproducts will evolve within the insulation system, and field operators will encounter the challenge of re-conditioning the insulation system of the transformer, removing as much as possible these aging byproducts on-line or off-line.

While a variety of methods are available for field dry-out, identifying the real problem inside the transformer and selecting the right process should be the first decision. Advanced condition assessment is performed nowadays in the field using dielectric frequency response (DFR) instruments capable of discriminating moisture in the solid insulation from dielectric oil conductivity. The dry-out process must later be evaluated, and remaining moisture in the insulating system requires an accurate estimate before the transformer is put back in service. In this work, thanks to the support of a local utility and the implementation of safe procedures for field dry-out processes, a power transformer is continuously monitored using DFR; analysis and validation is carried out comparing cold trap water volume.

In this document, DFR field application is demonstrated to optimize the dry-out process, providing immediate condition assessment of the insulation spectrum variation throughout the process, determining the efficiency of the process, and minimizing the risk of overstressing the mechanical structure of the solid insulation.

Analyzing the Phenomena of Wind-Induced Vibrations on Unloaded Davit Arms

Erik A. Ruggeri, P.E.

Background for the Study

Installing complete structures (both sets of arms) but only one circuit will be strung. Second circuit will be installed when electrical load demands such.

Pole suppliers recommended either suspending 150 lbs (Valmont) or 10% of the arm weight (T&B) at the end of the unloaded arms “as a rule of thumb”.

Xcel engineers wanted better science applied to the proposed solution to a common problem, “Put 150 lb weights on the arm as a rule of thumb”.

Axial and Lateral Capacity of Tapered Helical Piles for Transmission Pole Structures

Mark H. Fairbairn, P.E., Lee Goen P.E., Jason Herron, EIT, and Gary L. Seider, P.E.

The foundations for most transmission line structures constructed in North America today are drilled shafts. However, drilled shafts are not always a suitable foundation choice. This paper details one example where helical piles were used as the foundation at select tower locations on a transmission line project for Xcel Energy. The project was XCEL Stinson-Bayfront Line 3315 32.1 Mile Re-Build 115 kV line. The structures were steel H-Frame, made by Thomas & Betts Meyer. The tangent structures were direct embedded, and the running angle and dead-end structures were either helical piles or drilled shafts. The line is located in a remote area of northwest Wisconsin near Duluth, MN. Helical piles were used at tower locations with poor road access, and in areas considered environmentally sensitive where large vehicles would destroy the landscape and vegetation. Xcel, Hubbell / CHANCE, and Thomas & Betts teamed together to design this project. Xcel Energy produced the load and design drawings, Thomas & Betts designed the H-Frame Pole structures and the pile transition connections, and Hubbell / CHANCE designed the helical pile foundations. The helical piles were a tapered shaft design, consisting of 2-1/4" solid square bar shafts with three or four helix plates for the starter sections, then stepping up to 8" nominal pipe shaft extensions connected together via the use of transition couplers.

Prior to line construction, full-scale load tests of the helical pile / connection were performed at the Thomas and Betts Structure Test Facility located in Hager City, Wisconsin. The tests were done to verify the design of the piles and connections to the pole base. The running angle and dead-end pile and transition systems were successfully loaded and tested to values that meet or exceed the ultimate design structure ground line reactions. These results are presented. The piles, tested together in a multi-pile group, were subjected to a combination of axial tension, compression, and lateral shear. In addition, four full-scale load tests were conducted on the line right-of-way at the actual tower locations. The tests consisted of pile penetration tests, axial tension, and lateral shear tests. These test results are compared to the theoretical capacity of the piles based on site soil type and strength. The results of the tests allowed the helical pile design to be adjusted prior to start of construction to provide the contractor with minimum depth and installation torque requirements.

AUTHORS:

Mark H. Fairbairn P.E., Senior Civil/Structural Engineer, Thomas and Betts, W8020 150TH Avenue, Hager City, WI 54014, USA mark.fairbairn@tnb.com

Lee Goen, P.E. CHANCE®/Hubbell Power Systems, Inc., 210 North Allen Street, Centralia, MO 65240, jlgoen@hubbell.com

Jason Herron, EIT, CHANCE® / Hubbell Power Systems, Inc. 210 North Allen Street, Centralia, MO 65240, jwherron@hubbell.com

Gary L. Seider, P.E., CHANCE®/Hubbell Power Systems, Inc., 210 North Allen Street, Centralia, MO 65240, glseider@hubbell.com

Engineering and Constructing High Quality Drilled Shafts

Calvin Stripling, P.E.

A drilled shaft, to be considered high quality, must meet at least the following requirements: 1) Concrete throughout the shaft that meets specifications 2) Reinforcing steel correctly placed with concrete to steel bond 3) Load transfer from the shaft concrete to the in situ geomaterial surrounding the shaft and 4) Proper concrete cover over the steel reinforcing cage for corrosion protection.

To produce a good quality shaft that meets the four conditions listed above specific aspects of the shaft design and installation must be controlled. These aspects are: steel congestion because it can restrict concrete flow; excavation stability to prevent shaft defects; concrete rheological (fluid) properties so that concrete behaves as it should; drilling fluid because it can affect concrete-geomaterial bond as well as the quality of the shaft base; and the interaction between the plumbness tolerance of the drilled shaft and specified concrete cover so that there is adequate cover to resist reinforcing steel corrosion.

Simulating Real World Conditions for Relay Scheme Testing

Jason Buneo

Abstract

Many of today's relay testing methods employ techniques available 50 years ago and have not evolved. These test methods don't fully utilize the capabilities of either the protective relays or the available test equipment. In fact, current standard testing practices for microprocessor-based relays do not even adequately represent real system conditions. Moreover, these methods do not properly utilize the one theory that could help—namely, that of symmetrical components.

This paper looks at three distinct ways of using symmetrical components to more accurately simulate real world conditions, including:

- a current unbalance scenario in a motor protection relay,
- the removal of zero sequence current in a transformer differential relay,
- operating a phase time overcurrent and a neutral time overcurrent on the same trip output without isolation,

For each of these scenarios listed above, antiquated methods are generally used, or the scenarios are not even tested because of the perceived difficulty of the procedure. In many cases of field-testing relay schemes, the methods employed do not take into consideration symmetrical components in the determination of fault values.

Therefore, a more accurate method for evaluation and testing of protection relays is necessary. In this paper, the method is examined in detail, along with the solutions for the three scenarios, encouraging testers to utilize symmetrical components to more accurately represent the power systems that the relay is protecting. By embracing methods that utilize symmetrical components, the perceived difficulty in testing protective relays will be greatly reduced.

Introduction

The transition from electromechanical protective relays to microprocessor based protective relays has allowed users to better protect power systems than what was possible in previous generations of equipment. Microprocessor based relays have a lower burden, greater flexibility for protective functions and logic, and in many cases can be accessed through remote communications. The increased flexibility of microprocessor based relays has also allowed customers to reduce their wiring costs and simplify their elementary diagrams.

However, with these great enhancements also comes some drawbacks. Many of these drawbacks are related to commissioning and periodic testing of these microprocessor based relays. Since there now many protective elements in a microprocessor based relay, isolating a specific function to verify its correct operation can become a bit of a challenge. In many protective schemes, it is common to have a single output contact on a protective relay trip based on the operation of many different protective elements. For example, in a protective relay, there might be differential, current unbalance, phase time overcurrent, and ground time overcurrent programmed to the same output contact. Many customers may now require that the relay be tested with all elements active, but that the tests are performed so that each element can be properly tested without operating the other active elements. To say the least, this can be tricky.

This increasing complexity also doesn't help that the average tester won't look at a particular relay that often. Once or twice a year for certain relays of a certain type. It could be even longer for other relays that have continuous monitoring. If you tested a relay once, a few years ago, chances are that you are not going to remember all of the details necessary to quickly test it again. Especially, if there were some settings changes. Then all bets are off. You might as well be testing it again for the first time.

All of these factors together, plus some others (like deadlines and pressure) make testing protective relays a pain. This paper won't be addressing some of the factors like deadlines and pressure,

but it will discuss how to make the fault values you apply to the relay more realistic and make the relay think it is looking at a real power system. This is good from a practical standpoint, because many modern protective algorithms in relays can tell the difference between a real fault and a contrived one from old equipment and procedures. The best way to start make fault values applied to a relay appear more realistic is to apply the method of symmetrical components.

Symmetrical Components

Calculating normal and abnormal system conditions starts with an understanding of symmetrical components. Symmetrical components first came about in a paper written by Dr. C. L. Fortescue entitled, "Method of Symmetrical Coordinates Applied to the Solution of Polyphase Networks." [1] Dr. Fortescue stated that unbalanced three phase voltages or currents could be transformed into three sets of balanced three phase components. To do this mathematically, the method of symmetrical components utilize a variable called the "a" operator. This variable is a vector with a magnitude of 1 and an angle of 120°. In a three phase system, the "a" operator is applied to the reference voltage or current. By applying the "a" operator to the reference voltage and current phases they are each rotated counter clockwise by 120°. To get a 240° displacement, the "a" operator is squared. This is shown in Figure 1 below where the "B" and "C" phases of voltage are expressed in terms of "A" phase voltage. This same procedure would apply to current as well.

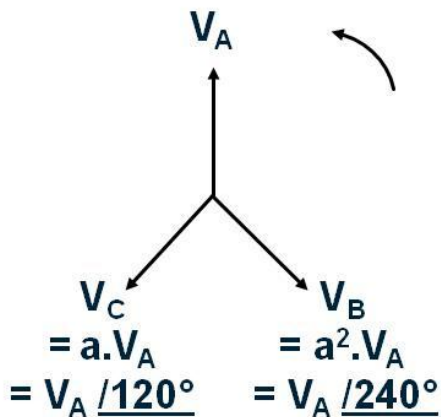


Figure 1. Application of the "a" Operator

Now that each of the phases are expressed in terms of a common reference, they can be broken down further into their actual sequence components. All three phases will each contain three components called positive, negative, and zero sequence. These are shown in Figure 2.

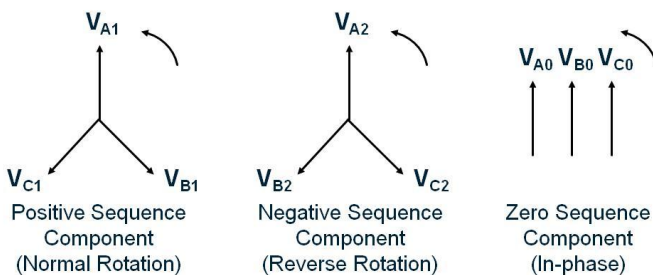


Figure 2. Positive, Negative, and Zero Sequence Components

Mathematically, the sequence components can be broken down into the following equations:

$$V_A = V_{A1} + V_{A2} + V_{A0}$$

$$V_B = V_{B1} + V_{B2} + V_{B0} = a \cdot V_{A1} + a^2 \cdot V_{A2} + V_{A0}$$

$$V_C = V_{C1} + V_{C2} + V_{C0} = a^2 \cdot V_{A1} + a \cdot V_{A2} + V_{A0}$$

Now that we have these equations, what do they mean? To put these equations in perspective, let's show how the relationship between phase voltages and currents with their sequence components. Figure 3 shows how each of the phase quantities are a vectorial summation of each of their respective sequence components.

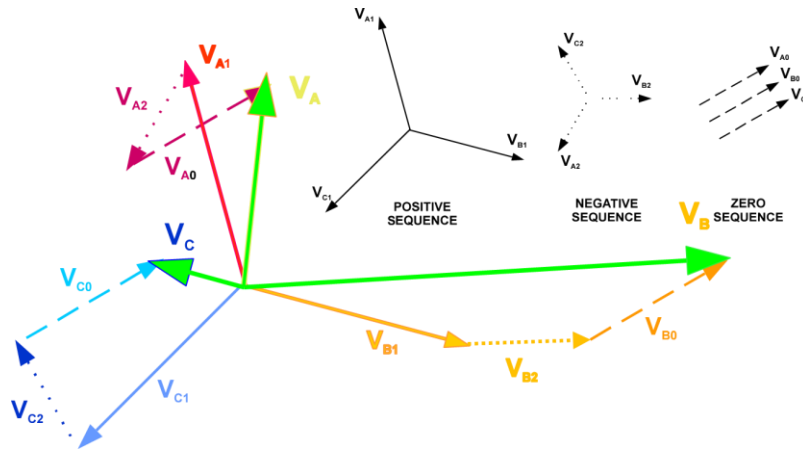


Figure 3. Relationship between symmetrical components and phase components

In power systems each of these symmetrical components would be measured by the protective relay in some form or another depending on what the current system conditions are. In a normally operating, balanced system, the protective relay will measure primarily positive sequence values. The negative and zero sequence values will be minimal because there are no unbalances or ground currents. During a three phase bolted fault, only positive sequence current will be measured because all three phases are still balanced symmetrically due to fault magnitude and phase angle. During a phase to phase fault, the relay will be measuring both positive and negative sequence currents. This is because that when a phase to phase fault occurs, the negative sequence component opposes the positive sequence component. When a line to ground or double line to ground fault occurs, positive, negative, and zero sequence values will be measured.

Application Example 1: Motor/Generator Current Unbalance Protection

Now that symmetrical components have been discussed in theory, it is time to put that new knowledge into practice. The first application symmetrical components will be used to test a motor or generator for current unbalance protection. This protection is designed to protect a motor or generator from uneven loading between the phases. In particular, the negative sequence current is monitored to keep it below a predefined magnitude as proscribed by the settings engineer.

To make the math easy, let's say this motor's full load amp rating in secondary current is 5 A, and that the percent unbalance pickup is 20%. In secondary amperes, the pickup current should be 1 A.

The traditional way of testing this protection has been to inject a single phase current into one of the phases of the relay and increase the magnitude until the unbalance element operated. Using this method the pickup would be actually be 3 A instead of 1 A. This is because the relay is splitting the positive negative and zero sequence components evenly, and it will take three times as much current to get a proper trip.

To get a proper 1 A trip, the symmetrical component quantities will need to be computed. Since this is an unbalance element, only positive and negative sequence components are required. The positive sequence current will be the full load secondary Amps which is 5 A. The negative sequence current is the 20% unbalance, which is 1 A. There is no mention of zero sequence current, so that will be set to 0 A. These values of symmetrical components can now be used to figure out what the phase currents should be. The phase A current can be solved as follows. The solution for leading and lagging angles will be given.

$$I_a = I_a^0 + I_a^+ + I_a^-$$

$$I_a^+ = 5 \angle 0^\circ, I_a^- = 1 \angle 180^\circ$$

Separate into Real and Imaginary Values :

$$I_{a_{Real}} = 5 \cos(0^\circ) + 1 \cos(180^\circ) = 4$$

$$I_{a_{Imaginary}} = 5 \sin(0^\circ) + 1 \sin(180^\circ) = 0$$

$$I_{a_{Magnitude}} = \sqrt{(I_{a_{Real}})^2 + (I_{a_{Imaginary}})^2} = 4A$$

$$I_{a_{Angle}} = \tan^{-1} \left(\frac{I_{a_{Imaginary}}}{I_{a_{Real}}} \right) = \tan^{-1} \left(\frac{0}{4} \right) = 0^\circ \text{ Leading} \rightarrow 0^\circ \text{ Lagging}$$

Where I_a^0, I_a^+, I_a^- are the zero, positive and negative sequence values

Continuing on, the B and C phase currents can also be solved in the following equations.

$$I_{b_{Real}} = 5 \cos(0 - 240) + 1 \cos(180 - 120) = -2$$

$$I_{b_{Imaginary}} = 5 \sin(0 - 240) + 1 \sin(180 - 120) = 5.196$$

$$I_{b_{Magnitude}} = \sqrt{(5.196)^2 + (-2)^2} = 5.568 \text{ A}$$

$$I_{b_{Angle}} = \tan^{-1} \frac{I_{b_{Imaginary}}}{I_{b_{Real}}} = -68.95^\circ \text{ Leading} \rightarrow 111.05^\circ \text{ Lagging}$$

$$I_{c_{Real}} = 5 \cos(0 - 120) + 1 \cos(180 - 240) = -2$$

$$I_{c_{Imaginary}} = 5 \sin(0 - 120) + 1 \sin(180 - 240) = -5.196$$

$$I_{c_{Magnitude}} = \sqrt{(-5.196)^2 + (-2)^2} = 5.568 \text{ A}$$

$$I_{c_{Angle}} = \tan^{-1} \frac{I_{c_{Imaginary}}}{I_{c_{Real}}} = 68.95^\circ \text{ Leading} \rightarrow 248.95^\circ \text{ Lagging}$$

The final calculated values are shown in Table 1.

Table 1. Calculated values for 20% unbalance

	la	lb	lc
Magnitude	4 A	5.568 A	5.568 A
Angle (Lagging)	0°	111.05°	248.95°

As can be seen the magnitudes and phase angles have drifted from the nominal balanced conditions. This is exactly a 20% unbalance with a 5 A nominal current. It is quite different from the 3 A single phase injection that was calculated earlier. This method is much closer to an actual system condition than the previous single phase injection method.

Application Example 2: Transformer Zero Sequence Current Removal

The next example of applying symmetrical components to protective relay testing that we will look at is verifying the removal of zero sequence current in transformer differential relays. Zero sequence current tripping is a common nuisance problem experienced by differential relays. When a sufficiently high magnitude line to ground fault occurs outside of the zone of protection of a differential relay the zero sequence current flowing through the relay may become large enough to cause a trip even though the transformer is not experiencing the fault directly. Fortunately, there have been various methods developed that can counter act this problem. Figure 4 shows a typical diagram for a two winding transformer differential protection scheme.

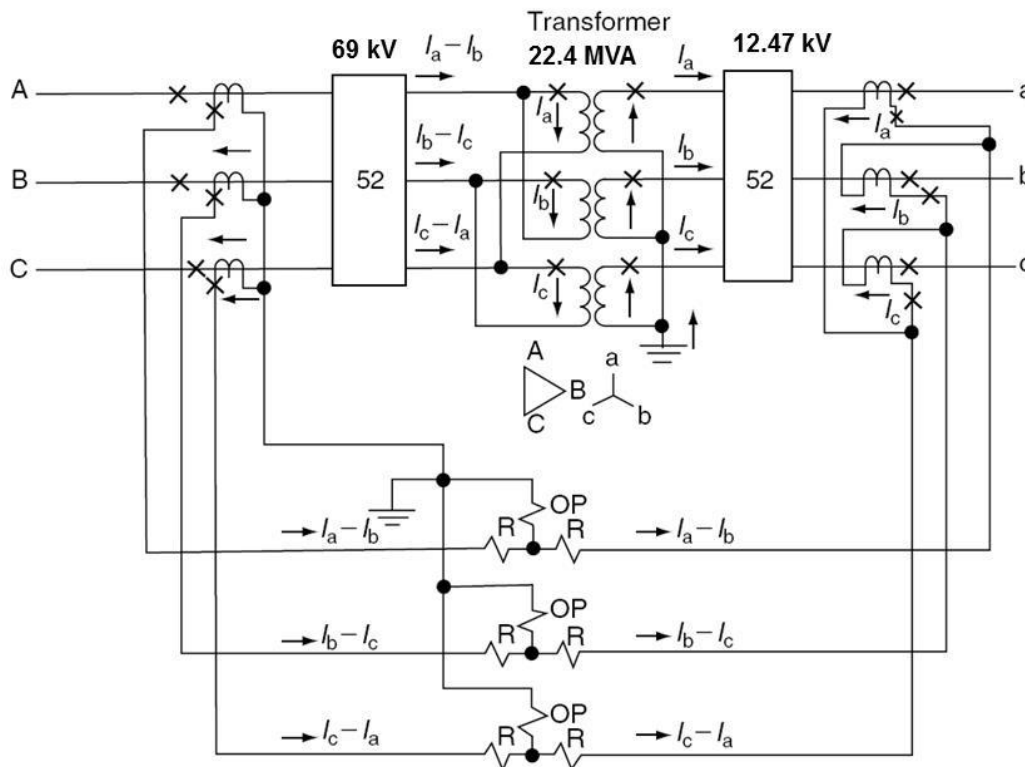


Figure 4. Two winding transformer differential protection [2]

In traditional electromechanical differential schemes, the zero sequence current could be eliminated by virtue of the current transformer (CT) connections to the relay. This was done by wiring the CT's in the opposite configuration of the winding that they are connected to. So, for the delta high side winding, the CT's are wired in a wye configuration. In the wye winding, the CT's are wired in a delta configuration. This configuration will cancel out the zero sequence current in both windings. This process is referred to as external zero sequence compensation.

Modern microprocessor relays no longer have to rely on specific CT configurations to eliminate the zero sequence current. They can do it internally through software. Almost all new protection and many retrofit commissioning is done with microprocessor relays. To use the internal compensation, the

CTs will be wired in a wye configuration for both windings. As we saw earlier, this will give rise to zero sequence current flow in the transformer, but the relay will be able to recognize it with its internal algorithms and essentially ignore this current. Let's take a look at exactly how this is done with a practical example.

For our example, let the transformer have the following settings:

- Transformer MVA** = 22.4
- High Side Voltage** = 69 kV
- Low Side Voltage** = 12.47 kV
- CT Ratio on the High Side** = 30:1
- CT Ratio on the Low Side** = 240:1

With these settings we can figure out the high and low side secondary current with the following equations.

$$I_{rated_HighSide} = \frac{MVA}{\sqrt{3} \times KV_{Ph-Ph(HighSide)}} = \frac{22.4 \times 10^3}{\sqrt{3} \times 69} = 187.65 \text{ A}$$

$$I_{base_HighSide} = \frac{I_{rated_HighSide}}{CTR_{HighSide}} = \frac{187.65}{30} = 6.25 \text{ A}$$

$$I_{rated_LowSide} = \frac{MVA}{\sqrt{3} \times KV_{Ph-Ph(LowSide)}} = \frac{22.4 \times 10^3}{\sqrt{3} \times 12.47} = 1038.3 \text{ A}$$

$$I_{base_LowSide} = \frac{I_{rated_HighSide}}{CTR_{HighSide}} = \frac{1038.3}{240} = 4.32 \text{ A}$$

Now that we have the secondary currents we can look at the relationship of the two windings of the transformer. For our example we will have the following relationship shown in Figure 5.

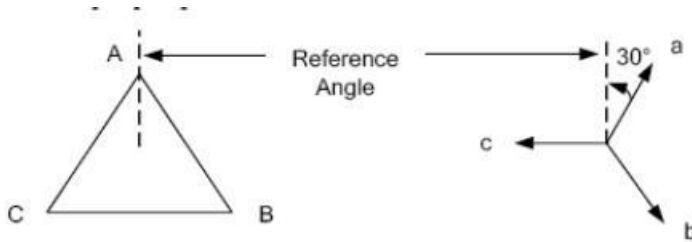


Figure 5. Phase angle relationship between winding 1 and winding 2 [2]

Winding 2 is shifted 30° from Winding 1. The relay will take this phase relationship and apply its zero sequence compensation by mathematically computing its phase components against a zero sequence matrix and applying a magnitude shift factor of $\sqrt{3}$ to the calculations. These calculations are shown in the following equations.

$$[ZeroComp] = \frac{1}{\sqrt{3}} \times \begin{bmatrix} 1 & -1 & 0 \\ 0 & 1 & -1 \\ -1 & 0 & 1 \end{bmatrix} \times \begin{bmatrix} I_a \\ I_b \\ I_c \end{bmatrix} = \begin{bmatrix} \frac{1}{\sqrt{3}}(I_a - I_b) \\ \frac{1}{\sqrt{3}}(I_b - I_c) \\ \frac{1}{\sqrt{3}}(I_c - I_a) \end{bmatrix} = \begin{bmatrix} \frac{1}{\sqrt{3}}(I_1 + I_2 + I_0 - a^2 I_1 - a I_2 - I_0) \\ \frac{1}{\sqrt{3}}(a^2 I_1 + a I_2 + I_0 - a I_1 - a^2 I_2 - I_0) \\ \frac{1}{\sqrt{3}}(a I_1 + a^2 I_2 + I_0 - I_1 - I_2 - I_0) \end{bmatrix}$$

As can be seen, each of the I_0 terms are eliminated in each of the equations. Depending on what the phase relationship is between windings the compensation matrix will be different. If an incorrect matrix is selected, then the zero sequence currents will not be properly eliminated. Verifying the relay is removing the zero sequence components is an important, but often overlooked test when commissioning transformer differential relays.

To determine if the differential relay is actually removing the zero sequence current, it is best to perform the following steps. First, calculate the values of the relay that would give you trip values based on the positive sequence current. When that value is calculated, apply the current that is slightly less than that so that the relay does not operate on a differential trip. The idea is to get the relay on the verge of tripping on a differential operation. When the relay is at this precipice, apply zero sequence current to the relay. The relay should not trip.

Taking the same transformer we have been working with, let us apply some differential settings to the relay. Since many manufacturers have various methods of calculating differential operation, let's take one of the most common methods where the operate current is the sum of the two winding currents and the restraint current is the average of the two winding currents.

Here are the differential relay settings of interest.

Slope = 25%

Winding 1 Secondary Current = 6.25 A

Winding 2 Secondary Current = 4.32 A

Using these settings we can solve for when the relay should be just on the threshold of operating. Note that when testing differential relays, the CT polarities will be facing opposite of each other when in service to establish a zone of protection around the transformer.

$$I_{OPERATE (PU)} = \frac{I_{Winding1} \angle \theta_{Winding1}}{Tap1} + \frac{I_{Winding2} \angle \theta_{Winding2}}{Tap2}$$

$$I_{OPERATE (PU)} = \frac{4.50 \angle 0}{6.25} + \frac{3.97 \angle 180}{4.32} = 0.721 \angle 0 + 0.919 \angle 180 = |-0.199|$$

$$I_{RESTRAINT (PU)} = \frac{\frac{|4.50 \angle 0|}{6.25} + \frac{|3.97 \angle 180|}{4.32}}{2} = \frac{0.720 + 0.919}{2} = 0.82$$

$$Slope = \frac{0.199}{0.820} \times 100 = 24.26\%$$

The value of slope applied by injecting 4.5 A of positive sequence current into winding 1 and 3.97 A of positive sequence current into winding 2 is just at the precipice of operation. Since these are positive sequence values, a total of six currents will be applied to the relay. Three in winding 1 and three in winding 2. Table 2 shows the magnitude and phase angle of all of the current inputs.

Table 2. Phase Quantities of Only Positive Sequence Current Values

	Magnitude (A)	Angle (Lagging)
I_A (Winding 1)	4.50 A	0°
I_B (Winding 1)	4.50 A	120°
I_C (Winding 1)	4.50 A	240°
I_a (Winding 2)	3.97 A	210°
I_b (Winding 2)	3.97 A	330°
I_c (Winding 2)	3.97 A	90°

By applying 1 A of zero sequence current to winding 2, we can calculate the phase quantities of the combined positive and zero sequence current. Like with the motor unbalance example, the calculations will have only two sequence component terms to worry about instead of three. Only the positive sequence and zero sequence values need to be used. These values are shown in Table 3.

Table 3. Phase Quantities of Positive and Zero Sequence Values

	Magnitude (A)	Angle (Lagging)
I_A (Winding 1)	4.50 A	0°
I_B (Winding 1)	4.50 A	120°
I_C (Winding 1)	4.50 A	240°
I_a (Winding 2)	3.144 A	219.15°
I_b (Winding 2)	4.862 A	335.90°
I_c (Winding 2)	4.094 A	75.86°

The values given in Table 3 should not trip the differential protection with the given settings.

Application Example 3: Phase and Residual Time Overcurrent Protection on Same Contact

With the previous two examples, extensive calculations were needed to calculate the positive, negative and zero sequence current values. Of course by now it is expected that the reader is an expert on symmetrical components and can now do these calculation in her or her head. In fact we will do so with the following example.

Many times a person tasked with testing protective relays will be given the constraint to individually test the elements using only the trip contact that will be used during actual faults. In addition, the other elements must remain active during the testing. In a lot of cases this is not a problem because it is relatively straight forward to isolate protective elements from one another based on the design of the test. For instance, and under frequency element is easy to isolate from an over voltage element by keeping the voltage magnitude below the over voltage threshold and ramping the frequency. Other element it is not so easy. Phase time overcurrent and residual time overcurrent elements can often interfere with one another if care is not taken. Both of these elements use the same current inputs to take their measurements. This is shown in Figure 6.

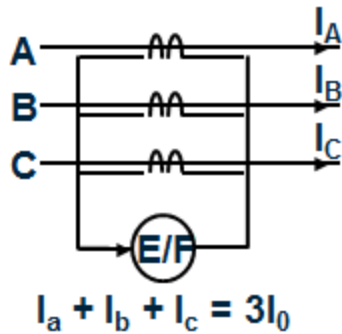


Figure 6. Current inputs for phase and residual time overcurrent [2]

The phase time over current element measures the positive sequence current and the residual time over current element measures the zero sequence current. In many cases, the residual time overcurrent element is set to a pickup value lower than the phase time overcurrent element. Many testing procedures have each of these elements tested the same way, by injecting a current into a single phase of the relay and ramping the magnitude until a trip occurs. The problem with this is that if the phase element is being tested, the residual will trip first preventing the user from measuring the true phase pickup value.

This can be easily solved by looking at what each of the elements is actually measuring. In the case of the phase time overcurrent, positive sequence is being measured. To ensure that the residual current does not pickup, the zero sequence current must be set to zero. This is done by applying a balanced three phase current to all three current inputs, and then ramping to the appropriate magnitude that will yield a trip. To test the residual element without affecting the phase element, the opposite can be applied. Apply only zero sequence current and make the positive sequence component zero. This is achieved by applying three equivalent currents with a phase angle displacement of zero degrees. Then ramp the current to the appropriate pickup magnitude. The residual element will trip and the phase element will not.

Conclusions

A solid understanding of symmetrical components is vital to understanding and testing the various protection algorithms of modern microprocessor relays. This paper has shown only three of the many scenarios where proper application of symmetrical component theory can aid in testing protection elements. More importantly, proper application yields more realistic fault values which in turn gives a more accurate picture of protective relay operations.

References

1. C.L. Fortescue, *Method of Symmetrical Co-ordinates Applied to the Solution of Polyphase Networks*, Annual Convention of the American Institute of Electrical Engineers, Atlantic City, NJ, 1918
2. J.Lewis Blackburn, *Protective Relaying Principles and Applications* Third Edition, CRC Press, 2006

Sweep Frequency Response Analysis: Failure Mode Analysis

Dinesh Chhajer and Volney Naranjo

Frequency Response Analysis: Failure Mode Analysis

By

Dinesh Chhajer
Volney Naranjo
Applications Engineers
Megger

Abstract

This paper will focus on Frequency Response Analysis (FRA) diagnostic technique as a tool to identify transformer failure modes. The paper summarizes and presents the most relevant aspects of IEEE FRA guide (PC 57.149) that includes FRA test requirements, measurement methodology, results interpretation and analysis. It is complemented with recommendations from other FRA standards (IEC, CIGRE and DL/T 2004) not included in the IEEE guide. Failure mode guidelines included in the IEEE guide to identify mechanical issues are reviewed in detail and are compared with real life cases from field experience. Additionally, it also provides recommendations on best practices to be considered while performing the FRA test in field environment. Paper also presents FRA case studies collected from utilities that helped in identifying mechanical issues and taking preventive actions to avoid catastrophic failure of power and distribution transformers.

I. INTRODUCTION

Power system operators constantly strive to improve the reliability and stability of the power system. Transformers, being integral parts of the system, need to deliver and operate without any fault or unexpected behavior. To minimize the probability of unexpected behavior, scheduled testing and maintenance is performed on transformers. In today's age, power system operators are offered a large variety of offline and online monitoring, along with advancements in measurement, signal processing and data acquisition. A big question remains: How to utilize these tools to improve the system reliability as well as prevent catastrophic failure of transformers?

Transformer windings are routinely tested using traditional methods such as excitation current, transformer turns ratio and winding resistance tests. Unexpected or questionable results will indicate issues, but additional tests will be required to confirm or determine the root cause. Problems associated with physical changes inside the transformer (such as winding displacement, core movement, winding deformation, radial and axial movement) are typically easily detected using diagnostic techniques like Frequency Response Analysis (FRA). This technique is most useful in diagnosing a transformer suspected of internal mechanical movement due to transformer transportation, natural disasters, short circuit faults or for advanced condition assessment after a transformer alarm or unsatisfactory electrical test results. This test will confirm the results of any traditional tests and is even sensitive enough to detect issues that normally remain unidentified in routine tests. Different failure modes can be detected in different frequency bands of an FRA curve. FRA test analysis is based on the comparison of a test result to a reference or baseline result. In the absence of a baseline curve, a comparison with a similar transformer (units are considered to be similar if they are identical in manufacturer, design, and construction) or a comparative analysis of the three phases may also yield valuable information.

This paper focuses in recommending the appropriate procedures to perform and analyze FRA tests as per the IEEE C57.149-2012 guide, advising on best field practices and presenting case studies on determining failure modes as per the IEEE guide and field experiences.

II. Recommended Practices by IEEE Std C57.149-2012 for FRA Measurement

IEEE C57.149-2012 is the Guide for the Application and Interpretation of Frequency Response Analysis for Oil-Immersed Transformers. The guide was work in progress for several years by incorporating inputs from various industry professionals, utility personnel, transformer and test equipment manufacturers. The final guide was approved in December 2012 and released on March of 2013. It provides users the recommendations for procedure and requirements for testing, field and factory application, test data analysis and interpretation.

A summary of the IEEE FRA guide in regards to test instrument specifications, test practices and test results analysis has been presented below:

1 Test Instrument

As an end user of FRA, it is important to select the appropriate instrument, understanding its capabilities and whether it follows the instrument guidelines recommended by IEEE guide. The following are the main requirements or characteristics defined by IEEE C57.149:

It specifically defines the following:

- Test instrument should be capable of recording minimum 200 points per decade.
- A three lead configuration (signal, reference, and test) should be used. They should be made of coaxial cables and the shield of the coaxial cable should be able to be grounded on both ends. All the leads should be of same length and each lead can have a length up to 30m.
- XML format for the data file is recommended for data storage and recollection of results for future.

For the rest of the instrument attributes, like calibration, output power, dynamic range and measurement impedance, it is indicated that they should be adequate, sufficient or capable for the purposes of the test.

Frequency range for FRA test shall be wide enough to be able to diagnose problems in the three main mechanical components of a transformer: core, clamping structure and winding/interconnections. The resolution should be adequate to provide clear diagnosis. It is important to note that test frequency range has not been defined explicitly in the guide.

2 Test Practices

a. Specimen Scope

IEEE guide is explicit for oil-immersed transformers, and it does not have an established limit in regards to nominal voltage, MVA rating or any other transformer characteristics.

The recommended criteria to decide when to perform a FRA test is after any situation that can cause mechanical movement or electrical damage to the transformer assembly. Some of these situations are:

- Factory short-circuit testing
- Installation or relocation
- After a significant through-fault event
- As a part of routine diagnostic measurement protocol
- After a transformer alarm (i.e., sudden pressure, gas detector, Buchholz)
- After a major change in on-line diagnostic condition (i.e., a sudden increase in combustible gas, etc.)
- After a change in electrical test conditions (i.e., a change in winding capacitance)

b. Test Conditions

FRA test analysis is based on the comparison of a test result to a reference or baseline result. Results are highly dependent on mechanical configuration, both internal and external. Hence, it is of great importance to prepare the specimen for the test, make an effort to minimize the external influence and to replicate to the maximum the test conditions in case a diagnostic test is run.

IEEE guide covers the topic in detail, dividing the subject in environment preparation and object preparation. In summary, the requirements are:

- Transformer should be completely isolated from any power source. All terminals, including neutrals and grounds, should be disconnected.
- Tank of the transformer should be grounded.
- Specimen should be as close to in-service condition, e.g., bushings installed and filled with oil. Testing with oil is the most common and preferred method of measurement.
- If possible, all test leads connections should go directly to the bushing terminal.
- Internal CT, if present, should be configured for in- service condition.
- Operation of the DETC is up to the decision of the owner.

Another aspect that influences the test result is the position of the LTC and/or the DETC. Every tap position is a different mechanical configuration, depending on the amount of turns and type of LTC.

The IEEE requirement is to perform the test in extreme raise position. If performed on neutral position, it shall be documented along with the direction from which neutral position is reached. It is preferred to arrive at neutral tap from raised position. The DETC position is to be determined by service conditions.

Transportation is a critical stage in the life of a transformer and FRA is a perfect tool to determine if it has affected the physical configuration or the geometry in any way. Shipping configuration is usually different than the normal physical condition of a transformer, thus generating a different FRA trace. Hence, any baseline measurement taken under shipping configuration is only good for the transportation stage until the delivery. There are four aspects that are specific in the shipping configuration of a transformer and should be observed during all the phases of the transportation process. This is to ensure that any entity holding custody of the transformer can perform repeatable tests:

- *Presence and level of the oil:* It can cause variations in the FRA test readings across a broad range of test frequencies. Test should be performed with the same level of oil.
- *Position of the DETC and LTC:* Test at the same position of the shipping configuration
- *Bushings and placement:* Since bushings are removed for transportation, it is recommended to install small FRA testing bushings. If the test is to be performed with the regular bushings they should always be placed in the same position.
- *Configuration of the tank and test groundings:* It may vary and can affect the FRA trace.

Once the transformer has been delivered and put back to its normal configuration, a new baseline response should be taken for future references. A similar rule should be applied if any of the transformer components are repaired or replaced.

c. Voltage

Instrument manufacturers use voltages that range from $2 V_{pp}$ to $20 V_{pp}$. Using the same voltage in a diagnostic test as in a baseline test is important to guarantee repeatability. The effect of using a different voltage is noticed below 10 kHz and is more pronounced on LV windings. IEEE recommends avoiding applying excessive voltages to transformers without oil.

d. Frequency Range

The importance of selecting the appropriate frequency range is to cover the entire spectrum of the transformer response to frequency and to avoid recording a response due to external factors.

IEEE has no specific recommendation or requirement for the frequency range setting. However, in a section corresponding to failure modes, it analyzes different failures in a frequency range from 20 Hz to 1 MHz. Additionally, in Annex 5, it describes the typical regions that depend on the dominant influence of the different structures of the transformer. These regions are framed between 10 Hz and 10 MHz. A response greater than 1 MHz is irregular and complex, it may contain important information from the leads of taps but it is also affected by the grounding leads.

e. Measurement Types

There are four main measurement types that can be performed on a transformer: end-to-end open circuit, end-to-end short circuit, capacitive inter-winding and inductive inter-winding.

Figure 1 illustrates the four measurement types. V_R is the applied signal and V_M is the measurement of the response. The connections shown below represent single phase configuration of a transformer. For three-phase configuration similar tests would be performed on each phase.

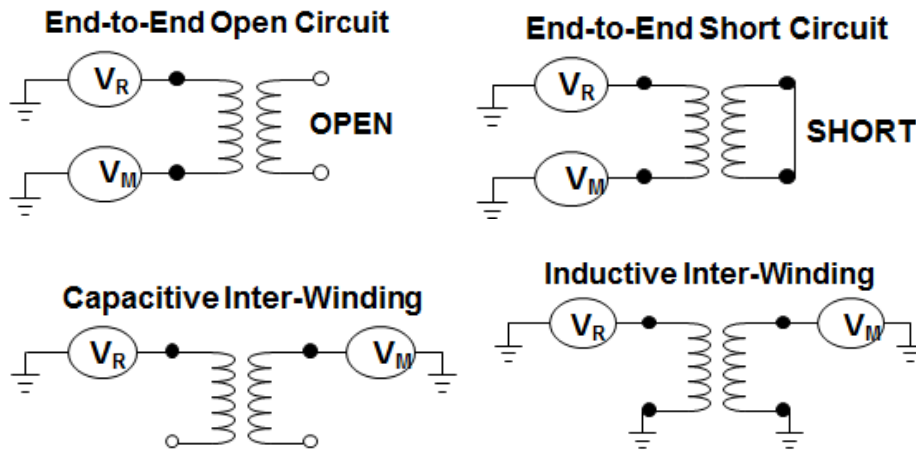


Figure 1: Measurement types

IEEE recommends performing all end-to-end open and short circuit tests, but the minimum requirement is to perform all open circuit tests. If the transformer has an LTC, it should be set in extreme position to include all tap windings in the circuit and DETC set as found.

f. Connections

Lead connections also have an impact on test results. To achieve good and repeatable measurements, it is important to consider where and how to connect test and ground leads for each winding/phase measurement.

- i. Sequence of connections:** The purpose is to test all windings. IEEE defines that all measurements should be done from head-to-tail and follow winding configuration (vector group). The guide has six tables that show the test connections for 0° and 30° groups of two and three windings transformers and autotransformers with, without and buried tertiary. Any other configuration or equipment shall be determined by the user following the vector group. Variations on sequence or polarity are accepted.
- ii. Shield grounding:** Shield grounding is an important aspect of the measurement and the method used to achieve the grounding will have a great impact on test results. The standard grounding method is to run an extension of the grounding cable from the top of the bushing (lead connection) to the flange of the bushing. IEEE requires that the grounding techniques, conductors, routing and any other aspect related to it should be precise, repeatable and documented.

g. Instrument and Tests Verification

Prior to running an entire set of tests, it is important to check the integrity of the instrument and verify that it is calibrated and working properly. Furthermore, once all tests are performed, it is a good practice to run a repeatability check to confirm that the connecting practices do not affect the results. IEEE recommends running, when possible, a self-check of the instrument on a standard test object with a known response. This checks both the instrument and the test leads.

3 Test Result Analysis

Any result analysis on FRA is mainly performed by comparing a response to a reference response. It can be a previous result on the same object, a response from a similar test object or the response from the other phases within the same transformer. In addition to the comparison, another way to perform the analysis is by identifying unexpected responses from the different type of measurements and transformers. This method helps to locate the section or structure where a fault is present.

In the IEEE FRA guide, the two basic analysis tools are a) trace comparison and b) identification of trace characteristics. The main purpose with any of these is to determine if the physical condition has not changed, and a secondary purpose is to detect or determine the type of mechanical failure, e.g., radial deformation, axial elongation, core defects and turn-to-turn short circuit, among others.

a. Trace Comparison

This is the primary tool for analysis using traces from a previous measurement, similar units or the other phases on the same unit as a reference. A comparison to a previous measurement should overlay almost perfectly. Thus, the main method for trace comparison is a plot inspection, and it is also the method used to determine the different failure modes.

Figure 2 below shows a typical response from 20 Hz to 10 MHz, a plot of admittance magnitude vs. frequency. The frequency normally is presented in logarithmic scale and the magnitude is usually shown in decibels. Linear scale for the frequency and the magnitude are used occasionally as well. The entire trace can be divided into four regions depending upon the predominant component influence: core, winding interaction, winding structure, leads of taps and grounding leads. The frequency range for different regions shown below in figure 2 can be used as a general guideline, however it may vary based upon different transformer designs.

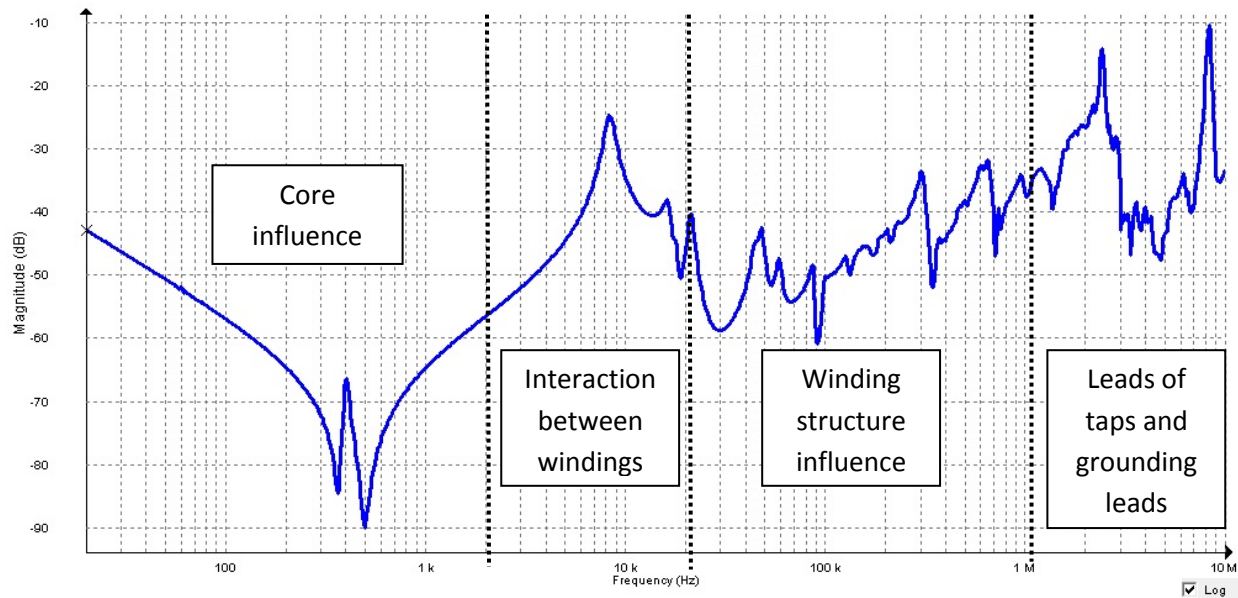


Figure 2: FRA trace showing influence of transformer components in different frequency regions

The plots are inspected to evaluate trace resonances and magnitude and phase deviations as well as the general patterns. Any deviation may be an indication of a mechanical change. The comparison can also be made by subtracting the diagnostic result from the baseline response, and analyzing difference plotting. Any deviation from zero requires a detailed evaluation. Difference plotting is to be used on magnitude plots, not phase plots, due to its sensitivity. A third option for trace comparison is correlation coefficients, which determines how random or similar two traces are. The goal of the analysis is to get an indication of correlation between two traces. FRA instrument manufacturers usually include the mathematical methods in their software tools.

b. Trace Characteristics

Despite the variety of transformer designs and ratings, there is a general characteristic response for each type of test and frequency region. Knowing how a response should look like is helpful in identifying problems and narrowing them to a specific component of the transformer. There are significant indicators for two general problems:

- Winding deformation/Insulation degradation:
 - New resonances or loss of resonances
 - Shift in frequency for an existing resonance
- Winding looseness:
 - Continuous increment of magnitude compared to the reference trace with a similar shape as frequency increases above 500 KHz.

Also, if a resonance point shows that it is attenuated (smoothed) when compared to traces, it is an indication of increased resistance.

Each of the four types of test has its own general expected characteristic. Responses out of the

predictable plot can indicate a mechanical change inside the transformer. The following are specific characteristics for each type of test:

- i. Open circuit (end-to-end open) Test.** This is the most common test. In the high voltage (HV) windings, it produces the most predictable pattern in the low frequency region.

For low frequencies:

- The response is mainly inductive (core magnetizing inductance), which causes the magnitude to decrease. The response shows a decreasing slope of approximately -20 dB per decade.
- HV wye-connected windings often show one distinct or two close resonances (minima) between 20 Hz and 5 KHz.
- HV delta-connected windings generally show two resonances (minima) spaced apart.
- Low- or tertiary-voltage windings follow the same pattern but influenced by the HV winding.
- The higher the voltage and power rating, the lower the response magnitude.
- The plots of the three phases of a transformer, around 60 Hz, should emulate the same behavior as the excitation current test: the two external phases have lower attenuation (higher current) than the central phase.

Mid Frequencies:

- Dominated by impedances created by the winding stack.
- Response can be either a complex or simple series of resonances.

High Frequencies:

- Usually above 500 KHz.
- Response similar to mid frequencies but more sensitive to specific and small sections such as tap windings, tap leads and deviated turns.
- At these frequencies, the response is more capacitive. It follows a rising trend with a linear slope of approximately 20 dB per decade.
- The higher the voltage and power rating, the higher the response magnitude.
- Insulation degradation and winding looseness can be identified in this region.

- ii. Short Circuit (end-to-end short) Test.** This type of test shows the response of a winding without the effect of the core. The configuration is similar to a short-circuit impedance test. The resulting plot is almost equal to the open circuit test from the mid frequencies and up. In the low frequencies region the impedance associated to the core reluctance is removed with the short circuit in the LV winding. Hence, the resonances in this region disappear, and the response has a higher magnitude.

If the short-circuit test produces a horizontal response at frequencies less than 30 Hz, any differences between phases (below 30 Hz), should be confirmed with a winding resistance test. In this region, the results are comparable to the winding resistance test, and no difference should appear between the traces.

- iii. Capacitive Inter-winding Test.** The main characteristic of this response in the low frequencies is an increasing magnitude as frequency increases, with few resonances. From the mid

frequencies and up, the increasing trend continues, and resonances will appear due to the impedance between windings of two voltage classes and by inter-winding resonances.

- iv. Inductive Inter-winding Test.** This test is mainly performed to measure the voltage ratio between two windings. The characteristic trace shows a flat magnitude response in the low frequencies region, and it is equal to the nominal voltage ratio. The mid and high frequencies are not examined in this test.

By showing the trace for the linear magnitude Vs. frequency, an indication of the turns or voltage ratio result can be obtained by calculating the reciprocal of the magnitude in the flat section, less than 60 Hz.

III. Recommendations from other Standards

In addition to the IEEE FRA guide there are three other important reference documents related to FRA: Chinese Standard DL/T911-2004, IEC Standard 60076-18 Ed.1, and CIGRE Technical Brochure No. 342.

All of these reference documents contain valuable information and on some topics have a different approach to FRA technique. Following are the highlights that complement the IEEE Standard and can be used to improve test practices or broaden the use of the technique for diagnostic purposes.

1 Frequency Range

Like IEEE, Cigré has no direct mention on what frequency range to set; however, it has a section that shows the typical ranges response for high voltage (HV), low voltage (LV), and regulating windings of large and medium MVA rating.

TABLE I
Frequency range for natural frequencies of large transformer windings [4]

Transformer component (> 100 MVA/limb)	Typical range for natural frequency	
	start [kHz]	stop [kHz]
HV disk winding	10	200
LV layer winding	10	1000
Regulating winding	100	1000

TABLE II
Frequency range for natural frequencies of medium transformer windings [4]

Transformer component (< 30 MVA/limb)	typical range for natural frequency	
	start [kHz]	stop [kHz]
HV disk winding	10	1000
LV layer winding	50	1500
Regulating winding	100	1500

The Chinese standard and the IEC clearly define a measurement range as per the following table.

TABLE III
Frequency Measurement Range [1] , [2]

Standard	Range
DL/T911-2004	1 KHz to 1 MHz
IEC 60076-18 Ed.1	≤20 Hz to 1 MHz for test objects >72.5 KV ≤20 Hz to 2 MHz for test objects ≤72.5 KV

For the high frequency limit, IEC recommends using at least 2 MHz in all tests for compatibility and simplicity.

2 Sequence of Connections

For star-connected windings with neutral, IEC recommends applying the source to the line terminal and taking measurements on the neutral. For the delta windings and others without neutral, follow the terminal numbering or labeling in ascending order. It also defines the connections for zigzag windings, autotransformers, phase shifting transformers and reactors.

The Chinese standard follows the same criteria as IEC but swaps the location of the leads; it states to connect the source to the tail and the measurement to the head.

It also provides a table to specify additional measurements if required. The purpose of the table is to collect the connection terminals for each test: signal/reference, response, grounded, floating, shorted; tap position and previous position.

TABLE IV
Format for Specifying Additional Measurements [2]

Measurement	Tap	Previous tap	Source and reference (V_{in})	Response (V_{out})	Terminals earthed	Terminals connected together	Comments
1							
2							
3							
-							
-							
-							

3 Shield Grounding

IEC is more specific than IEEE and defines more than one method. First method (preferred by IEC) is to use a grounding braid from top of bushing to flange of it and allows interpretation up to 2 MHz. Another method is identical to the first one except that the earth connection from the measurement leads to the flange at the base of the bushing may be made using a fixed length wire or braid, in this scenario connection is not the shortest possible. The position of the excess earth conductor length in relation to the bushing may affect amplitude (dB) measurements above 500 kHz and resonant frequencies above 1 MHz.

The Cigré recommendation is to use a grounding extension that is as short as possible, i.e. IEC preferred method, without coiling, and made with a flat braid of 20 mm minimum. It recommends not using wire for this purpose.

The requirement of the Chinese standard is to be firmly connected to an obvious grounding terminal and the cable to be as short as possible, avoiding coiling.

4 Instrument and Tests Verification

Prior to testing, Cigré recommends running integrity verification either with an object of a known response or by means of connecting the test leads together, which should give a 0 dB response.

Cigré also recommends to run a repeatability check, especially across bushings rated 400 kV and higher. This is due to repeatability issues at frequencies higher than 500 kHz and to determine the maximum usable frequency for results analysis. It consists of repeating a test after removing the test leads and reconnecting them. The maximum usable frequency is determined at the point where the two results start to deviate significantly. For bushings of lower voltages, the issues of repeatability are above 1 MHz.

IEC specifies three checks:

- Instrument performance: This is same as the integrity verification of Cigré.
- Repeatability: It recommends repeating the first test after completion of the measurements.

- Zero check: This is optional and its purpose is to determine the highest frequency usable for interpretation on each side of the transformer. It consists of making two measurements, first with all the test leads connected to one of the HV terminals and then to one of the LV terminals.

IV. IEEE FRA guide Failure Modes

Changes in the response of a FRA test can be due to a single failure mode or a combination of any number of them. Each failure mode produces characteristic changes in the response, which can be identified easily especially if a failure mode is more predominant over the other type of failures. The main plots used by IEEE guide in the failure mode analysis are the open and short circuit tests. The following is the summary of the characteristic changes of nine failure modes [3].

Radial Deformation			
	Frequency Range	Open Circuit	Short Circuit
<p>It is a radial (inward) compressive failure. The result is a buckling along the winding.</p> <p>Deformation can occur in two forms, free and forced, and forces are concentrated on the inner windings.</p>	20 Hz - 10 kHz	Generally unaffected	Slight attenuation
	5 kHz - 100 kHz	Minimal shifts or new resonances	
	50 kHz - 1 MHz	Obvious shifts or new resonances	
	> 1 MHz	Unaffected	

Axial Deformation			
	Frequency Range	Open Circuit	Short Circuit
<p>The winding will be stretched and its radius will be reduced.</p> <p>The response might show multiple resonances shifting in a broad frequency range.</p>	20 Hz - 10 kHz	Generally unaffected	Change in magnitude
	5 kHz - 100 kHz	Obvious shifts or new resonances	
	50 kHz - 1 MHz	Possible shifts or new resonances	
	> 1 MHz	Unpredictable	

Bulk Winding Deformation

Corresponds to the movement of coils due to high currents, shocks during transportation or natural disasters.	Frequency Range	Open Circuit	Short Circuit
	20 Hz - 10 kHz	Generally unaffected	Generally unaffected
	5 kHz - 100 kHz	Obvious new resonances Possible shifting	
	50 kHz - 1 MHz	Possible shifting at the higher frequencies	
	> 1 MHz	Possible shifting	

Core Defects

A physical change in the transformer core: shorted or burnt laminations, disconnected core ground or unintentional core grounds, and joint movements.	Frequency Range	Open Circuit	Short Circuit
	20 Hz - 10 kHz	Changes in the primary resonance. Discard magnetization effects.	Generally unaffected
	5 kHz - 100 kHz	Possible shifts or new resonances	
	50 kHz - 1 MHz	Possible shifting at the higher frequencies	
	> 1 MHz	Possible shifting	

Contact Resistance

More than a failure mode it is an indication of poor contact on the bushing to winding connection, LTC or DETC that can cause changes in low and high frequencies.	Frequency Range	Open Circuit	Short Circuit
	20 Hz - 10 kHz	Generally unaffected	Affected winding will show offset
	5 kHz - 100 kHz	Possible shifts or new resonances	
	50 kHz - 1 MHz	Possible shifts or new resonances	
	> 1 MHz	Possible shifts or new resonances	

Turn-to-turn short circuit

<p>Low or high impedance shorts between turns easily detected with a FRA test.</p> <p>The open circuit diagnose response will look like a short circuit test.</p>	Frequency Range	Open Circuit	Short Circuit
	20 Hz - 10 kHz	Response similar to a short circuit test	Obvious differences. Affected winding shows offset
	5 kHz - 100 kHz	Possible shifts or new resonances	
	50 kHz - 1 MHz	Possible shifts or new resonances	
	> 1 MHz	Possible shifts or new resonances	

Open Winding

<p>High impedance due to loose connections or burned through coils from thermal failure.</p> <p>Complete open circuits will show results close to the noise floor.</p>	Frequency Range	Open Circuit	Short Circuit
	20 Hz - 10 kHz	Changes in the primary resonance Discard magnetization effects	Obvious differences. Affected winding shows offset
	5 kHz - 100 kHz	Obvious new resonances. Possible shifting	
	50 kHz - 1 MHz	Possible shifts or new resonances	
	> 1 MHz	Possible shifts or new resonances	

Winding Looseness

<p>It is a spreading of the disk-to-disk or turn-to-turn axial distances caused by the loosening of a clamping structure.</p> <p>Commonly caused by transportation.</p>	Frequency Range	Open Circuit
	20 Hz - 500 kHz	Generally unaffected
	500 kHz – 2 MHz	Some detectable increasing differences
	1 MHz – 5 MHz	Largest increasing differences.

Floating Static Shield with Carbonization		
	Frequency Range	Open Circuit
Loose electric contact of the copper bonding braid on the aluminum shield strips	<100 kHz	Some differences
	100 kHz – 500 kHz	Possible large differences in magnitude of resonances
	1 MHz – 3 MHz	Largest differences in magnitude of resonances

V. Real Life Failure Mode Analysis

Case 1:

Four single-phase regulating autotransformers, 130/130/16.5 MVA, $230/\sqrt{3} / 161/\sqrt{3} / 69$ kV, in process of installation and commissioning experienced a major earthquake of very high intensity. It was decided to investigate the condition of transformers before putting them in service. The manufacturer of the autotransformers was consulted to provide their recommendation.

Fingerprints taken at the delivery of the autotransformers were compared to test performed after the earthquake and significant deviations were detected on three out of the four autotransformers. The deviations were noticeable on the short circuit test [H1-H0X0 with shorted X1-H0X0].

The figures 3, 4 and 5 show the FRA short circuit test results comparison before and after the earthquake for those three transformers

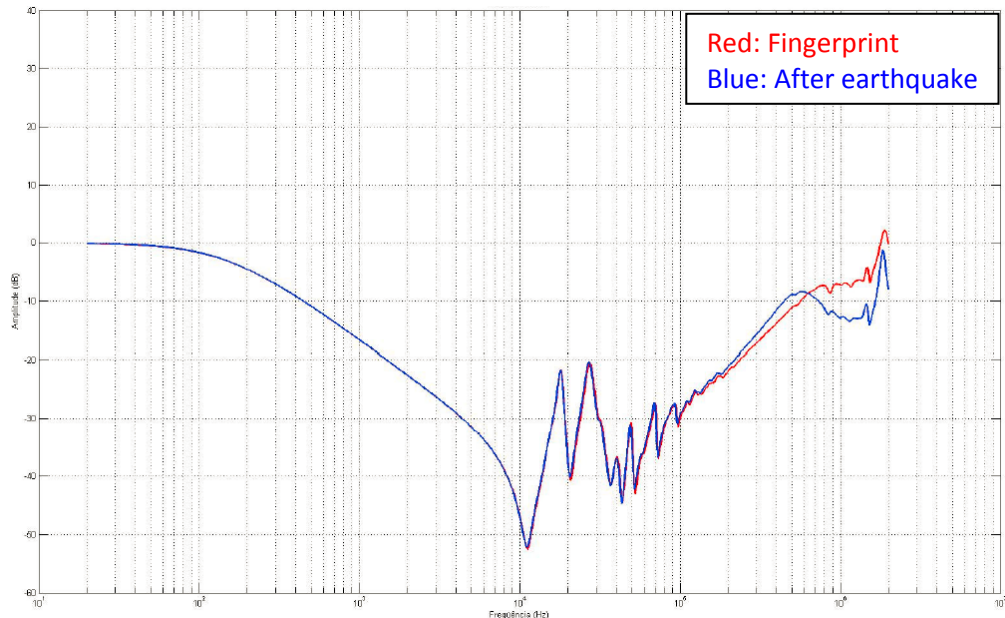


Figure 3: Autotransformer 1, comparison of short circuit responses before and after earthquake

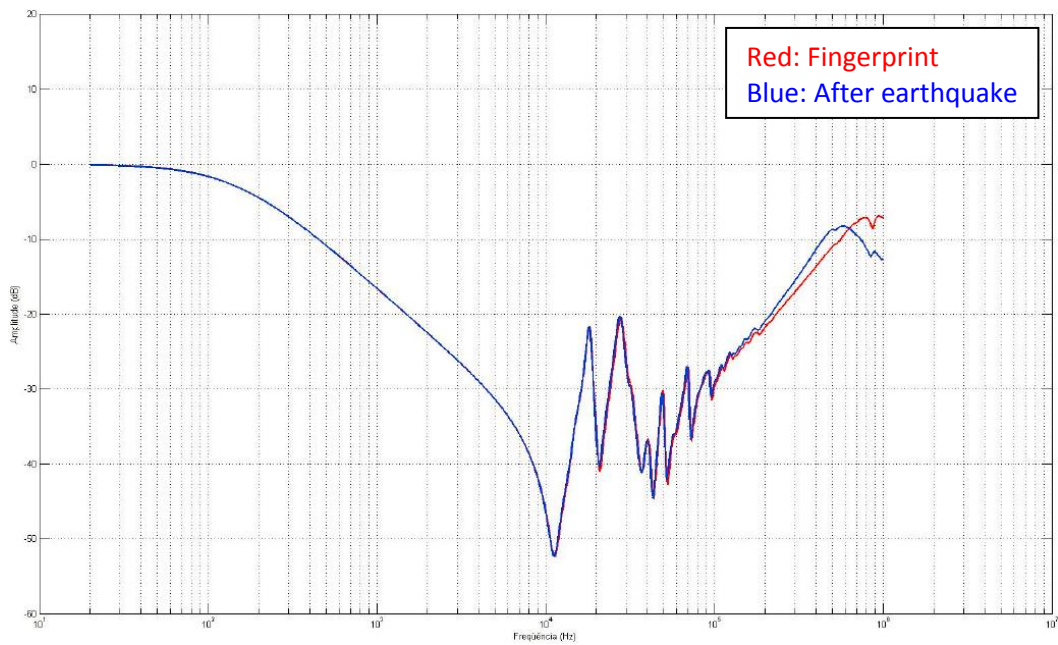


Figure 4: Autotransformer 2, comparison of short circuit responses before and after earthquake

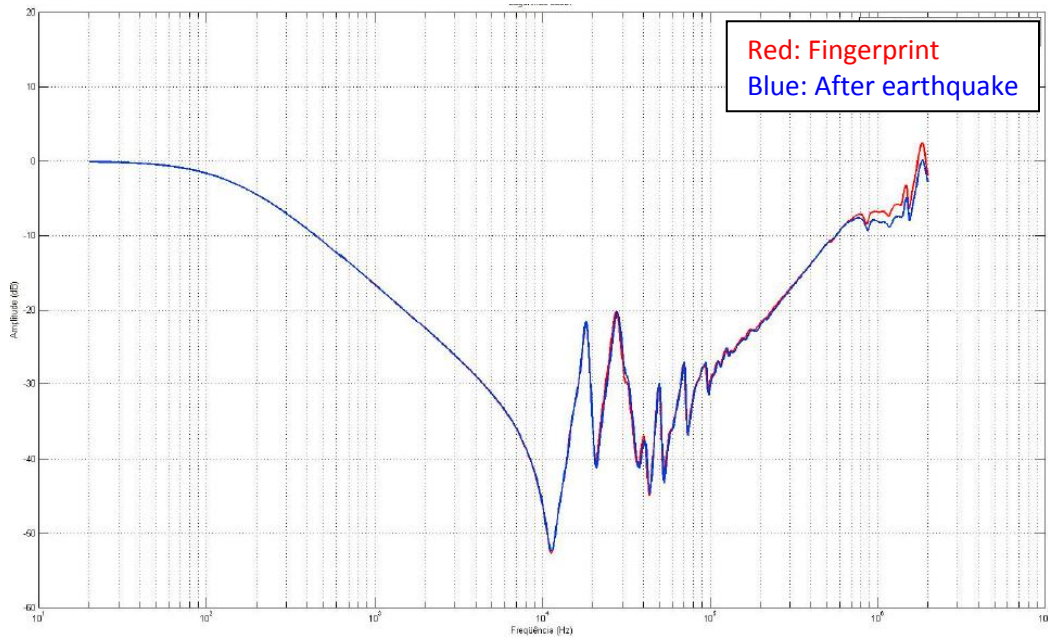


Figure 5: Autotransformer 3, comparison of short circuit responses before and after earthquake

On evaluating the above short circuit results, significant differences were observed in the following high frequency ranges:

Autotransformer 1: 150 KHz to 2 MHz

Autotransformer 2: 200 KHz to 1 MHz

Autotransformer 3: 700 KHz to 2 MHz

A common characteristic for each comparison is an increasing magnitude difference in the high frequencies area. This is a typical indicator of winding looseness as described in the failure modes sections of IEEE C57.149.

It was decided to inspect the transformers on site. Visual inspection was performed and it was found that the three autotransformers were longitudinally displaced. There was a bigger separation between the turns of the winding due to the loosening of the blocking structure.

The FRA diagnosis was able to detect the internal winding movement and issue was resolved at site by transformer manufacturer before the commissioning of the auto transformers.

Case 2:

A 40 MVA, 115/13.8 kV wye-wye transformer, showed an increase in Insulation Power Factor (PF) and LV side capacitance readings after maintenance was performed as a result of reported oil leaks. Under scheduled maintenance the following year, LV side capacitance showed a further increase in readings.

The transformer was again taken out of service to perform additional testing. An FRA test was performed as a part of advanced diagnosis. There were no baseline curves available for the transformer.

FRA open circuit tests were performed on both high and low side windings of the transformer. The following results were observed when all three LV windings were analyzed.

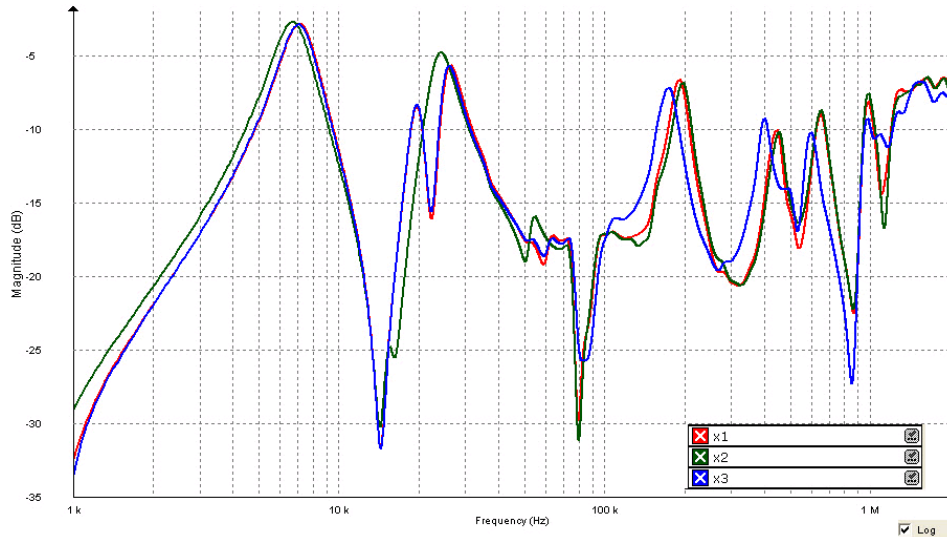


Figure 6a: FRA Open Circuit Test of LV windings for all phases

All three phases were compared to determine any mechanical changes within the transformer. As shown in Figure 6a above, the three LV windings showed a lot of asymmetry in the frequency range of 50 kHz- 1 MHz. Possible LV winding geometry change was suspected based upon the FRA curves. Results were further analyzed to compare A (X1-X0) and C (X3-X0) phases traces that should have similar resemblance.

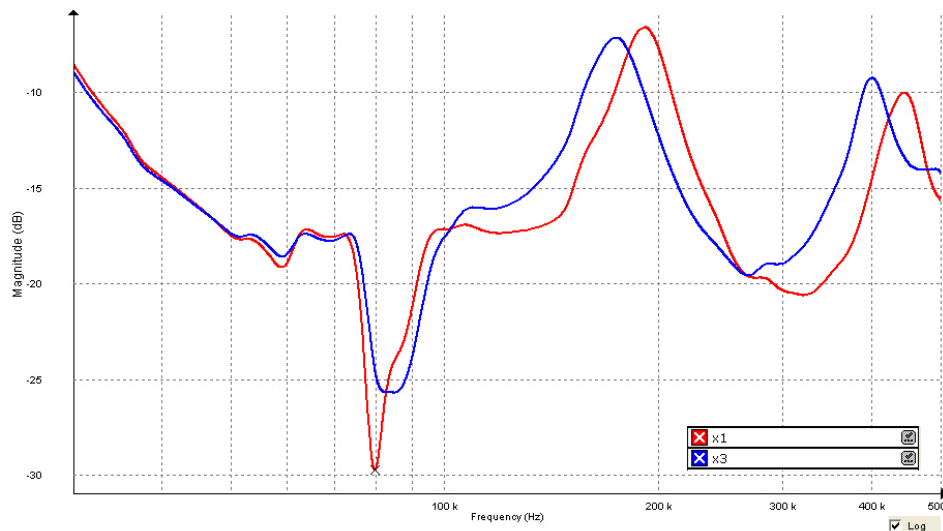


Figure 6b: FRA Open Circuit Test of LV windings for phases A & C comparison in 50 kHz to 500 kHz range

As shown in Figure 6b above, traces were compared in the frequency range of 50- 500 kHz that corresponds to the main winding section. Two traces showed extensive asymmetry; suspected geometry change was further strengthened. IEEE failure mode analysis for open circuit test in above frequency range suggested this being radial winding deformation (hoop buckling).

Transformer was placed under watch list. It was put back in service. In the same year, 2003, a few months later the transformer tripped out due to a fault. It was decided not to put this transformer back in service based upon a further increase in LV side capacitance (PF test) after the fault.

Transformer was sent for inspection and repair. Upon de-tanking and tear down, it was found that all three low side windings were severely deformed showing signs of radial buckling due to lack of strength to withstand through fault conditions.



Figure 7: All three LV windings showing radial deformation (hoop buckling) and close up on phase C

After diagnosing the problem, the transformer was rebuilt and put back in service at a different location. A new FRA fingerprint (as shown in Figure 8) was taken before putting it back in service for any future investigation and analysis.

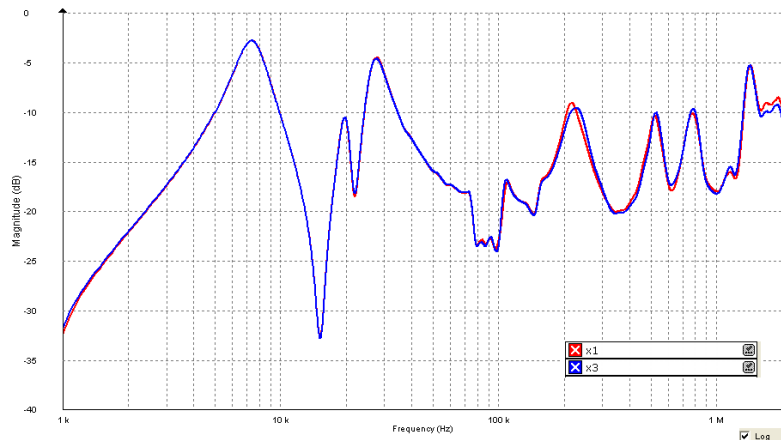


Figure 8: FRA Open Circuit Test of LV A and C phase windings after rebuild

FRA analysis helped in identifying a winding deformation problem and prevented a near future catastrophic failure of this transformer.

VI. Recommendations on Best Practices

- 1) The test equipment should always be checked for its performance and validity before initiating the FRA test on a specimen. This can be achieved by performing a self check using a standard test object with known FRA trace. For self check, test equipment should always be used with the supplied test leads on a standard test object. A standard test object is usually offered by the test equipment manufacturer. In the absence of that, as an alternative self check can be performed by shorting the test leads together, the user should expect a zero dB response.
- 2) Applied voltage can affect the FRA response in the lower frequency region up to 10 kHz. To obtain repeatable test results for comparison, it is recommended to use same test voltage applied in past for obtaining baseline results or when comparing traces between similar transformers. It is advisable to check the voltage used in previous tests before running a test or if the traces do not match below 10 KHz.

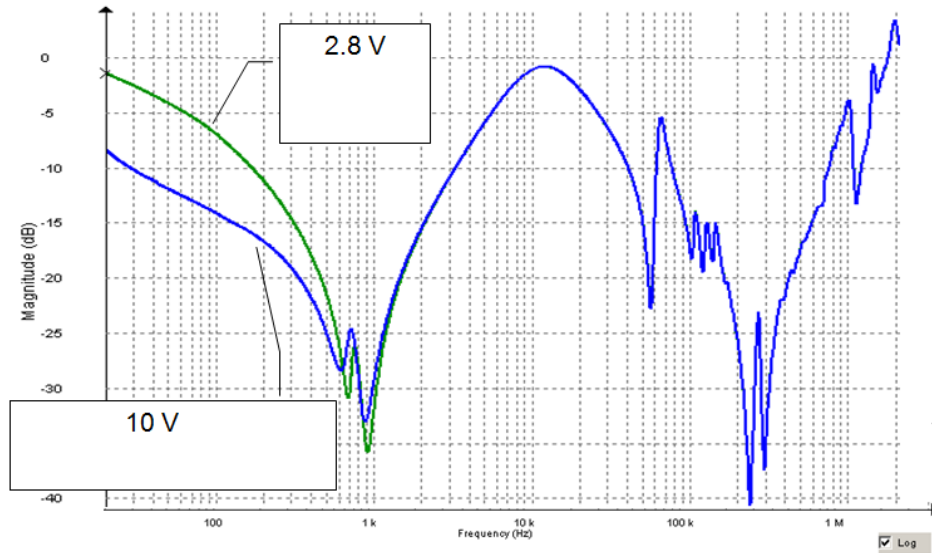


Figure 9: Comparison of tests performed at different voltages

- 3) Core's residual magnetism can affect the FRA response in lower frequency region up to 2 kHz. It is advisable to demagnetize the transformer before performing the FRA test. In the field, if resources are not available to demagnetize the transformer, it is recommended to perform FRA test before the dc winding resistance to minimize the effect of residual magnetism on FRA results.
- 4) Ground connection is the reference for both source and measuring leads. It is very important to apply the same grounding practices each time to obtain consistent and repeatable results. Inconsistent grounding practice can greatly affect the high frequency region of the FRA trace. One of the methods to accomplish this is to use "shortest possible ground" technique. The goal should be to provide the source and measuring leads the closest ground (reference) point with shortest length of ground braid. Figures 10a and 10b below shows the best grounding practices to be used in field.

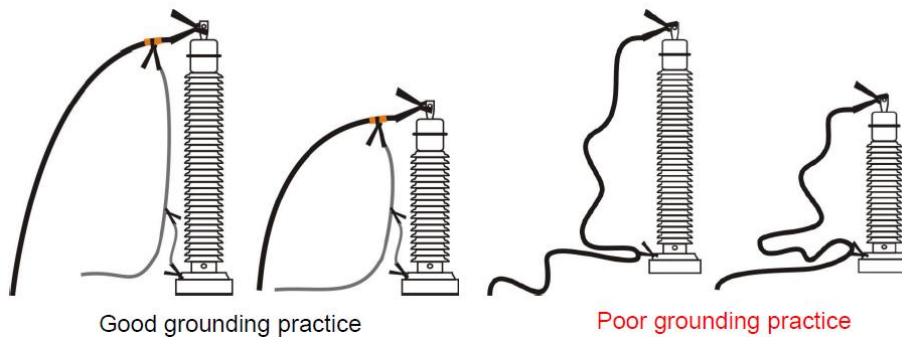


Figure 10a: Effective use of flat braid ground wire

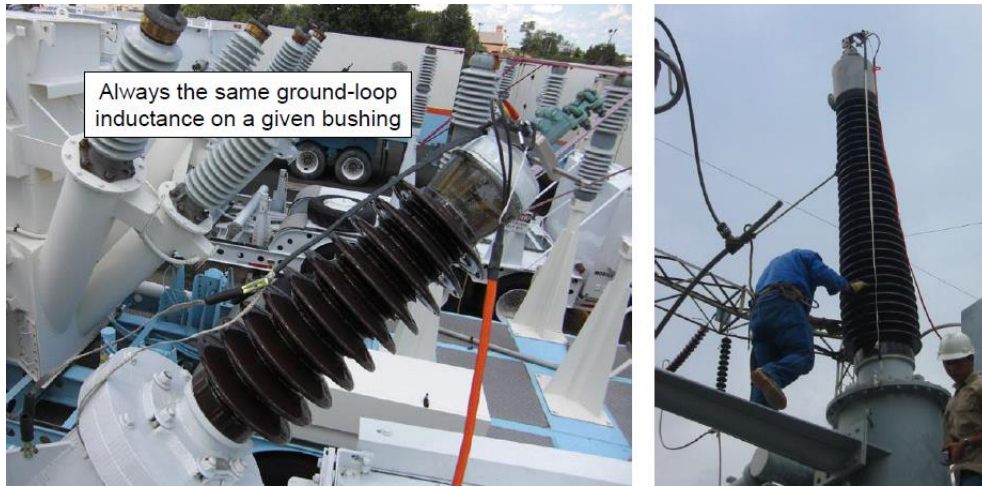











Figure 10b: Best grounding practices in field environment

5) Transformer configuration will vary from one specimen to the other. Placement of source and measuring leads need to be consistent and follow a set procedure. In the IEEE guide, it is recommended to connect from head (source) to tail (measuring) of the vector for any phase measurement. In almost all test software offered by test equipment manufacturers, on selecting the template for any particular transformer vector configuration, the labeling of individual test is marked from head to tail. In other words, first terminal represents where the source lead would go and follow up terminal represents connection for measuring lead. Figure 11 example below shows where to connect the leads for each test.

Source lead	Measured lead		
	H1	H3 [open]	<input checked="" type="checkbox"/>
	H2	H1 [open]	<input checked="" type="checkbox"/>
	H3	H2 [open]	<input checked="" type="checkbox"/>
	X1	X0 [open]	<input checked="" type="checkbox"/>
	X2	X0 [open]	<input checked="" type="checkbox"/>
	X3	X0 [open]	<input checked="" type="checkbox"/>
	H1	H3 [short X1-X2-X3]	<input checked="" type="checkbox"/>
	H2	H1 [short X1-X2-X3]	<input checked="" type="checkbox"/>
	H3	H2 [short X1-X2-X3]	<input checked="" type="checkbox"/>

3 phase, 2 winding
transformer test template

Figure 11: Test lead placement indication

- 6) De energized tap changer (DETC) on high side and on load tap changers (LTC) on low side are very common in North America and their position may affect the FRA trace. To obtain repeatable results, use the same tap position for each comparison test. It is recommended to use in service tap for DETC and extreme raise position for LTC. If nominal tap is to be used for LTC, it is recommended to note down the previous tap position before nominal.
- 7) FRA measurement on a transformer involves a number of tests to be performed and speeding up of test is recommended yet not sacrificing the repeatability and accuracy of the measurement. It is advisable to have less measurement points (50 per decade) in lower frequency region and as frequency increases, more measurement points per decade are added (200 per decade in highest frequencies). This would help in fast measurement time and yet getting the desired resolution and accuracy both in low and high frequency regions. Figure 12 below shows the different measurement points per decade based upon the frequency range. User can always increase or decrease the points per decade to get a balance between more resolution and test time duration.

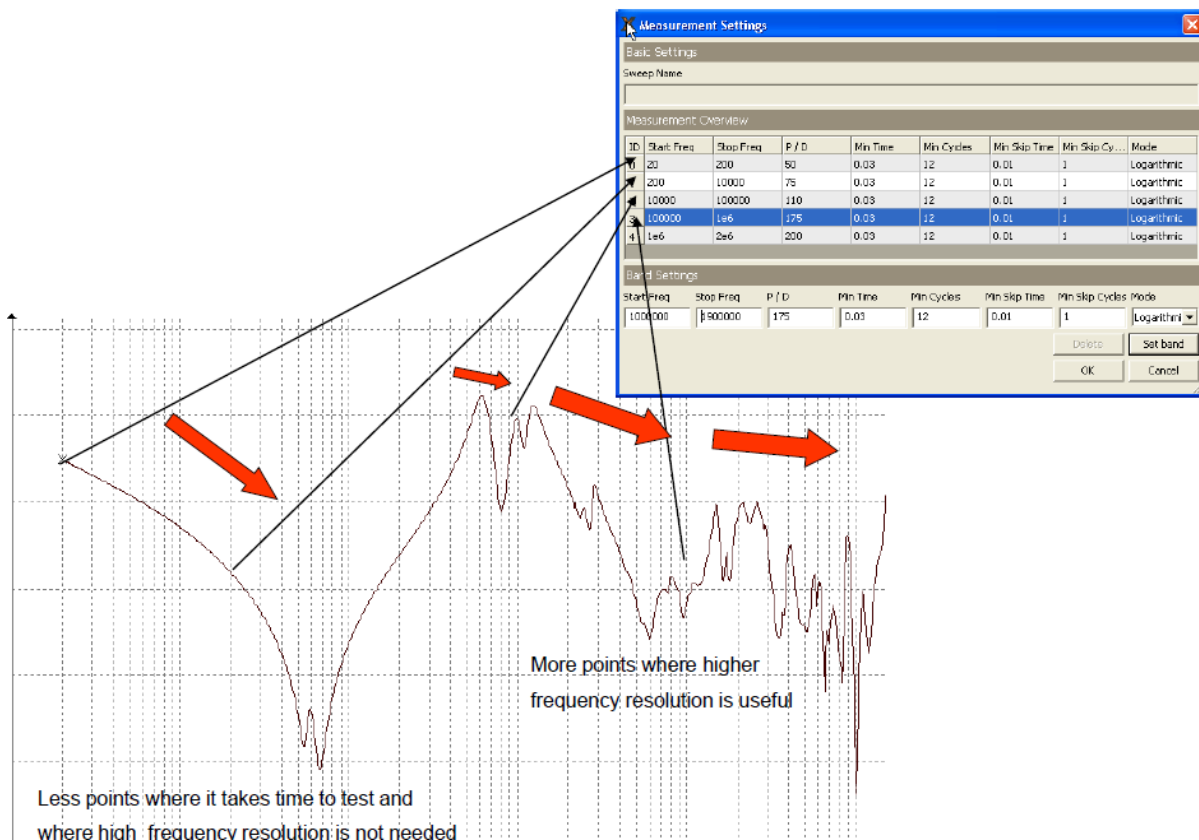


Figure 12: Measurement sampling settings for different frequency ranges

- 8) Connections to the transformer terminal are very important for repeatable measurements. It is recommended to connect directly to the bushing terminals. In the FRA tests where shorting leads are used it is advisable to use shortest possible shorting leads and they should be isolated from ground. Inconsistent connections can affect the response mostly in mid and high frequency range. Be sure to have tight connections on both, test and shorting leads.
- 9) It is advisable to document as much as information as possible like manufacturer and serial number of transformer, vector configuration, test instrument used, operator, tap position, pictures of transformer, testing, shorting and grounding leads and other relevant information. This would help in replicating the same conditions for future FRA measurements.
- 10) In addition to comparing the traces against baseline and similar transformers, difference plotting and inspecting for expected pattern of the trace based upon transformer configuration, voltage level and frequency range is recommended for addition analysis. This would include using correlation analyzers and correlation coefficients to investigate the dissimilarity between the traces and calculate how much the difference is between the two traces in different frequency bands. Using these mathematical models provides a quantification to support conclusions on the condition of the transformer after a fault and after repairs.

All of the above field recommendations would help in obtaining more consistent, repeatable and accurate FRA measurements that would aide in diagnosing any mechanical changes associated with transformer under investigation.

VII. FRA Case Studies

Case Study 1:

A 22 kV/4160 V delta wye transformer showed questionable readings on routine electrical tests. Winding resistance readings on low side B phase showed a difference of more than 17% as compared to A & C phase. Even though power factor and transformer turns ratio came out good, the excitation current showed very high values on B phase when compared against A and C phase excitation currents. Additionally, because of such high excitation current, it was only possible to perform the test at 5 kV to avoid test instrument tripping out.

FRA test was performed to do advanced diagnostics. No baseline results or similar transformer traces were available to compare the traces. The three phases were compared against each other to perform the diagnosis.

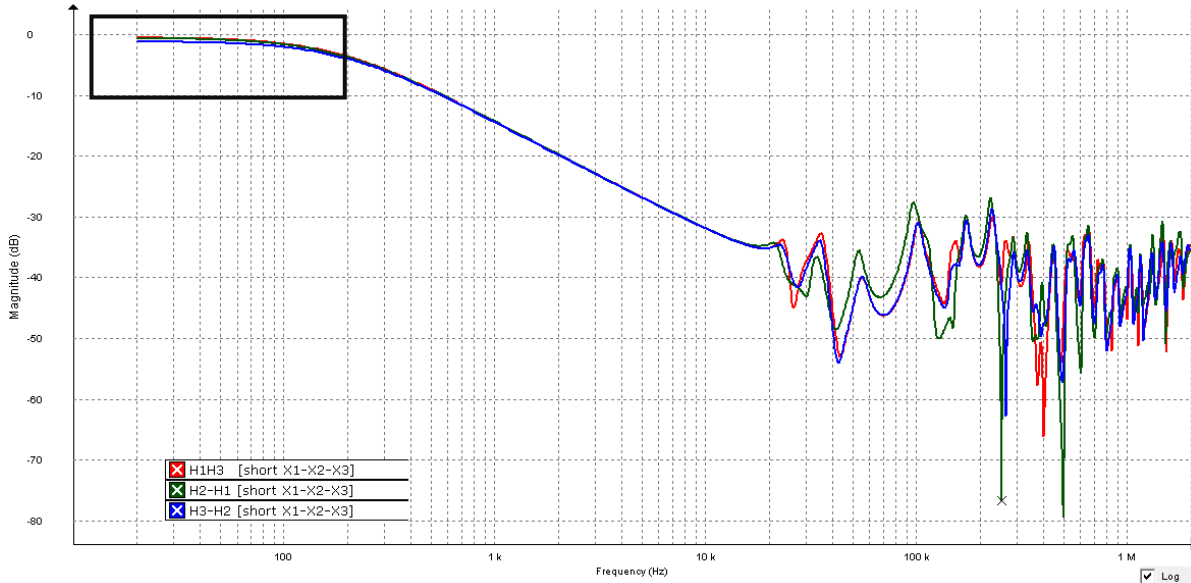


Figure 13: Comparison of the short circuit results of the three phases

When comparing FRA short circuit results with DC winding resistance tests, the IEEE guide mentions that if the short-circuit test produces a horizontal response at frequencies, less than 30 Hz, then the FRA results can be compared to the DC winding resistance results. Any differences between phases at these low frequencies should be checked with a DC winding resistance test.

When above FRA trace is zoomed in for frequency less than 100 Hz, a noticeable difference between the three phases can be observed as shown in figure 14. This analysis supports the questionable readings obtained in winding resistance test.

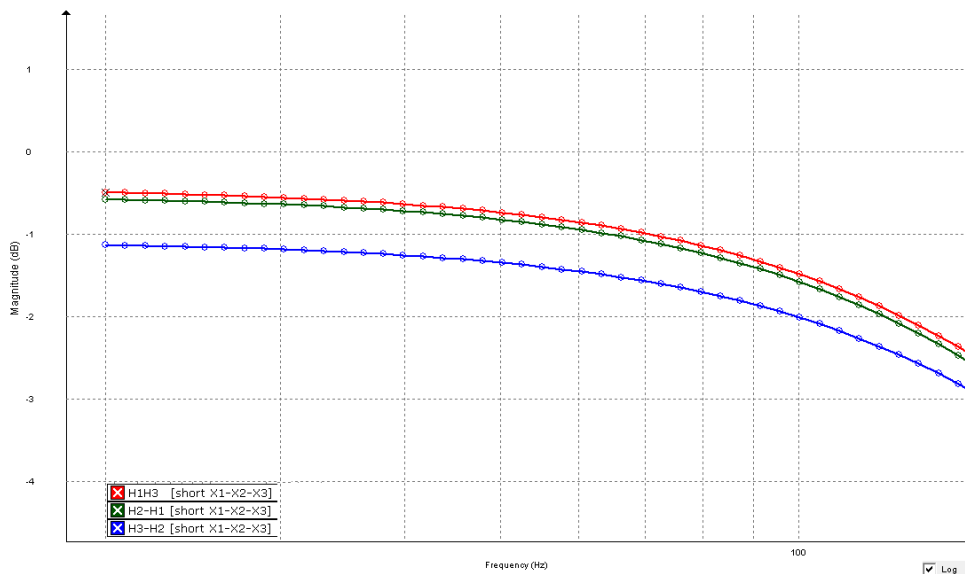


Figure 14: Detail of the short circuit results below 100 Hz

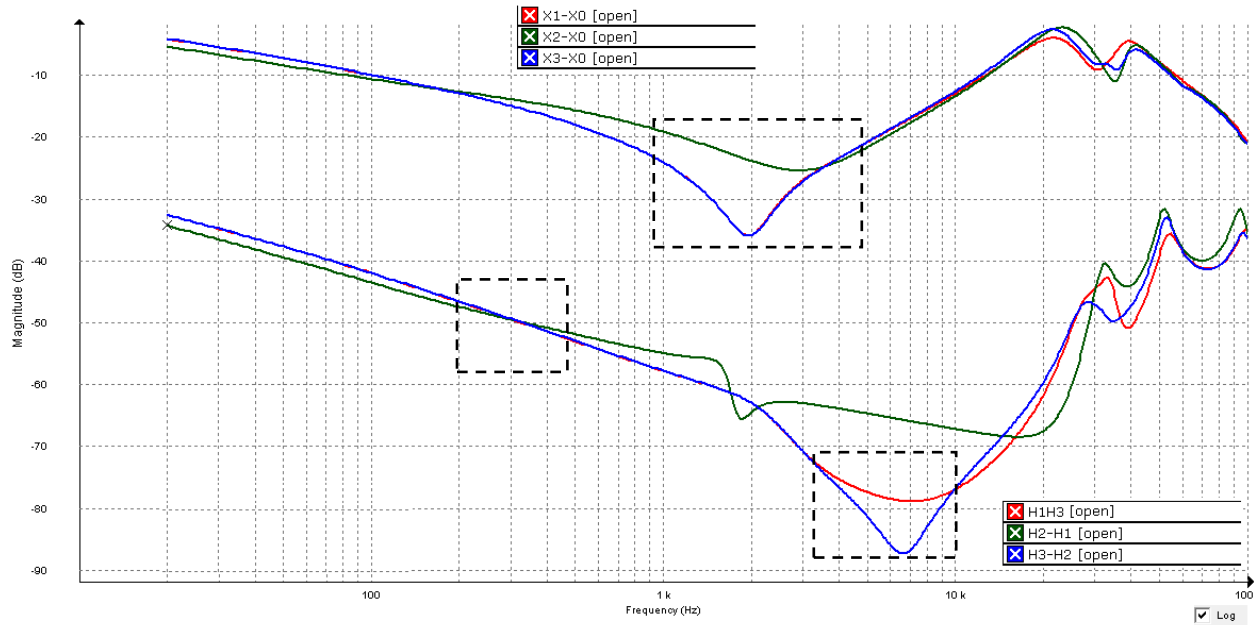


Figure 15: Open circuit results for HV and LV sides for all the three phases

When defining the typical trace characteristics of an end to end open circuit test, the IEEE guide explains that Delta connected windings will usually show two further resonances spaced apart in frequency range from 20Hz to 5 kHz. In the HV winding open circuit test results for A and C phases, the two resonances as described in guide were missing. When analyzing the minima (anti resonance) in low frequency region, A phase minima was attenuated, smoothing the sharpness of parallel LC resonance. This is usually the effect of resistance representing the conductor and dielectric losses.

Additionally, it was observed that B phase trace which usually have a distinct pattern and offset throughout the low frequency region up to 1 kHz showed a cross over point where it crossed A and C phase traces. This kind of response is unusual and typically not expected.

On analyzing the low side open circuit traces, the same cross over phenomena was observed for B phase. A and C phases matched very closely in low frequency region, however the B phase showed a great amount of resonance shift and attenuation.

Conclusion: Short circuit results confirmed the problem identified with the winding resistance test. In the absence of baseline measurements, when the three phases open circuit results were compared, a lot of anomalies were found that indicated problem related to core and windings. Similar conclusion was made with the excitation current measurements. FRA trace characteristics analysis helped in confirming the questionable readings obtained from other electrical tests. Transformer was in service for more than 50 years therefore it was decided to retire the transformer to avoid any possible future catastrophic failure.

Case Study 2:

A 66 MVA 115/34.5 kV Autotransformer without tertiary showed an increase in winding capacitance to ground of 7% in scheduled maintenance test. DGA analysis showed high levels of hydrogen gas. Additionally, there was significant increase and sharp jump in Ethane (C₂H₆) levels compared to DGA analysis of oil sample taken previous year.

On further investigation, it was informed that transformer saw a full short circuit fault because of B phase explosion of three phase station service transformer connected to the low side bus of the auto transformer.

A FRA test was performed on the auto transformer 1 as per the IEEE guidelines. In the absence of baseline measurements, the three phases were analyzed together. The comparison between the phases was inconclusive. It was decided to perform the FRA test on sister autotransformer 2 in the same substation. Both the auto transformers had similar nameplate information and serial numbers were consecutive.

The FRA results of the two auto transformers were compared to support the results obtain from capacitance & power factor and DGA tests.

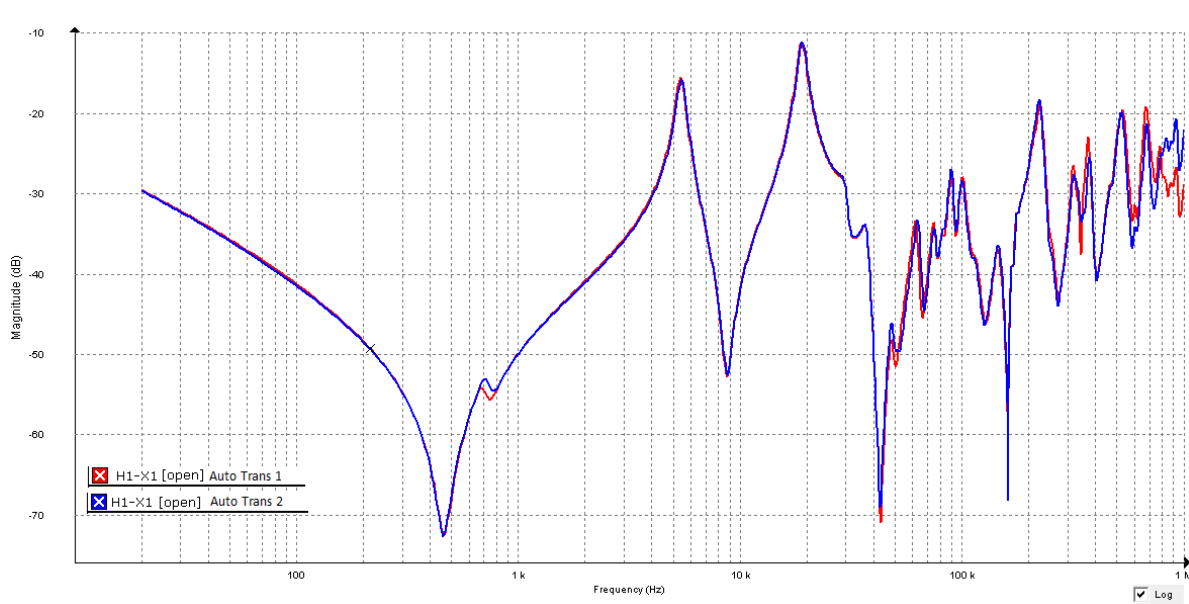


Figure 16: Comparison of phase A of autotransformers 1 and 2

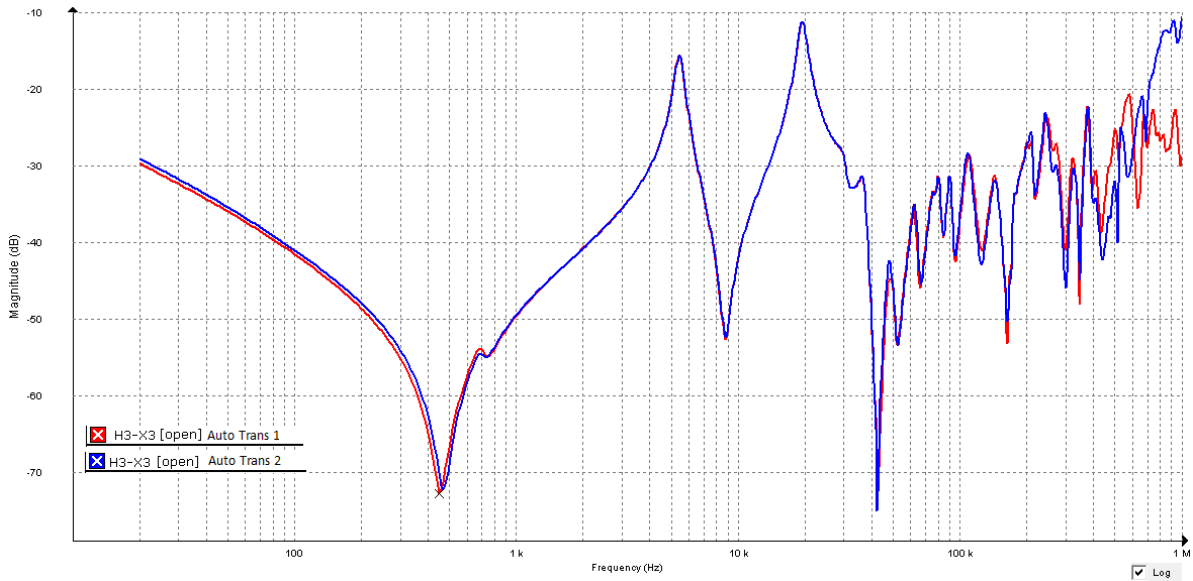


Figure 17: Comparison of phase C of autotransformers 1 and 2

Figures 16 and 17, FRA trace comparisons between respective phases of two auto transformers shows that A and C phases have a lot of symmetry with some curve mismatch in mid to high frequencies.

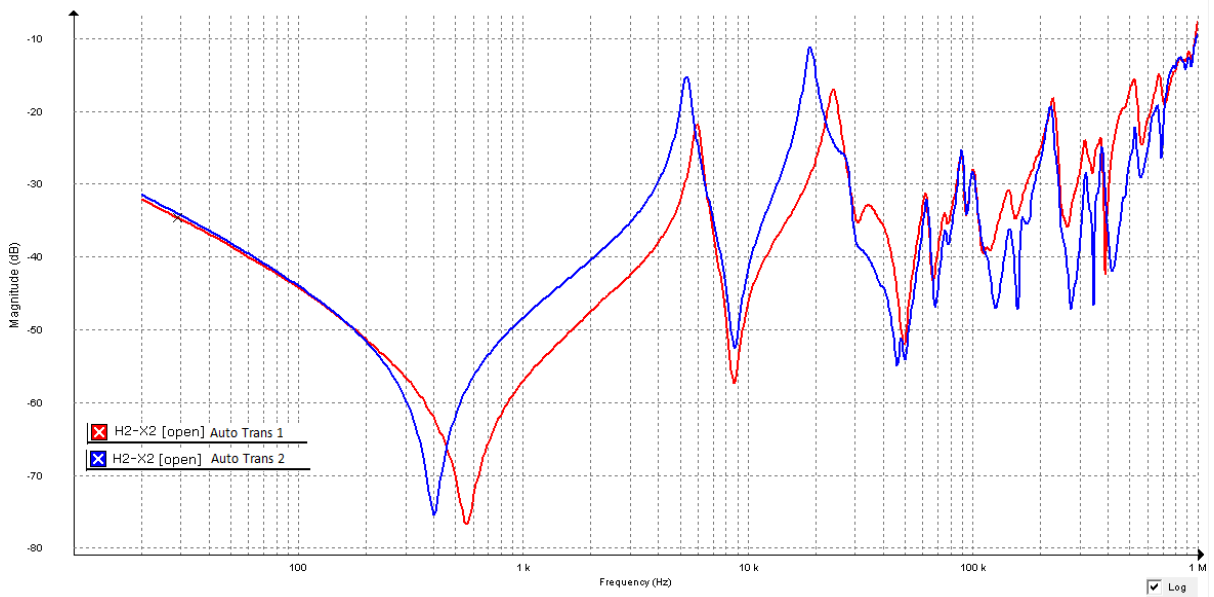


Figure 18: Comparison of phase B of autotransformers 1 and 2 showing mismatch throughout the frequency range

Phase B comparison shows shift in resonance, change in magnitude and loss of resonances in frequency range from 200 Hz to 600 kHz. On analyzing the above traces in different frequency bands, the following observations were made:

20 Hz - 10 kHz:

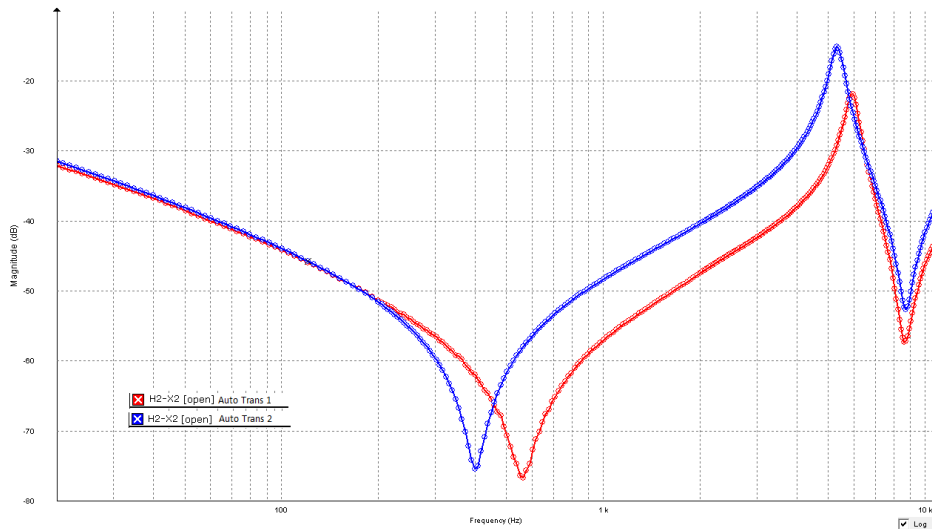


Figure 19: Comparison of autotransformers 1 and 2, low frequency area detail

Core magnetization can affect the results in this region. However, no shift and change in magnitude (in lower portion of this frequency range) was observed as shown in figure 19, which rules out a core magnetization problem. It is easy to see change in primary resonance between the two traces. This shift could indicate problems associated with core defects like shorted or burnt laminations, disconnected core ground or unintentional core grounds and joint dislocations.

5 kHz – 100 kHz

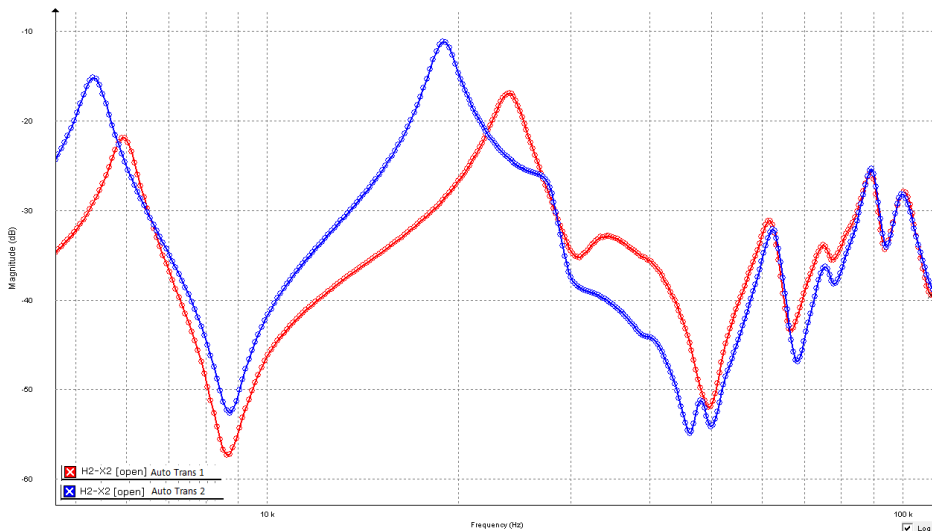


Figure 20: Comparison of Autotransformers 1 and 2, mid frequency area detail

As shown in figure 20, in this frequency band, we can observe multiple resonance shifts in broad frequency range. Additionally, some change in magnitude and loss of resonances were observed as well. Traces exhibiting these symptoms could indicate problems associated with winding movement and in particular axial deformation.

Based upon the FRA comparison of two auto transformers, it was determined that there has been some winding deterioration and movement in B phase of auto transformer 1. Other components of the transformer may have been affected as well. That strengthened the conclusion drawn by other electrical tests performed on the transformer. Based upon the analysis, this transformer has been put under watch list with oil samples taken every 3 months and scheduled maintenance testing reduced from eight years to one year. Decision on when to replace the transformer would be taken based upon DGA analysis and scheduled maintenance test results in coming time.

VIII. Conclusion

Transformers are a critical part of any power system. To maintain a reliable system, we need to identify which ones need attention and maintenance to extend the remaining healthy life of these transformers. Deciding upon correct maintenance in aged populations of transformers can save significant money due to postponed investment costs.

FRA method helps in identifying internal mechanical changes that can greatly affect the useful life of a transformer. Summary of IEEE FRA guide and recommendations from other standards provide the tools to perform the measurements correctly and interpret the FRA results to detect any defects in mechanical integrity associated with windings, core and other components of a transformer. FRA failure mode analysis assists in narrowing down the type of problem and related faulty section of the transformer. The case studies and its analysis based upon failure mode characteristics provide techniques and process to identify issues and utilize FRA measurements for advanced diagnosis.

IX. References

- [1] The Electric Power Industry Standard of People's of China, "Frequency Response Analysis on Winding Deformation of Power Transformers," Std. DL/T911-2004, ICS 27.100, F24, Document 15182-2005, June 2005.
- [2] IEC 60076-18 Ed.1: Power transformers – Part 18: Measurement of Frequency Response, July 2012. .
- [3] IEEE PC57.149-2012 Guide for the Application and Interpretation of Frequency Response Analysis for Oil Immersed Transformers.
- [4] CIGRE Technical Brochure No. 342: "Mechanical Condition Assessment of Transformer Windings using Frequency Response Analysis" (FRA), April 2008.
- [5] ABB report BRPT10-0887, Transelec Substation Lagunillas CL, June 29, 2010.



Dinesh Chhajer, PE received his M.S. degree from the University of Texas at Arlington in 2006. Currently, he is working as an applications engineer for Megger. At Megger, his responsibilities include providing engineering consultation and recommendations in relation to the testing of transformers, circuit breakers, batteries and other substation assets. Dinesh has previously worked as a substation maintenance engineer and substation design engineer with POWER Engineers, Inc. He is currently a licensed professional engineer (PE) in the state of Texas.



Volney Naranjo is an applications engineer for substation products at Megger for over 2 years. Prior to Megger, Volney worked for GERS USA – Consulting Engineers, for over 10 years in several positions, such as field engineer and project manager, gaining experience in the power engineering environment, including providing professional services for design and testing and commissioning power systems. He graduated from the University of Valle in Cali, Colombia with a Bachelor of Science in Electrical Engineering and is a member of IEEE.

345kV Transmission Line Thermal Upgrading Using Connector Shunts

Douglas P. Harms, P.E.

345kV Transmission Line Thermal Upgrading Using Connector Shunts

Douglas P. Harms, P.E.
Sr. Consulting Engineer
Transmission Engineering
CenterPoint Energy (Ret.)

Presented At The
46th Annual Transmission and Substation
Design and Operation Symposium (TSDOS)
September 11-13, 2013
Addison, Texas

Transmission Project Background

In early 2012 an existing independent electric power generator notified CenterPoint Energy that they would add generation to increase their output capacity from 1,021 MW to 1,236 MW by January, 2014. System load flow studies modeling the generation output increase revealed that the capacity of the two existing 345kV transmission lines interconnecting the generator would be overloaded.

The best long term system solution was determined to require rebuilding and reconductoring approximately twenty-six (26) miles of existing latticed steel tower structures with two-conductor bundled 795kcmil ACSR Drake conductors with new steel monopole structures and three-conductor bundled 959.6kcmil ACSS Suwannee conductors. The estimated time required to engineer the project, obtain certification, acquire property rights, procure materials and complete the rebuild construction was in excess of 24 months at an estimated cost of \$67 million! The time frame for this solution was not acceptable.

Line Upgrading Decision Points

The CenterPoint Energy Transmission Engineering, System Planning and System Operations groups began working to find if there were any possible short term acceptable alternatives to rebuilding the lines.

In 2002, CenterPoint Energy had LiDAR surveyed the 345kV transmission lines to evaluate if they could be thermally uprated. The requirement was to increase from a continuous operating temperature of 75°C with a 4hr emergency thermal limit of 90°C to operate continuously at 90°C with a 4hr emergency thermal limit of 120°C. It was determined that with some modifications to a few structures along the lines, appropriate line to ground clearances could be provided. The lines were subsequently thermally uprated to 90°C continuous / 120°C 4hr emergency.

In 2012; it was determined after additional review, that thermally uprating the line above 120°C was not possible without rebuilding the line because of numerous line to ground clearance limitations.

Higher Thermal Operating Option

The CenterPoint Energy System Planning and Operations groups ran studies and developed operating solutions whereby the lines could be rated at equivalent values of 120°C/120°C. They determined that load flows would rarely exist where the continuous operating temperature would reach 120°C and a remedial action plan could be implemented under contingencies to maintain a 4hr emergency thermal limit of 120°C.

The lines had been constructed in 1970 with the 795kcmil ACSR Drake conductor. Based on the projected line flows, conductor annealing calculations showed that there would be negligible reduction in the strength of the conductors. However, there was concern about the condition of the conductor connectors all along the lines. The connectors would be subjected to routinely higher normal load flows resulting in higher conductor/connector temperatures and there would be a higher probability of reaching 4hr 120°C loadings under contingencies.

Transmission Line Connector History

The connectors installed on the 345kV lines in 1970 were in compliance with the then applicable ANSI C119.4 Standard. However; at that time the standard test criteria for overhead bare connectors only

required Class A (Heavy duty) heat cycle testing because the Class AA (Extra Heavy duty) heat cycle testing was not added to the standard until the late 1980's. The following is a comparison of Class A and Class AA test criteria contained in the ANSI C119.4-2011 Standard (Ref. 1).

The C119.4 - 2011 Standard contains performance criteria and test methods for qualifying connectors used on standard conductors, i.e. AAC, AAAC, ACAR, ACSR and Copper.

- The following is **Table 1 from the ANSI C119.4 – 2011 Standard** which lists the combinations of connector class and heat cycle durations covered in the test protocol:

<i>Connector Current Class</i>	<i>Number of Test Cycles for:</i>	
	<i>CCT Method</i>	<i>CCST Method</i>
<i>Class AA (Extra Heavy duty)</i>	<i>500</i>	<i>Not Applicable</i>
<i>Class A (Heavy duty)</i>	<i>500</i>	<i>100</i>
<i>Class B (Medium duty)</i>	<i>250</i>	<i>75</i>
<i>Class C (Light duty)</i>	<i>125</i>	<i>50</i>

- The following section of from the ANSI C119.4-2011 Standard and specifies the Current Cycle Temperature Conditions for the Connector Current Class:

6.8.1 CCT Current and Temperature Conditions

The current cycle test current shall be adjusted during the current-ON period of the first twenty-five (25) cycles to result in a stable maximum temperature rise in the control conductor of 100^oC (212^oF) to 105^oC (221^oF) above ambient temperature for Classes A, B, and C. For Class AA, the temperature rise of the control conductor shall be 175^oC (347^oF) to 180^oC (356^oF) above the ambient temperature. This current shall then be used during the remainder of the test current-ON periods, regardless of the temperature of the control conductor.

The above temperatures are Connector Performance Test Temperatures and are NOT meant to indicate any line operating temperatures. Class AA was developed for installing connectors on aged conductors. The test protocol is designed for a maximum line operating temperature of 93^oC.

Testing Connector Performance Above 93^oC

CenterPoint Energy and other utilities wanted to determine what the effects are if conductors and connectors are operated above the 93^oC operating temperature limit specified in ANSI C119.4. Testing was performed by the Electric Power Research Institute (EPRI) (Ref. 2) to evaluate the high-temperature operation of various types of tension connectors on traditional conductors. The first tests were to determine if the connectors could be operated continuously up to 150^oC while under tension to simulate actual line operating conditions.

A variety of tension connectors classified as ANSI C119.4 Class AA were installed in accordance with the manufacturer's specifications on new 795kcmil ACSR Drake conductor to be tested. Figure 3-1 (Ref. 2) below shows the conductor test temperature/current cycle profile used to heat the conductor to a surface temperature of 150^oC for 1,500 cycles. The conductor/connector segments were installed on a test frame and tensioned to 25% rated breaking strength (RBS) of the Drake conductor. The conductors and connectors were monitored with numerous thermocouples to measure the temperature of the surface of the conductors, temperature at the internal steel core wire, and temperature of the connectors at various locations. The test setup is shown below in Figure 3-3 (Ref. 2).

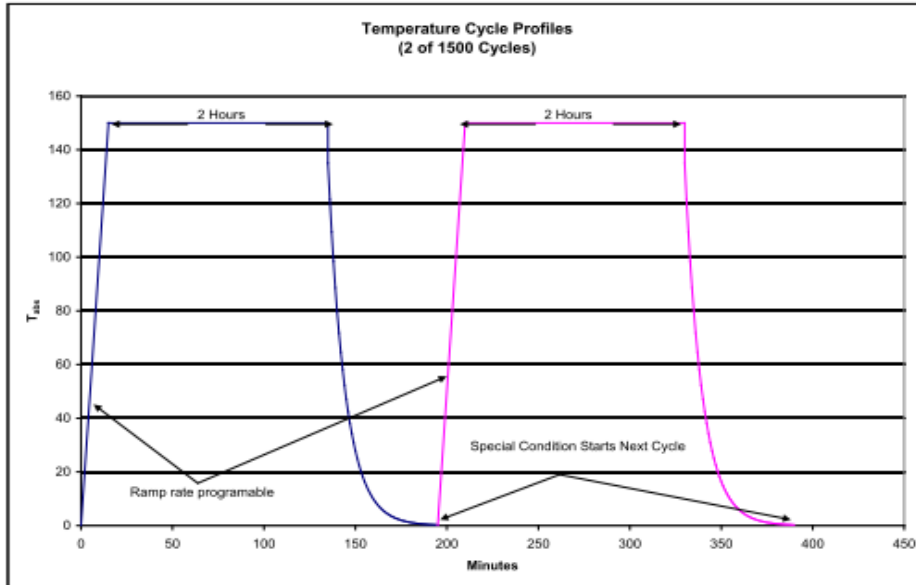


Figure 3-1
Thermal Cycle Design



Figure 3-3
Haslet High-Temperature Connector Test Frame

Connector Test Results

ANSI C119.4 specifies that a properly operating connector maintains a temperature lower than the temperature of the conductor surface to which it is attached. A total of forty (40) connectors were monitored in the test assembly: twenty-four (24) in-line tension connectors and sixteen (16) line deadend connectors. A total of twenty (20), or 50% of the connectors tested went into thermal runaway (connector temperature exceeded the conductor temperature) reaching temperatures ranging to over 400°C. This showed that even new connectors installed on new conductors could not be operated up to conductor temperatures of 150°C on a continuous basis.

A second set of tests were performed to determine if there might be a possibility for the connectors if the line conductors were only operated continuously at a lower temperature. The same test protocol was repeated with the temperature cycle profile set to a maximum of 125°C.

A total of thirty-two (32) connectors were monitored in the test assembly: sixteen (16) in-line tension connectors and sixteen (16) line deadend connectors. A total of seventeen (17), or 53% of the connectors tested went into thermal runaway (connector temperature exceeded the conductor temperature) reaching temperatures ranging to over 350°C. This showed that even new connectors installed on new conductors could not be operated up to conductor temperatures of 125°C on a continuous basis.

Improving the 93°C Connector Performance Limits

The connector testing showed that the 93°C operating temperature limit stated in the C119.4 Standard means what it says. The facts are that the ANSI C119.4 Standard thermal heat cycle test protocol was developed with the expectation that line connectors would be operated continuously at a maximum temperature of 75°C with a maximum emergency operating temperature of 93°C. Utilities have been pushing transmission line loadings higher and higher without fully understanding the limits of the line connectors.

What do we do with the line connectors now? What is the condition of newer connectors even if they have been operated at temperatures below 93°C? What is the condition of older connectors that have been in service for a long time not knowing their thermal history? How do we determine the condition of connectors in service? What do we do when we find bad connectors? There were many questions to be answered.

Infrared (IR) thermal imaging of connectors has been used to show when a connector is operating hotter than the line conductor. This condition typically exists only if the line is very heavily loaded and the connector is already in thermal runaway failure mode. At this point the failed connector must be replaced.

A connector's internal conductor/connector interface resistance can be measured with an instrument such as the SensorLink® Radio Ohmstik Micro Ohmmeter (Ref. 4). The resistance measurement must be taken with the ohmstik when the circuit is energized. The measured conductor/connector resistance is then compared with the resistance of an equivalent length of conductor. A conductor/connector interface resistance less than the conductor resistance indicates a healthy connector. A conductor/connector interface resistance greater than the conductor resistance indicates a problematic connector. The higher the differential ratio of the resistances; (connector resistance/conductor resistance), the higher the deterioration of the conductor/connector interface. The higher the resistance ratio, the greater the danger is that the electrically failed connector in thermal runaway condition will fail mechanically.

The most important fact about any conductor connector installed on a bare conductor on a transmission line is that the connection will never be any better than the moment at which it is installed. Once it is put in service and current flows through it, it begins to deteriorate. There are many factors which contribute to the deterioration of the conductor/connector interface: cleanliness of the conductor surface, cleanliness of the connector surface, amount and type of connector corrosion inhibiting compound present at the interface, moisture in the connection interface area, condition of the compression dies, compression tool and the compressive force applied when the connector was installed. Unfortunately, the only perfect connection is a thermal fusion weld between the conductor and connector. Even connectors installed with external explosive compression techniques do not approach thermal fusion welding of the materials. EPRI and Oak Ridge National Laboratories (ORNL) are working in partnership on research to try to develop practical “doping materials” that can be applied to the interface of the connector and to develop improved compression connectors that maintain higher connector compression forces over a wider range of operating temperatures. This will be great in the future, but we must deal with existing connectors operating on our transmission lines.

In response to utility company concerns about connectors and increasing incidents of catastrophic connector failures, manufacturers have developed devices called “connector shunts”. These shunting devices are designed such that the connector is left in place and the shunt device is installed to bridge across and divert the current flowing through the connector to flow through the shunt device and to provide mechanical strength to reinforce the mechanical strength of the connector. Since these devices are relatively new, what is the long term high temperature performance of these devices?

Testing Connector Shunts

CenterPoint Energy and other utilities wanted to prove out through testing the high temperature line performance of various connector shunt devices. Testing was performed by the Electric Power Research Institute (EPRI) (Ref. 3) to evaluate the high-temperature operation of various types connector shunts installed across various types of connectors installed on traditional conductors. The EPRI project was developed to evaluate the shunt devices installed across the population of various connectors that had been tested in the high operating temperature connector test (Ref. 2) and to test their stand-alone performance with no connector present. The test setup is shown below in Figure 3-1 (Ref. 3).

A variety of tension connectors classified as ANSI C119.4 Class AA were installed in accordance with the manufacturer’s specifications on new 795kcmil ACSR Drake conductor to be tested. The conductor/connector segments were installed on a test frame and tensioned to 25% rated breaking strength (RBS) of the Drake conductor.

A total of six (6) test lines were installed in the test rack but only five (5) test lines were used to evaluate connector/connector shunts high-temperature performance. One (1) of the lines was used to monitor conductor temperature and balance the test setup power supply currents. The five (5) test lines consisted of a total of ten (10) standard deadend connectors and seven (7) standard tension connectors. At the beginning of the testing, connector shunts were installed across eight (8) deadend connectors and six (6) tension connectors. Four (4) shunt devices were installed independently and were carrying all of the line current and only connecting conductor ends with no standard compression connector installed. Two (2) deadend connectors and one (1) tension connector were not shunted for performance comparison.

The conductors, connectors and connector shunts were monitored with numerous thermocouples to measure the temperature of the surface of the conductors, temperature at the internal steel core wire, and temperature of the connectors and connector shunts at various locations. Figure 3-2 (Ref. 3) below shows the conductor test temperature/current cycle profile used to heat the conductor to a surface temperature of

180°C for 1,500 cycles. This was designed to emulate as nearly as possible a long term high temperature duration field condition tension performance test with temperatures nearly emulating ANSI C119.4 Class AA performance test temperatures.



Figure 3-1
Test Conductors

Figure 3-2 shows three thermal cycles completed as measured on Line 1.

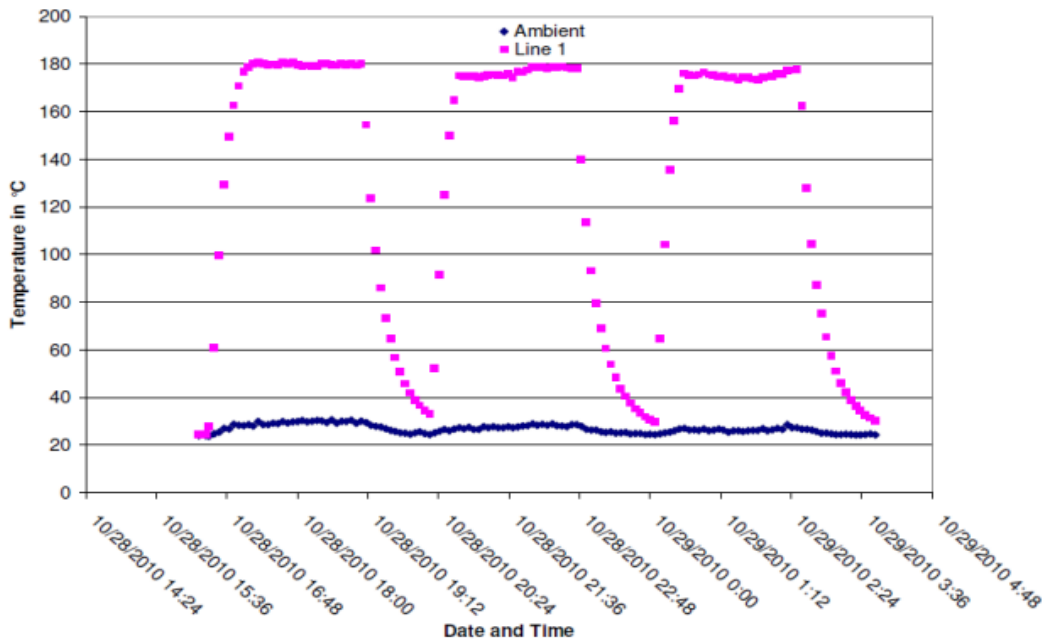


Figure 3-2
Thermal Cycle Temperature Response

Connector Shunt Test Results

The commercially available shunt devices tested were the ClampStar® shunt manufactured by Classic Connectors and the Preformed® shunt manufactured by Preformed Line Products. The gauge of effectiveness for the shunts thermally protecting the underlying compression connectors was comparison of the surface temperature of the conductor internal to the shunt device relative to the temperature of the shunt device relative to the test line conductor temperature. Early on in the testing, both the deadend connectors and the tension connector which had been left unshunted went into thermal runaway and shunts had to be install across all of these connectors.

On average throughout the 1,500 cycles of testing with current flows sufficient to create a test line surface temperature of 180°C, the temperature of the conductor internal to the shunts ranged from 50°C to 60°C while the temperature of the shunt devices ranged from 80°C to 100°C. For the connectors which were initially left unshunted, went into thermal runaway and had to be shunted during the test, similar temperatures were measured. Shunts installed without any connector and therefore; carrying the full test current, reached temperatures ranging from 100°C to 110°C.

Both manufacturers rate the mechanical strength of their devices to be greater than 60% of the rated breaking strength (RBS) of the line conductor. After the thermal cycling testing, mechanical tension tests were performed on the devices. The devices which had been installed over connectors were tension tested in this combination assembly. All tension tests resulted in the total assembly strengths being in excess of 95% of the RBS of the line conductor. Tension tests of the shunt devices which had been thermal cycled without any connector resulted in the devices having strengths greater than 60% of the RBS of the line conductor.

The results of these tests showed that these connector shunt devices provided thermal and mechanical protection for the underlying connectors.

CenterPoint Energy's Decision for Uprating the 345kV Transmission Lines

In early summer 2012 a decision had to be made regarding the line upgrade. Planned construction on other 345kV lines in the CenterPoint Energy transmission system required that any work done on these generation increase interconnection circuits had to be completed by May 2013. This did not allow any time to obtain any data to try and make a condition assessment of the connectors. From a line flyover and historical inspection photographs of the lines, it was determined that there were a total of 88 tension connectors and 168 jumper connectors. As mentioned previously in this report, a thermal upgrade was done approximately ten (10) years ago requiring installation of new connectors and therefore some of the connector population was not very old. However, with the results of the connector and connector shunt testing projects, there was concern about pushing the line loading higher on the forty-two (42) year old line connectors and there was uncertainty about the newer connectors. It was decided to install connector shunts on 100% of the connectors on the lines. The estimated cost to install shunts on all connectors was approximately 2% of the estimated line rebuild cost. To gain experience with both types of connector shunts which had been tested and because of particular line conductor configurations, Preformed® shunts were chosen to be installed on the tension connectors and ClampStar® shunts were chosen be installed on the jumper connectors.

There was an opportunity to obtain an assessment of the condition of the line connectors before the shunt devices were installed. A resistance measurement of each connector would be made with a SensorLink® Radio Ohmstik Micro Ohmmeter (Ref. 4) prior to installing the connector shunt.

Because of various land and water obstructions along the length of the transmission circuits, installation of the connector shunts had to be installed at various locations using both ground and air techniques and in various combinations of the line dead and energized. Both types of shunt devices can be installed by ground or air and on the line either energized or de-energized. The following photos show examples of installing the connector shunts.

Installing a Preformed® Connector Shunt:



Installing a ClampStar® Connector Shunt:



Results of Ohmstik Connector Resistance Measurements

Measurements with the SensorLink® Radio Ohmstik Micro Ohmmeter (Ref. 4) were taken at various times and by various means over a period of approximately four (4) weeks. All measurements had to be made with the lines energized. Measurements were taken from a helicopter using a side mounted platform and from a lineman suspended from a long-line under the helicopter; from the structures using ladders and from an insulated bucket truck.

CenterPoint Energy construction personnel developed an identification methodology to catalog each connector resistance reading. Each connector was first identified as a tension or jumper connector. The location of the connector was cataloged by recording its physical location on the line relative to adjacent structures by recording the adjacent structure's unique identification number. The conductor position of the connector was then cataloged as to its phase position and then its position on a particular conductor in the two (2) bundle configuration. The final identification of the resistance reading was then to catalog on which side of the connector the reading was taken by its location relative to the adjacent structure's unique identification number.

Example:

Code Recorded: 2876 – **S T I W** – 2877 = 21 $\mu\Omega$

Meaning: **S**pan between Str. 2876 and 2877 – **T**op phase – **I**nside conductor – **W**ire Resistance = 21 $\mu\Omega$

Code Recorded: 2876 – **S T I H** – 2877 26

Meaning: **S**pan between Str. 2876 and 2877 – **T**op phase – **I**nside conductor – **H**igh Tower Number Side of Connector (2877) = 26 $\mu\Omega$

Resistance Ratio = 26 $\mu\Omega$ / 21 $\mu\Omega$ = 1.24

The ratio of the conductor/connector interface resistance divided by the equivalent conductor length resistance gives an indication of the health of the connection. SensorLink® (Ref. 4) recommends the following:

A ratio from 0.3 to 1.0 : Normal connection – No action needed

A ratio from 1.0 to 1.2 : Poor condition – Re-inspect in 1yr or after next fault

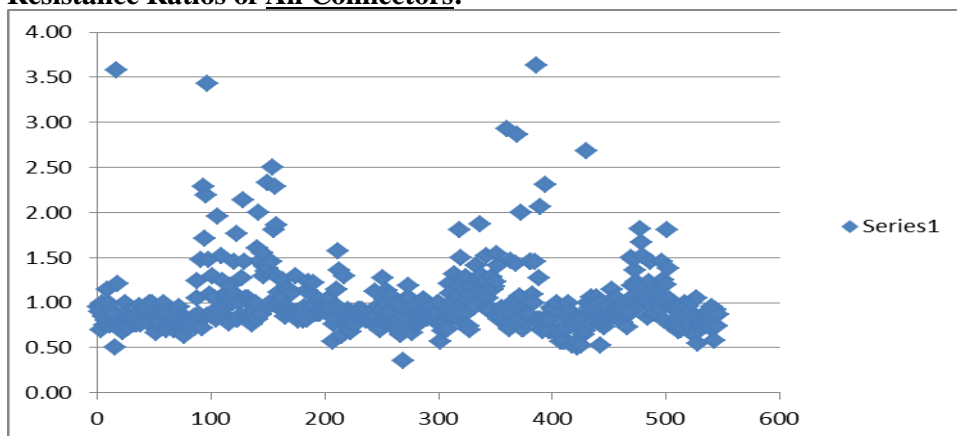
A ratio from 1.2 to 1.5: Poor condition – Re-inspect after next fault

A ratio from 1.5 to 2.0: Poor condition – Schedule replacement in three months

A ratio from 2.0 to 3.0: Bad condition – Schedule replacement as soon as possible

A ratio greater than 3.0: Failing – Replace as soon as possible

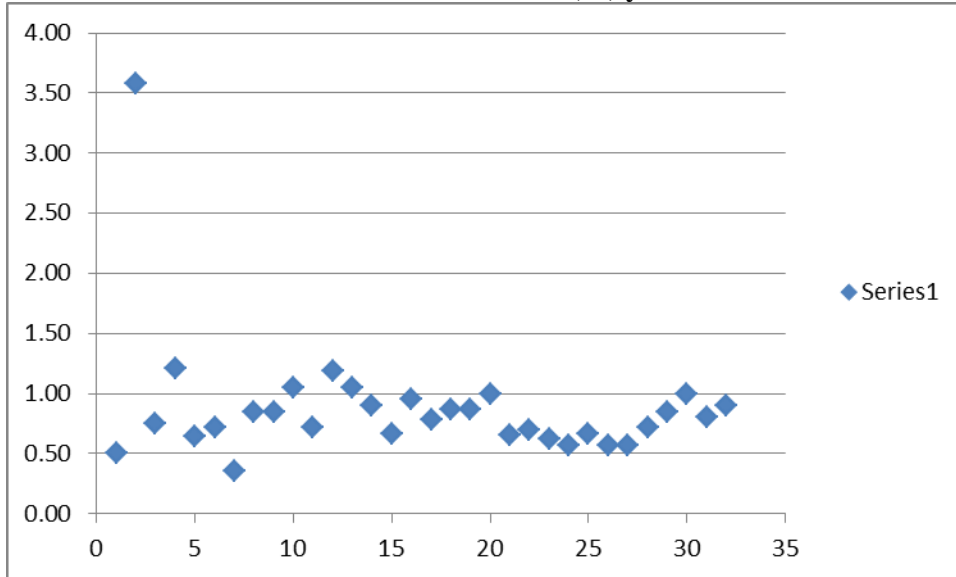
Resistance Ratios of All Connectors:



The the two graphs below show a breakdown of the resistance ratios of the tension connectors by age.

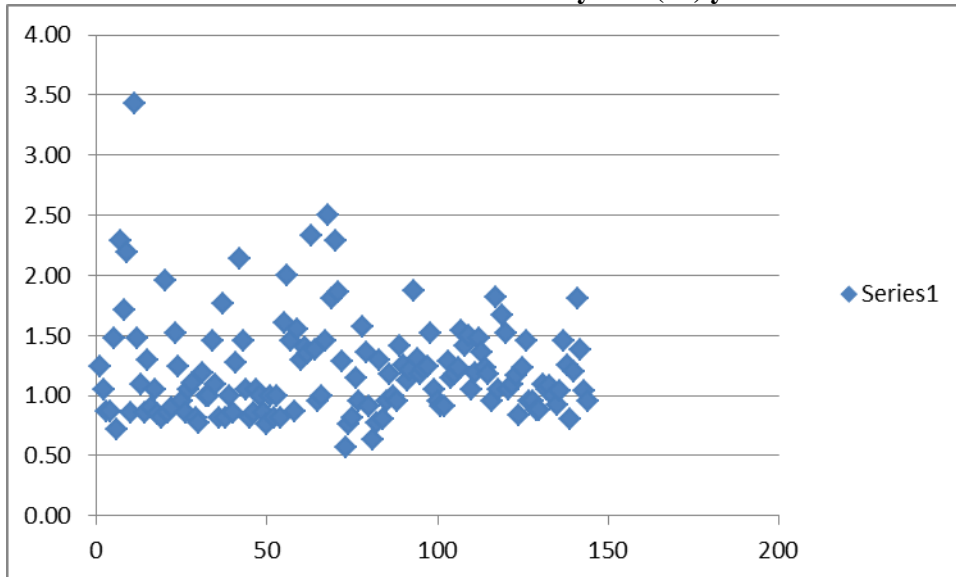
There were only a few connectors in the ten (10) year old category with a resistance ratio above 1.0; however, there was one connector above 3.5 indicating a failing condition.

Resistance Ratios of Tension connectors Ten (10) years old:



There were quite a few of the original tension connectors with a resistance ratio of 1.5 – 3.0 indicating that they are due for replacement. Obviously, there was one connector in the critical range of 3.5.

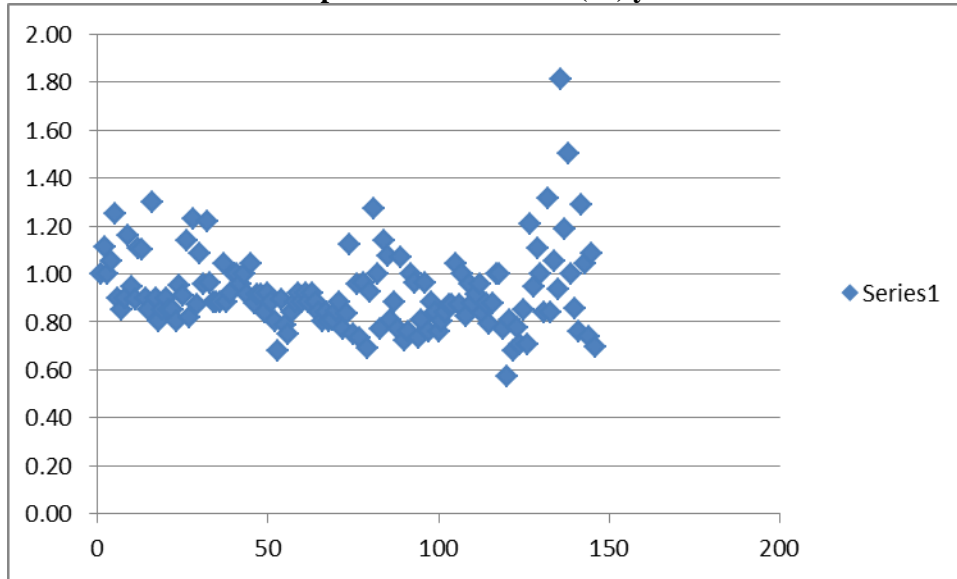
Resistance Ratios of Tension Connectors Forty-two (42) years old:



The two graphs below show a breakdown of the resistance ratios of the jumper connectors by age.

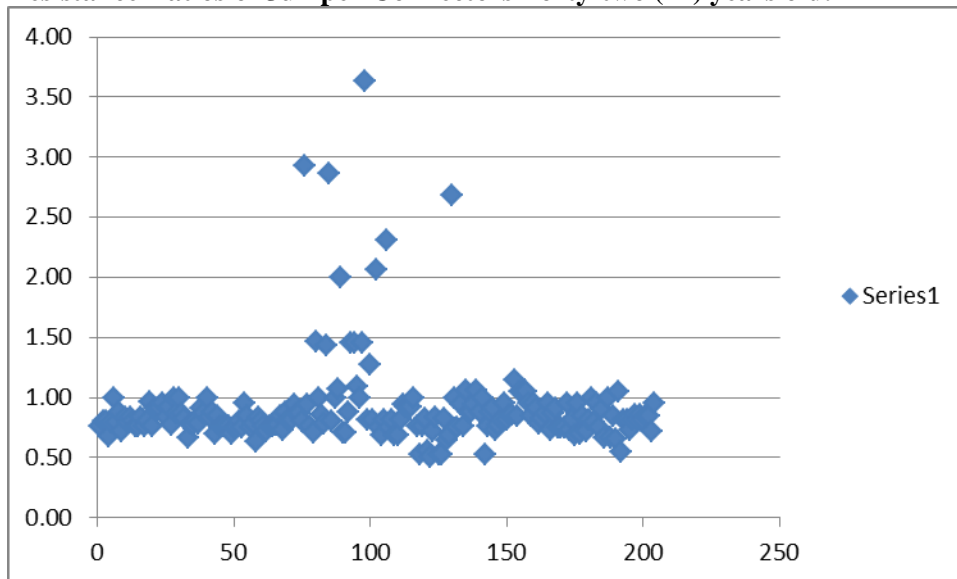
It is interesting that there were quite a few jumper connectors in the population of ten (10) year olds with a resistance ratio greater than 1.0, and quite a few above 1.2 indicating that they are on the move in the failure mode.

Resistance Ratios of Jumper Connectors Ten (10) years old:



It was surprising to find that in the population of forty-two (42) year old jumper connectors, there are not as many above 1.0 relative to the ten (10) year olds. Although one would jump to an assumption that the forty-two (42) year olds jump to a higher resistance when they begin to fail, we presently do not have a way to predict the rate of deterioration of a connector once it goes into failure mode.

Resistance Ratios of Jumper Connectors Forty-two (42) years old:



345kV Transmission Line Thermal Upgrading Project Summary

This project was the first of its kind for CenterPoint Energy. The particular connector shunt devices selected were based on the conductor size, connector size, line hardware and line jumper configurations on these lines. There are many different conductor sizes, connector sizes, line hardware and line jumper configurations that exist. Each line configuration has to be evaluated to determine the type and size of connector shunt device suitable for a particular line for both tension and jumper connectors.

The tension connectors on these 345kV lines represent only one type of connector installed forty-two (42) years ago on new conductor and one different type of tension connector installed ten (10) years ago on the conductor after it was service aged for thirty-two (32) years. The jumper connectors installed originally forty-two (42) years ago are of similar type to those installed ten (10) years ago with the exception that the newer ones are slightly shorter and they were installed on the service aged conductor.

CenterPoint Energy used this project to learn how to make a field assessment of line connectors using the SensorLink® Radio Ohmstik Micro Ohmmeter (Ref. 4). Training sessions were held prior to beginning the project for CenterPoint Energy engineering and construction personnel and for the contract construction personnel who would work on the project. Even with this training, there was a learning curve once mass acquisition of data began. Helicopter and ground line mechanics had to learn the particular techniques of setting up the instrument for the particular connector measurement and recoding the data in accordance with the resistance measurement documentation methodology that had been established. To assure the consistency of resistance measurements for each connector, a conductor resistance measurement was taken before the conductor/connector interface resistance was taken. There were numerous locations on the line jumpers where formed wire type bundle spacers were installed too close to the end of the jumper connectors to be able to take resistance readings. At each of these locations the formed wire spacer had to be removed before the conductor/connector resistance reading could be taken. The formed wire spacer was then replaced with a bar type spacer far enough away from the jumper connector to not only allow for the resistance measurement to be taken, but to allow sufficient space for the shunt device to be installed over the connector.

This project was CenterPoint Energy's first field application of the Preformed® connector shunt device and the ClampStar® connector shunt device. Training sessions were held prior to beginning the project for CenterPoint Energy engineering and construction personnel and for the contract construction personnel who would work on the project. Even with this training, there was a learning curve once mass installation of the devices began. The connector shunts are connectors and the conductors over which they are installed must be thoroughly bright cleaned and coated with inhibitor compound just as when installing a compression connector. Helicopter and ground line mechanics had to use various wire v-brush and abrasive wire wheel brush techniques to thoroughly clean long lengths of conductor and then apply inhibitor compound to the conductor before the shunt device was installed. CenterPoint Energy also used this project to test various installation methods for each of the devices, de-energized and energized from helicopter, insulated bucket, and insulated ladders. Both types of devices were able to be installed by all of these methods. As mentioned above, there were numerous formed wire type bundle spacers that had to be removed in the jumpers and replaced with bar type spacers farther away from the connectors to provide space for the connector shunt device. There were also some locations along the lines where formed wire type bundle spacers had to be removed and replaced with a bar type spacer far enough away from the tension connector to allow sufficient space for the shunt device to be installed over the connector.

Five (5) years ago CenterPoint Energy began using a conductor solution cleaning system known as ConductaClean®. The cleaning system is used on both new and aged conductor to effectively clean the

conductor before inhibiting compound and a compression connector is installed. This system requires that the end of the conductor be free to be placed into the solution agitation device. CenterPoint Energy is working on a research project with EPRI to try to develop a device which can be placed over the in-service line conductors to effectively clean long lengths of line conductors for not only connector shunts but for line tap connector installations.

CenterPoint Energy was able to accomplish the required thermal uprating of the 345kV transmission lines using the connector shunts in a timely manner. The project began in February 2013 and was completed in May 2013, seven (7) months ahead of the need date. With shunts installed on 100% of the connectors on these lines, the connectors are now protected. However, the connector resistance measurements that were taken on these two 345kV circuits for this project indicate that attention should be directed toward determining the electrical condition of connectors on other circuits.

References

- 1) ANSI ASC C119.4 – 2011 - **American National Standard** for Electric Connectors—*Connectors for Use Between Aluminum-to-Aluminum, and Aluminum-to-Copper Conductors Designed for Normal Operation at or Below 93°C and Copper-to-Copper Conductors Designed for Normal Operation at or Below 100°C.*
- 2) *Performance of Compression Fittings at Elevated Temperatures*, Final Report August 2009, EPRI Report 1018782, EPRI Project Manager J. Chan
- 3) *Evaluation of Connector Mitigation Measures for Lines Operating at High Temperatures*, Thermal and Mechanical Test Results, Technical Update, November 2012, EPRI Report 1026560, EPRI Project Manager J. Chan
- 4) SensorLink® *Operators Manual*, Radio Ohmstik, Radio Linked Micro Ohmmeter

CenterPoint Energy Contact

Questions or inquiries regarding the topics in this paper can be directed to:
Chester Kowalik, Sr. Consulting Engineer, Transmission Engineering, CenterPoint Energy, PO Box 1700
Houston, TX 77251-1700; email: chester.kowalik@centerpointenergy.com Tel. 713-207-6720

Baseplate and Flange Weld Inspection of Transmission Tubular Steel Structures

Ed Jacobs, Al Clare, Paul Cameron



Baseplate and Flange Weld Inspection of Tubular Steel Transmission Structures

The purpose of this paper is to inform our industry on the importance of the proper inspection of tubular steel transmission structures and the potential pitfalls that could occur in the process.

Ed Jacobs *Director of Quality, R&D, and Solid Modeling*
Al Clare *NDT Manager*
Paul Cameron *Plant Quality Manager, CWI*
Jon Loveless *Quality Engineer*

July 19, 2013



Table of Contents

Abstract: Baseplate and Flange Weld Inspection of Transmission Tubular Steel Structures	2
Introduction /Background	3
Framework of AWS D1.1	4
The Shortcomings of AWS D1.1	5
A Proper Inspection Program.....	6
T&B Destructive Testing Results and Validation of NDE	7
T&B Enhancements to AWS D1.1 for Full Penetration Welds in T-Joints.....	8
Considerations for a New Standard	10
Conclusion	10

Abstract: Baseplate and Flange Weld Inspection of Transmission Tubular Steel Structures

Thomas & Betts Corporation

8155 T&B Boulevard, 2D-15, Memphis, TN 38125; Ph. (901)-252-5349; Fax (901)-252-1312

Ed Jacobs *Director of Quality, R&D, and Solid Modeling*

Al Clare *NDT Manager*

Paul Cameron *Plant Quality Manager, CWI*

Jon Loveless *Quality Engineer*

The purpose of this paper is to discuss the shortcomings of the AWS D1.1 weld inspection standards when applied to tubular steel transmission structures, and to inform our industry of the importance of the proper inspection of tubular steel transmission structures and the potential pitfalls that could occur in the process.

The AWS D1.1 standard has been the most widely accepted standard for tubular steel transmission structures and has provided the industry with guidance for many years. However, AWS D1.1, which was originally adopted for building and bridge construction, does not recognize or adequately address the unique characteristics of tubular steel transmission structures. Using AWS D1.1 as a starting point, we can, however, remedy the existing weaknesses and gaps, and develop a more robust inspection process which will validate the structural integrity of the weld.

Our experience indicates that a single structure can be tested by multiple UT (Ultrasonic Testing) Level II personnel, certified in accordance with ASNT (American Society for Nondestructive Testing), with each inspector arriving at conflicting results. Interpretations of the results can also vary. The key to sound inspection practices lies in knowledge of the joints and fabrication methods, consistent equipment and techniques, and an objective basis for the interpretation of results. Properly trained individuals can understand the geometry of a steel pole and interpret any indication found by applying a consistent, repeatable and, most importantly, accurate UT testing methods.

This paper will:

1. Explain the framework and shortcomings of AWS D1.1 when utilized for UT inspection of tubular steel transmission structures, in particular, T-joints.
2. Communicate how critical it is to establish a repeatable UT inspection practice to ensure that results are consistent and accurate.
3. Discuss forensic metallurgical examinations and validations of NDE (Non-Destructive Examinations).
4. Recommend a "standard" for the inspection and identification of structurally significant defects in tubular steel transmission structures.

Introduction /Background

History of the American Welding Society and AWS D1.1.

The roots of the American Welding Society go back to World War I. Sudden demands for producing military equipment brought about the need for standardization of the manufacturing industry.

President Wilson created a *Welding Committee of the Emergency Fleet Corporation*, which worked with the already existing *National Welding Council*. By 1919, industry leaders agreed that dependable and objective information on welding was crucial for further U.S. industrial development. The two organizations merged to create the *American Welding Society*. Comfort A. Adams was the first president of the *American Welding Society*. Today's Society president is Nancy C. Cole.

In 1928, the American Welding Society published the first edition of the *Code for Fusion Welding and Gas Cutting in Building Construction, Code 1 Part A*. It was revisited and revised in 1930, 1937, and 1941. After its 1941 revision, it was given the *AWS-D1.0* designation.

The first bridge welding specification was published separately in 1936. It was eventually designated *AWS-D2.0, The Specification for Welding Highway and Railway Bridges*. AWS Codes were developed by three basic types of users; designers and builders of buildings; designers and builders of bridges; and starting in 1972, designers and builders of tubular-steel structures used in the off-shore oil and gas industry.

In 1972 *D1.0* and *D2.0* combined to form *AWS D1.1 - Structural Steel Code* and eventually *Section 10, Tubular* was added. This created a Buildings Group (Section 8) a Bridges Group (Section 9) and a Tubular Group (Section 10).

In 1988 the Bridges Group separated when the joint *AASHTO/AWS D1.5 Bridge Welding Code* was published. It addresses the specific requirements of State and Federal Transportation Departments. After that separation the AWS-D1.1 code changed references of buildings and bridges to statically loaded and dynamically loaded structures, respectively, in order to make the document applicable to a broader range of structural configurations.

In the 1990's Section 10, Tubular was removed and the committee decided to merge all inspection criteria into Section 6, Inspection (now Clause 6). This change was significant to the tubular steel transmission structure industry. It was the Tubular Group that developed the alternative UT techniques that were eventually incorporated into Annex K (now Annex S). Annex S is included in the *Informative* (Non-Mandatory) Annexes, meaning it is included in AWS D1.1 for informational purposes only, yet it contains some critical information necessary for the proper evaluation of tubular steel transmission structures.

AWS D1.1/D1.1M:2010, *Structural Welding Code - Steel* is maintained and revised by volunteer members of the American Welding Society. It is developed in accordance with the rules of the American National Standards Institute (ANSI). This is a voluntary consensus standard that is currently on a 5 year review cycle.

Framework of AWS D1.1

There are advantages to having a standard that is recognized throughout the industry. The words, “All Welding per the latest revision of AWS D1.1” have become a standard requirement found in virtually all structure specifications and fabrication prints. Such references should let all involved in the fabrication know what is expected in the design, qualification, fabrication and inspection of welds up-front. It has, however, become the default standard that most specification writers reference over and over without consideration of what is actually in AWS D1.1. In the case of Ultrasonic Testing (UT), it could even involve two different acceptance standards.

The steps to qualifying both the process and persons are clear and well laid out in Clauses 3 & 4 of D1.1. Many of the required steps for qualification found in D1.1 are used in other codes and standards published by the American Welding Society. They are time proven and understood by Welders, Inspectors and Engineers.

AWS D1.1 also lays out an alternative means of inspection. Understanding the wide range of weldments that can be fabricated under this code, the AWS-D1 committee included alternative methods for the UT. [See Annex S]

The American Welding Society has a very solid and well-recognized inspector certification program (QC1) for visual inspection (VT), but for the qualification of inspectors in all other forms of Nondestructive Testing (NDT) it turns to another widely recognized organization, the American Society for Nondestructive Testing (ASNT). ASNT’s Recommended Practice Number SNT-TC-1A is a recommended practice that becomes a requirement of AWS-D1.1 in paragraph 6.14.6 – Personnel Qualification. SNT-TC-1A lays out the requirements for a NDT inspector qualification program and includes certification requirements to:

1. Level I – Receives instruction and supervision from a Level II or Level III. This person is qualified for very specific calibrations and evaluations.
2. Level II – Gives guidance to Trainee and Level I personnel. A Level II also sets up and calibrates equipment, evaluates results, and is thoroughly familiar with the scope and limitations of the method(s) qualified.
3. Level III – Capable of developing, qualifying, and approving NDT procedures. Establishes and approves techniques, interprets codes, standards, and specification, and is capable of qualifying Level I & II personnel.

AWS D1.1 Clause 6 Part F details a very comprehensive process for the calibration of Ultrasonic Test equipment. Using the recognized IIW Type Block and other reference standards, Part F covers the equipment requirements, how that equipment is calibrated, and the specifics of the inspection. In addition, Annex S also includes a very comprehensive process for alternative techniques for UT examination.

The Shortcomings of AWS D1.1

The primary disadvantage for the Tubular Steel Transmission Structures industry is that AWS D1.1 covers such a wide range of designs and conditions that it's not specific enough for our industry. Some sections of Clause 6 are not practical for some of the industry's proprietary joint designs.

Although AWS-D1.1 gives clear guidance for the UT inspection acceptance criteria for statically and cyclically loaded non-tubular connections of 5/16" weld sizes and greater (Tables 6.2 & 6.3), there are no criteria for materials less than 5/16" or for tubular connections. In our industry, we use 1/4" and 3/16" thick steel. This opens up a point of contention for both the fabricator and end user. As a result, a standard must be developed by the fabricator to establish alternate inspection and acceptance criteria for production welds, which can vary greatly from fabricator to fabricator.

Another short-coming is that AWS D1.1 does not consider UT inspection on galvanized structures.

On a groove weld in a T-Joint with material thicknesses typical of steel structure tower walls, the AWS D1.1 scan requirement would be from a single side (Face-A). So, unless there is a signal from the base metal/weld metal interface, no scanning from Face-C is required. A more appropriate approach is to scan both the A and C Faces. [See Figure 4]

Although based on 40-50 yrs. historical information for UT inspection, AWS D1.1 does not account for modern technology. The current code is written based on cathode ray technology, not digital equipment that we use today. In addition, new UT technologies such as Phased Array have yet to be fully represented in AWS D1.1 with a clear calibration and comprehensive acceptance criteria.

Charpy V-Notch (CVN) testing has been an industry requirement since the 60's and has proven to be a beneficial test to ensure weld toughness. CVN testing is noted in the Clauses of AWS-D1.1, but perhaps visual acceptance criteria for weldments meeting a specific CVN requirement would be beneficial to our industry.

In other steel fabrication industries, the frequency of UT inspection on Complete Joint Penetration (CJP) welds is generally based on a sampling of maybe 10% or 25% as determined by the project specifications. Using the AWS D1.1 criteria for UT and scanning at a high sensitivity level takes a lot more time and makes sense when you're only inspecting a small percentage of the CJP welds. Some might be called the "Inch wide, Mile deep" approach where you have an intense inspection of a small sample. If that small sample passes the intense inspection, then the process is considered sound and will provide reliable welds throughout the project with no further UT inspection required.

AWS D1.1 acknowledges that some defects are more critical than others. Near surface, linear, crack-like defects are more critical than slag inclusions near the center of the weld. Also, AWS D 1.1 says that the orientation of the defect is more critical if it is perpendicular to the load.

However, our industry design standard requires 100% inspection of CJP welds and the goal for UT inspection should be to identify the critical defects and not spend time identifying and evaluating non-critical defects that you will find with scanning at a higher sensitivity level. Therefore, a lower scanning level is more appropriate in order to identify and evaluate the critical defects that could affect the weld reliability.

In summary, when it comes to weld inspection, AWS D1.1 is more of a general structural welding code and not specific to any industry. It's a big square peg, and we're trying to fit it into a 12-sided hole. It is not a perfect fit for our industry, and some adjustments are necessary to ensure reliable welds are produced.

A Proper Inspection Program

AWS D 1.1 says that each industry should determine the suitable acceptance criteria for the intended service. Clause 6.8 lays the ground work for determining a more suitable acceptance criteria, however, the tubular steel transmission structure industry, as a whole, has not yet undertaken this task.

The goal of an inspection program should be to identify the critical defects that may affect the performance of the structure for its intended purpose, not to identify every imperfection that will have no consequence to the structure's performance. Any NDT program should start with good visual (VT) inspection. Visual inspection of welds begins long before an arc is struck. Before welding begins the inspector needs to ensure they are familiar with the codes, standards, specifications, and drawings for the project.

Ensuring that base, filler metals, and fluxes are correct for the project, are tested in advance, and are specified in the fabricator's Weld Procedure Specifications (WPS) is critical. It is the inspector who will ensure that the electrodes, fluxes, and filler metals are stored to the manufacturer specifications and governing code requirements. The inspector will also ensure proper joint fit-up and cleanliness are maintained, that all welders are qualified to the processes and positions, and that the proper pre-heat is applied.

Once welding begins, good visual inspectors monitor welding parameters, technique and bead placement along with interpass temperature and cleaning. When inspection is carried out before and during welding inspection, the after welding is far more successful. After welding is complete, the inspector is simply looking to verify that the finished weld meets the visual acceptance criteria (such as that in AWS D1.1-Table 6.1), and the weldment meets its dimensional requirements.

Although most codes allow for the qualification of welding inspectors to be an internal program, the preferred method of qualification for visual inspectors is through third party certification such as those developed by such organizations as AWS, Canadian Welding Bureau (CWB), and ASNT. Inspector certification through third parties ensures that inspectors are objectively qualified and that their qualifications are documented.

In the case where more than visual inspection is required, other NDE methods can be utilized. All NDE methods require skilled and qualified inspectors. A good inspection program will seek to consistently minimize variation between inspectors. Conducting studies and identifying key differences will aid in establishing sound inspection practices and procedures. This enhances a fabricator's ability to get repeatable results to ensure reliable welds. Certain criteria critical to performance are transducers (defined by procedure), certifications (by ASNT course), qualifications (by a Level III in method tested), experience (specific to

industry), and calibrated equipment (traceable to a national standard). Mockups should also be developed and used as training for inspectors applying VT and UT methods.

It sounds easy enough, but eliminating the human variables that influence inspection is the most difficult factor to control. The key elements to eliminating the human variables are industry experience and proper training. To be effective, an inspector must know and understand the complexities involved in welding tubular members to perpendicular plates. A program developed to train an inspector in the geometry and design of tubular steel transmission structure is critical to enable the inspector to make proper decisions utilizing established acceptance criteria.

T&B Destructive Testing Results and Validation of NDE

Based on several destructive forensic metallurgical examinations, Thomas & Betts has found that the vast majority of UT and radiographic NDE indications are dispersed slag inclusions at the root of weld repairs that were made during the original fabrication of the structure. Finite element analysis (FEA), metallurgical analyses, and full-scale testing have confirmed that structural integrity was not compromised by the sub-surface indications in any of the structures we have examined.

Lessons Learned

The below figures represent the analysis of a single indication that was found in an inspection of a base plate to tower weld. Multiple cuts were made to analyze the indication found.



Figure 1.

A single indication was reported by UT. It was characterized as 2.0" L x 0.75" W x 0.12" D. The section containing that defect was sent for metallurgical analysis.



Figure 2.
Examination of the cut slices revealed a defect.

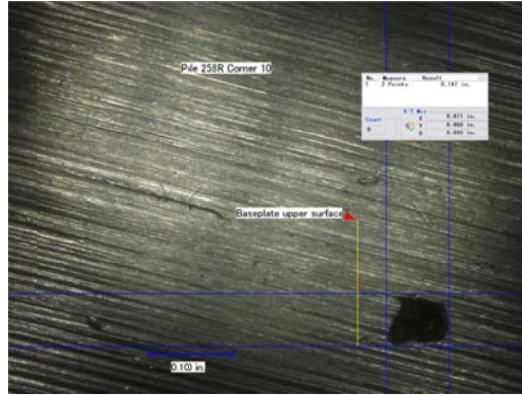


Figure 3.
Under 20X magnification, an indication is shown. Exhibited a small slag defect in the center of the weld at the base of the weldment. Actual flaw was less than 0.1" on a side and only 0.5" long.

Thomas & Betts inspection protocol was used, and this indication found was rejectable in accordance with AWS D1.1. It should be noted that:

- The indication was rejectable as measured by UT.
- The metallurgical examination confirmed the indication being rejectable. However, there was a major reduction in the size and geometry reported than was measured using UT.
- This indication was of a size and in a location which would have had no effect on the structural integrity of the pole.

Other industry inspection protocols, such as building, bridge, or pipeline fabrications, are usually focused on identifying visual cracks as a means to ensure structural integrity has not been compromised, and rely less on comprehensive UT inspections where no surface indications are present.

T&B Enhancements to AWS D1.1 for Full Penetration Welds in T-Joints

After 50+ years of industry experience, performing multiple Gage R&R Studies to hone inspector's skills to achieve consistent repeatable results, and years of researching testing requirements and UT evaluation, Thomas & Betts recommends specifying ultrasonic testing of tubular steel transmission structures full penetration welds in accordance with AWS D1.1, except modified per Clause 6.8 as follows:

1. Scanning and evaluation

Scan and evaluate at +7db's (after calibrating to 80% full screen height on the 0.060 side drilled hole), and add 2db per inch after 2 Inch of Sound Path. AWS D1.1 scans at +14db and calibrates on side drilled hole between 50-75%. AWS D1.1 uses an evaluation of 1 db. difference for all its class of defects A, B, C, D.

Rationale: One db. during the calibration of a machine can be easily misconstrued. The code also uses a + or – 2 degrees for angle of sound, this means that the difference between two transducers maybe a total of four degrees.

A second scan is necessary from Face C as shown in Figure 4 below.

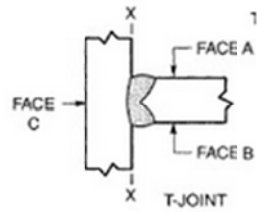


Figure 4.

2. Acceptance criteria

Evaluate from Scan Level:

80% FSH for 0.060 hole plus 7db

Alter the Acceptance Criteria to:

80% FSH Reject Regardless of Length

40% - <80% FSH Reject after 1 inch of Length

20% - <40% FSH Reject after 2 inches of length

Comparatively the AWS D 1.1 acceptance criteria are:

Indication level (a) – Reference Level (b) – Attenuation Factor (c) = Indication Rating

Compare Rating to Table 6.2 and determine acceptance.

Rationale: This method will simplify and speed up the evaluation of indications without compromising the detection of structurally significant defects. AWS D1.1 requires more calculation once an indication is identified.

3. Length evaluation from Maximum Indication:

Scan Left and Right until indication drops below 10% FSH

Comparatively, AWS D1.1 Method is to scan Left and Right until indication drops by 50% (6db). This could still be 37.5% FSH. This would not be less than 25% FSH

Rational: This Thomas & Betts Recommended Method provides the advantages of exceeding AWS requirements, being more critical on longer lengths and allowing evaluations after 2nd, 3rd, and 4th leg (that is crucial on thinner materials).

4. Post Galvanizing Inspection:

The word “galvanized” cannot be found anywhere in the 540 pages of AWS D1.1.

Galvanizing is prevalent in our business, and the galvanizing process can have a profound effect on weldments made with multiple brake lines and greatly varying material thicknesses. Post galvanizing toe crack inspection should be a requirement. Although this is considered above and beyond typical industry requirements, T&B firmly believes that post-galvanizing inspections including visual inspection and ultrasonic testing should be required.

Rationale: Toe cracks are associated with galvanized structures. Toe cracks historically were considered to be mostly a tower wall problem after galvanizing. There is a theory that the toe crack was also associated with a base plate to tower plate thickness ratio and that if

the ratio was small enough, there would be no toe cracking. Nevertheless, toe cracks occur regularly in galvanized structures and should be evaluated like other surface or near surface defects.

Considerations for a New Standard

API 2X and D1.8 Seismic Supplement, having similar requirements, should be considered for the basis of a modified standard. Also, fitness for use should be examined.

API 2X Recommended Practice

AWS-D1.1-Annex S is the AWS version of the API 2X Recommended Practice. It contains some of the same ideas but it has much more detail. It was written with the needs for Tubular Steel Off-Shore Structures in mind while AWS D1.1 was written with steel building in mind. Both would be an adaptation to use either with the tubular steel transmission structure industry. API uses a distance amplitude curve (DAC) and a transfer loss comparison. The transfer correction method would also account for any loss due to coatings. The API code does recognize fitness for purpose, FEAs, or fracture mechanics. API also recognizes certain flaws may be better left in the weld than to try to repair them.

D1.8 Seismic Code

Intended to ensure that welded joints that are designed to undergo significant repetitive, inelastic strains as a result of earthquakes and connect members designed to resist such inelastic strains, have adequate strength, notch toughness, and integrity to perform as intended. Certain defects are more critical than others (i.e. bigger lengths if deeper in). AWS D1.8 Commentary recognizes that “*when the repair may result in more harm to the joint than benefit*”, alternative acceptance criteria may be called for.

Fitness for Use

The ultimate goal of the new standard should be to determine whether or not the structure should be expected to perform as intended. Inspectors should look at the type of defect and the location and orientation of the defect, and thoroughly evaluate whether or not the defect could affect the structural integrity of the structure. Include a safety factor for the inaccuracies of the examination. Only defects that would affect the structural integrity would be rejected.

Conclusion

Simply specifying that tubular steel transmission structures be subject to ultrasonic testing in accordance with AWS D1.1 is inadequate due to the fact that AWS D1.1 is based on incomplete and outdated requirements with respect to our industry.

The shortcomings can be resolved in a production environment by adding requirements encompassing all thicknesses, inspection from two faces of a baseplate weld, and specifying post galvanizing inspections. The long-term approach for the industry is to work within our industry committees to collectively develop, as AWS D1.1 recommends, a standard suitable specifically for tubular steel transmission structures.

Adventures in Routing: A Case Study From the Big Hill to Kendall 345 KV CREZ Project in Kerrville, TX

Nathan Laughlin, P.E. and Curtis D. Symank, P.E.

**ADVENTURES IN ROUTING: A CASE STUDY FROM THE BIG HILL TO KENDALL
345 KV CREZ PROJECT IN KERRVILLE, TX**

Nathan Laughlin, PE, Senior Engineer, Lower Colorado River Authority,
Curtis Symank, PE, Senior Project Manager, POWER Engineers
Transmission & Substation Design & Operation Symposium, Dallas, TX
September 13, 2013

ABSTRACT

In designing and constructing its Big Hill to Kendall 345 kV CREZ transmission line project, the Lower Colorado River Authority (LCRA) encountered many unique challenges. These challenges included a CCN proceeding with over 1,200 intervenors, procuring construction and material resources in a constrained marketplace, designing through rugged terrain and developed areas along an interstate highway, and obtaining the necessary regulatory permits from several agencies, including the U.S. Fish and Wildlife Service (USFWS), the Federal Aviation Administration (FAA), and the Texas Department of Transportation (TxDOT).

A successful coordination process with TxDOT was particularly critical to the success of the project. The route approved by the Public Utility Commission of Texas (PUCT) paralleled TxDOT roads for approximately 98 of its 139 miles, including 85 miles along Interstate 10, with approximately 35 road crossings. Also, the PUC specifically directed LCRA TSC in its Final Order to “engage in discussions with TxDOT and use its best efforts to reach agreement with the Department to use state ROW along the proposed project where it parallels I-10.” This directive was new to LCRA’s experience, and the two-year permitting process that followed called for a more collaborative approach than is typical with TxDOT.

With the directive from the PUC as a starting point, LCRA TSC engaged TxDOT personnel at both the State and District levels in a series of meetings to identify opportunities for co-location. Out of these meetings, LCRA TSC and TxDOT found about 20 locations where co-location was feasible and mutually acceptable in concept. The accommodations discussed included aerial overhang of conductors, temporary construction access, and in some cases, placing 345 kV pole structures within TxDOT right-of-way. After the conceptual phase, LCRA worked closely with the TxDOT’s San Angelo and San Antonio Districts to implement the co-locations in a manner that was safe for both LCRA’s construction crews and the travelling public, both during the construction phase and the long-term operation of the transmission line. Above all, the success of this process required that good working relationships be developed on all levels of LCRA and TxDOT, including (and especially) the construction crews working with local TxDOT offices.

This paper will provide a case study of how LCRA worked with TxDOT and other parties on a particular design solution that routed the line through the intersection of Interstate 10 and State Highway 16 in Kerrville, Texas. This intersection had numerous design challenges around it, including several homes and businesses near the right-of-way, traffic constraints along the two highways, and a roadside monument with landscaping. Through its collaboration with TxDOT, and negotiations with other parties, LCRA’s design team developed a solution that placed four structures and 4400 feet of the line within TxDOT right-of-way, avoided several homes and businesses in a congested area, preserved the character of the roadside monument, and most importantly, protected the safety of construction crews and the travelling public during construction. The success of this process illustrates how a well-executed collaborative process can resolve complicated design issues where multiple stakeholders are involved.

A DIRECTIVE TO COLLABORATE

Through the PUCT regulatory process for what became the Big Hill to Kendall project in 2009 and 2010, LCRA encountered a wide variety of issues raised by intervenors and policymakers in the project area, which was approximately as large as Connecticut. The most significant routing issue argued by intervenors involved the relative merits of paralleling Interstate 10, the major existing infrastructure corridor in the study area, versus taking a more direct route through less populated and developed areas. This routing issue represented a conflict between two PUCT routing criteria, as the routes along Interstate 10 were more desirable in that they had a greater percentage of their length paralleling existing infrastructure corridors, while routes that did not parallel the interstate were more desirable in that they encountered less human development, as quantified by habitable structure counts.¹ Ultimately, in its Final Order in January 2011, the PUCT selected a route among the shortest routes at 139 miles in length that paralleled or closely followed TxDOT right-of-way for 98 miles, with 85 of those miles along Interstate 10. Figure 1 shows the route selected by the PUCT.

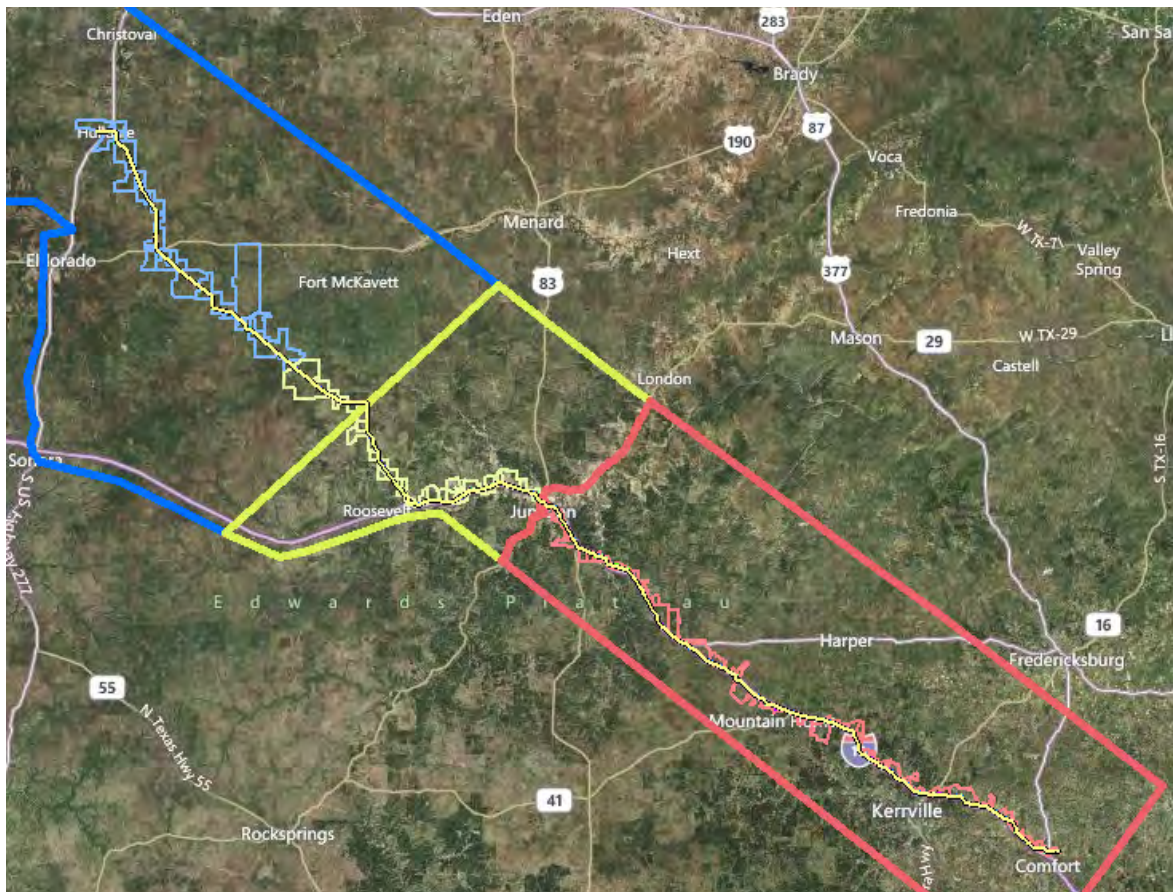


Figure 1: Big Hill to Kendall Project Map

¹ See Section 25.101 of the Texas Administrative Code for PUCT regulations pertaining to routing criteria for electric transmission lines.

In its Final Order authorizing the project, the PUCT gave LCRA two directives to work with other parties on modifications to the route during the detailed design phase of the project. The first addresses route modifications on individual landowners with language similar to that in many other PUCT proceedings:

LCRA shall cooperate with directly affected landowners to implement minor deviations in the approved route to minimize the impact of the project. Any minor deviations in the approved route shall only directly affect landowners who were sent notice of the transmission line in accordance with P.U.C. PROC. R. 22.52(a)(3) and shall directly affect only those landowners that have agreed to the minor deviation, excluding public rights-of-ways. Any agreed minor deviations shall not delay the project beyond its Commission-required completion date, nor shall any minor deviation add any significant cost to the project.²

In a later ordering paragraph, PUCT also directed LCRA to work with TxDOT on co-location opportunities for the line within highway right-of-way:

LCRA shall engage in discussions with the Texas Department of Transportation and use its best efforts to reach agreement with the Department to use state right-of-way along the proposed project where it parallels 1-10. These discussions shall not unreasonably delay the completion of this project and, in any event, if agreement has not been reached on or before September 1, 2011, then LCRA shall proceed with construction on the proposed project.³

The instructions to work with landowners on route modifications was common in previous experience with PUCT proceedings, and in fact, LCRA evaluates landowner-requested route modifications on most of its CCN projects. However, the directive for TxDOT and LCRA to work together was new in LCRA's experience, and would require a different approach than that used for typical route modifications on private property, and a much more extensive process than is typical for TxDOT permitting. In the months that followed PUCT approval, LCRA and TxDOT worked together first to define the process *by which they would work together*, then to identify opportunities for accommodation of the transmission line and associated construction activities within TxDOT right-of-way.

THE CHALLENGE: I-10/SH 16 INTERSECTION IN KERRVILLE

To further understand the process, it is helpful to frame it around the intersection of Interstate 10 and State Highway 16 in Kerrville, which is the primary gateway into the city of Kerrville, and which presented many constraints for both line design and construction, and was the most significant design challenge on the project. As shown on the map in Figure 2, the design constraints on the PUCT-approved route through the vicinity of the intersection included:

- 17 manufactured homes in the potential right-of-way
- A car dealership
- A US Department of Agriculture research facility
- A gas station
- The highway intersection, and
- A "Kerrville" highway monument within TxDOT right-of-way

² Final Order in PUCT Docket #38354. Ordering Paragraph 5

³ Final Order in PUCT Docket #38354, Ordering Paragraph 21

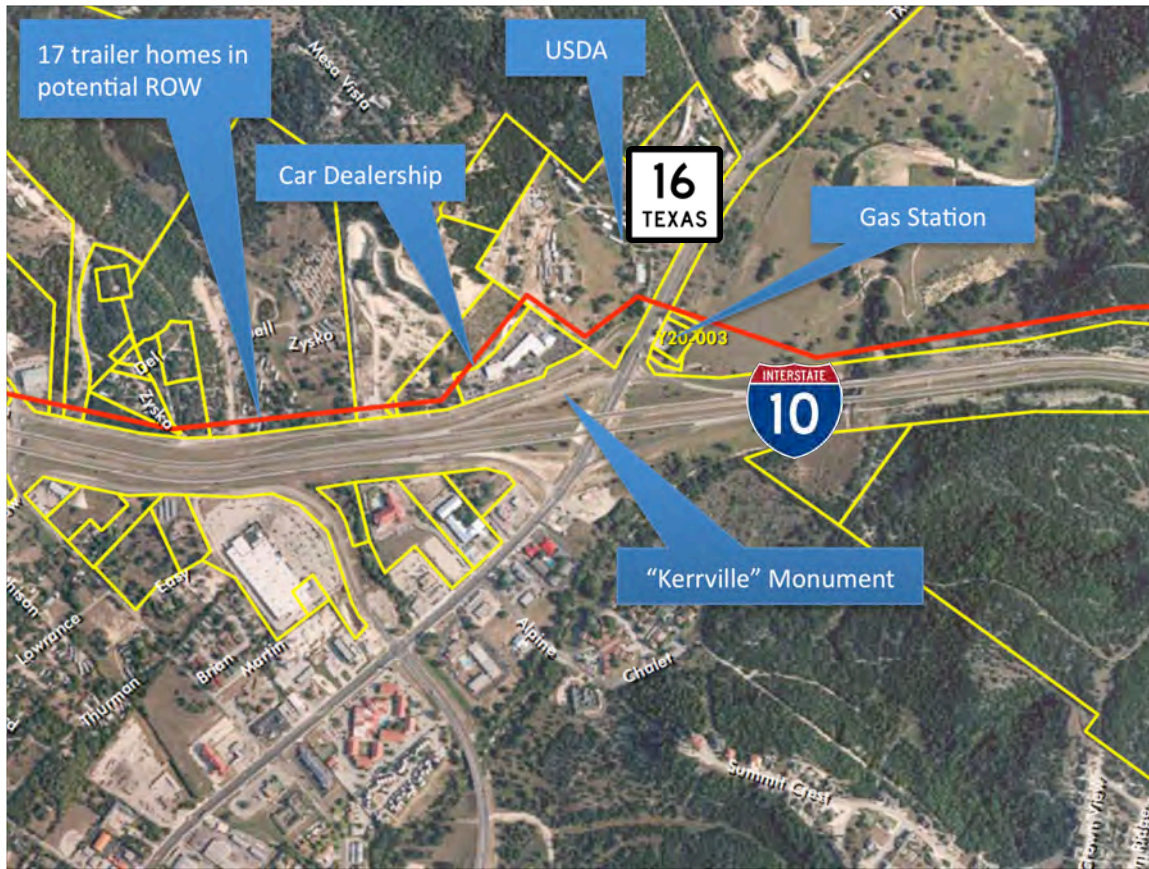


Figure 2: Constraints in Vicinity of Interstate 10/SH 16 Intersection in Kerrville, TX

The “Kerrville” monument in particular was emblematic of the concerns expressed by the City of Kerrville throughout the design process. Several years ago, the City worked with TxDOT on the design of the monument, which consists of a stone sign with irrigated landscaping and trees behind it, and which is situated between the main lanes of I-10 and the westbound entrance ramp. The monument is shown on the lefthand side of Figure 3, with the vegetation behind it. The City’s concerns with the line through the vicinity of the intersection were twofold – that the line would damage the value of the real estate around the intersection, and that the line would have a negative visual impact on their “gateway”.



Figure 3: “Kerrville” Monument

While the presence of all of these constraints on the Approved Route presented a challenge to the design team, they also presented an ideal opportunity to work with TxDOT on a mutually beneficial design solution under the “work together” language in the Final Order that would reduce the effects of the project on the public and private interests around the intersection.

THE COLLABORATIVE PROCESS

In early meetings after the PUCT approved the project, LCRA representatives met with TxDOT officials in Austin to discuss, on a high level, what collaboration between the two entities would look like. In the early discussions, it was agreed to that this process would be different from the typical TxDOT permitting process. Where permitting with TxDOT is typically a “bottom-up” process, with permits requesting exceptions going up from the local level to the District level to the State level, this process would be “top-down” – that is, LCRA engineers would start by working directly with the state-level TxDOT personnel and the supervisors at the District offices on potential accommodations, and when these accommodations were agreed to in concept, then the details of the accommodations would be worked out with local personnel prior to filing the actual permit. This way, LCRA would be working with personnel at TxDOT with decision-making power on extraordinary accommodations, and could work to a consensus with TxDOT more quickly.

After a few months of the design process on Big Hill to Kendall, LCRA TSC identified 3 types of accommodations that it would work with TxDOT on to come up with a mutually acceptable agreement:

- Overhang of wires
- Temporary construction access
- Structures in right-of-way

These three types of accommodations require exceptions from the parts of the Texas Administrative Code that govern what TxDOT would typically allow for utility accommodation. Such exceptions are allowed under the Texas Administrative Code, given that the exceptions meet certain stringent criteria:

1. The exception must be recommended for approval by the District Engineer, then authorized by either the Right-of-Way Director or the Maintenance Director of TxDOT.
2. The utility must show extreme hardship or unusual conditions provide justification for the accommodation, maintains the intent of the administrative code, and is backed up by design data.
3. The accommodation in the exception will not adversely affect the safety, design, construction, operation, maintenance, or stability of the highway, will not be constructed or serviced by the direct access from a freeway or entrance ramp, and will not interfere or impair the present or future use of the highway.⁴

With these guidelines in mind, LCRA brought 20 potential exception accommodations to TxDOT during the summer of 2011 in the form of exhibits. The exhibits that LCRA provided during this time were critical in “telling the story”, and in communicating the intent of the line design and how the line design related to TxDOT’s existing facilities. The exhibits included maps that were developed by LCRA’s GIS department in the first round of summer meetings, which were then marked up based on TxDOT’s input, such as the one in Figure 4a for the I-10/SH 16 intersection. At the second round of summer meetings, LCRA brought refined maps (including the one in Figure 4b), and worked with POWER Engineers on a series of visualizations showing the intersections in Kerrville from various vantage points, which were

⁴ Texas Administrative Code, Title 43, Part 1, Chapter 21, Subchapter C, Rule 21.35 “Exceptions”

extremely helpful in these discussions with TxDOT and in later discussions with Kerrville regarding the design through the intersection (as shown in Figures 5a and 5b).

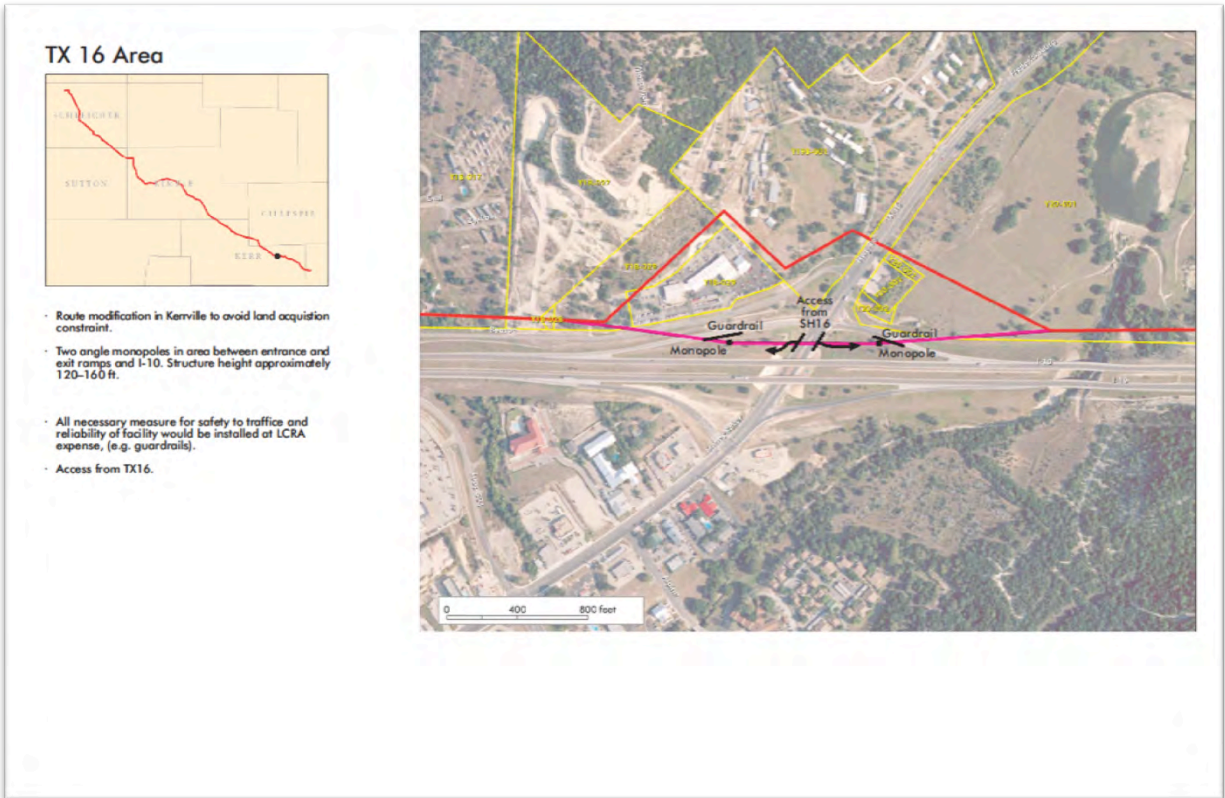


Figure 4a: First Exhibit for I-10/SH 16 Intersection brought to TxDOT

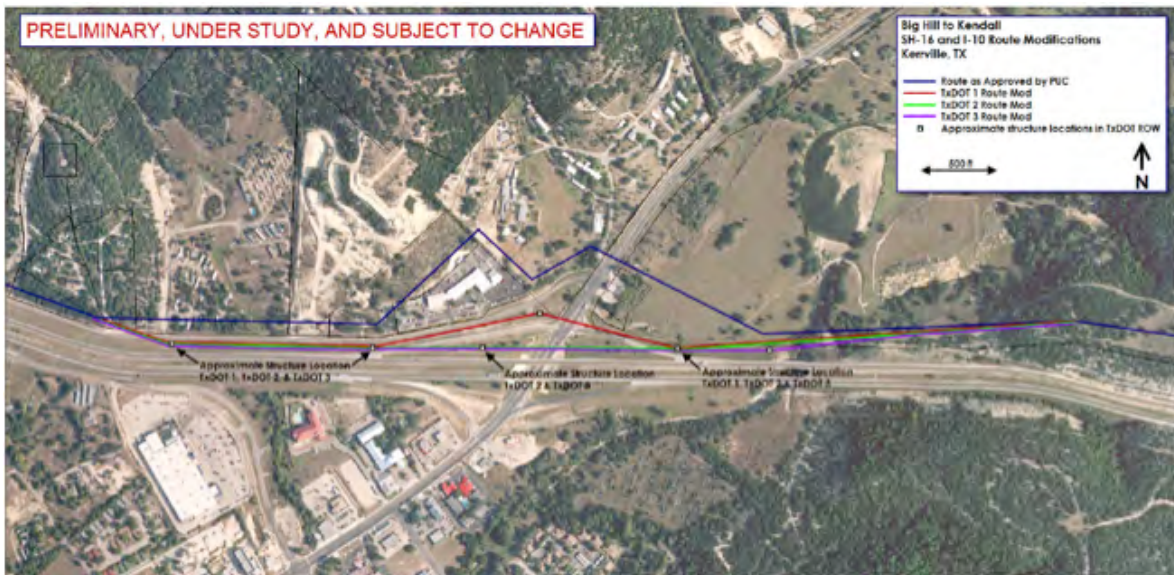
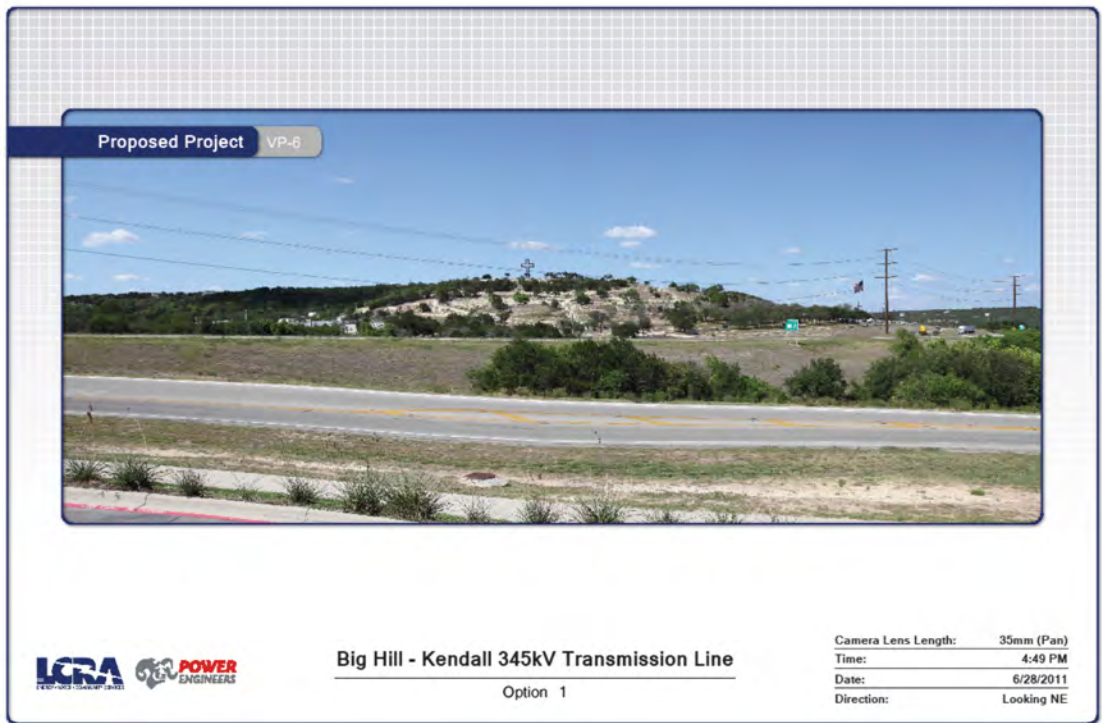
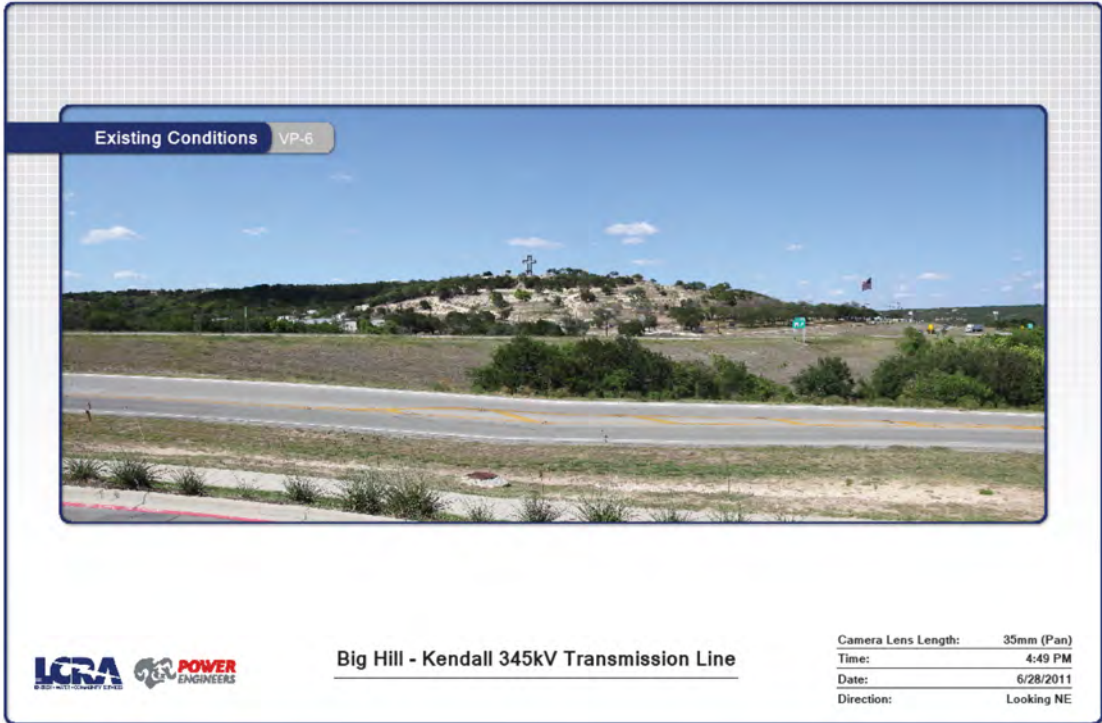


Figure 4b: Revised Exhibit for I-10/SH 16 Intersection with Multiple Alternative



Figures 5a and 5b: Visualizations of Existing Conditions and Proposed line near Intersection

While most of the 20 exceptions involved LCRA and TxDOT exclusively, and were resolved with relatively little drama, the I-10/SH 16 intersection drew in a third stakeholder in the City of Kerrville. The City took an initial position of opposition to the approved route, but when this position did not work out, they inquired into the collaborative design that LCRA and TxDOT were working through for the intersection. Partly with their input, the series of alternatives shown in Figure 4b were narrowed to an alternative that would, in concept, place multiple structures in TxDOT right-of-way in locations where they would not pose a hazard to the travelling public, and that would route the line over the “Kerrville” monument with a structure somewhere in the monument area. If implemented, the proposed routing through the intersection would avoid all constraints on private property, including the 17 manufactured homes and the car dealership, though bypassing them on state right-of-way. All parties agreed to this arrangement in principle in September 2011, and LCRA commenced work on the detailed design of the transmission line.

The next phase of the collaborative process between TxDOT and LCRA took place on a local level, and involved LCRA’s Construction Management personnel as much as the engineers. LCRA’s construction inspectors and contractor representatives, who had been on site for several months working with landowners already, began working with the county TxDOT offices on locating construction entrances, coordinating the movement of heavy equipment and setting up traffic control plans for areas where temporary construction access would be employed. Meanwhile, the engineering team incorporated the exception accommodations that received conceptual approval into the design and prepared exception letters and design documentation to formally submit to TxDOT. From September 2011 through summer 2012, the project team prepared for construction activities along TxDOT highways to commence in June of 2012, with activities in Kerrville slated for early 2013. The process progressed steadily (and most critically, ahead of construction crews) until one final issue reappeared in late summer of 2012.

BACK TO THE INTERSECTION IN KERRVILLE

After seeing a draft of the design in July 2012, officials from the City of Kerrville objected to the design as proposed, claiming that LCRA had not followed through with the earlier agreement. While LCRA disagreed with this assessment of the situation, they engaged the City through TxDOT and found that the City was primarily concerned about the proximity of the pole in the monument area to the “Kerrville” sign, and in the amount of vegetation that would be removed as a result of the draft design. Seeing an opportunity for a final resolution of its differences with Kerrville, and the potential for a mutually beneficial solution, LCRA’s engineering team revised the design to increase the height of the structure to maintain a safe clearance over existing vegetation and maximize the distance from the pole structure to the “Kerrville” sign. Also, in order to protect the travelling public during a complicated construction sequence, LCRA worked closely with TxDOT on the placement of barricades, the installation of new guardrails, the timing of crane and helicopter operations, and the deployment of law enforcement to carry out the traffic control plan. With the revisions to the design and all construction arrangements made, LCRA submitted the permit for the intersection in Kerrville and obtained approval in January 2013. By May 2013, structures were installed, wire was pulled in, and construction was complete through the intersection. Figure 6 is a photo of the line constructed through the intersection.



Figure 6: Big Hill to Kendall Transmission Line through Intersection, June 2013

WHAT WAS ACCOMPLISHED AND LESSONS LEARNED

Through collaborating with TxDOT on a design of the Big Hill to Kendall line through the intersection of I-10 and SH 16 in Kerrville that took into account the interests of stakeholders such as the City, LCRA accomplished the following: accommodations that it would work with TxDOT on to come up with a mutually acceptable agreement:

- Four structures and 4400 feet of the line were installed within TxDOT right of way in a manner that protected the safety of the public and of construction personnel, and that will keep both LCRA's facilities and TxDOT's facilities safe and reliable for the foreseeable future.
- The effects of the project on public and private entities near the intersection were greatly reduced, as constraints such as the car dealership, USDA, the gas station, and 17 manufactured homes (and their residents) were avoided by the line.
- The vegetation on the monument area can be maintained at its current height, and with almost all remaining in place during construction.
- LCRA and TxDOT built a good working relationship that allowed both entities to comply with the PUCT's directive to a far greater extent than anyone anticipated.

Though the circumstances of this project were unique, and the road to its success was far from a straight line, there are several lessons that can be carried forward from LCRA's experiences to other projects with complex permitting situations.

1. Take a collaborative approach in regulatory approval matters, including stakeholders where they are willing to contribute.
2. Build working relationships with all levels of each organization, from management level to construction personnel.
3. Recognize interests behind positions of stakeholders your organization has differences with, and work to find best solution for all parties.
4. Maps and pictures tell the story visually, and can be an invaluable resource in effective collaboration.
5. Build a good team of committed professionals that work well together.

Finally, the authors of the paper wish to express their gratitude to the many members of the Big Hill to Kendall Project team, both inside and outside of LCRA, who all brought something valuable to the table through its five year journey from birth to completion, and whose camaraderie, dedication, and good humor in the face of adversity made this project a joy to work on. Its success was far from a guaranteed, but by working together to get thousands of little things right, the big thing was finished: BH2K is complete, available, energized, and serving the ratepayers of Texas. Team, we're honored to have worked with you. Thanks.

Nip / Tuck Method: A Solution to Providing Additional Conductor-to-Ground Clearances for Transmission Lines

Michael E. Belanger, P.E. and Garrett Luszczki, E.I.

Nip / Tuck Method

A Solution to Providing Additional Conductor-to-Ground
Clearances for Transmission Lines

Michael E Belanger, P.E., M.ASCE
Garrett E Luszczki, E.I., A.M.ASCE
TRC
Augusta, Maine



Presented At The
46th Annual Transmission and Substation Design and
Operation Symposium (TSDOS)
September 11-13, 2013
Addison, Texas

SUMMARY

With the advent of sophisticated survey methods such as LiDAR, and interactive design programs like PLS-CADD, the engineer has more options, and more accurate tools than ever before to solve clearance problems. This paper explores the use of the Nip/Tuck method to solve clearance violations on transmission lines. The Nip/Tuck method uses a multi-span analysis in which a more accurate prediction of sag behavior can lead to more economical solutions. One possibility is to remove a section of a conductor (Nip) to allow local decreases in sag. Another, is ‘sliding’ the conductor through an insulator string (Tuck), allowing for a shifting of sags. With either approach, the engineer has more economic options to consider.

INTRODUCTION

In October of 2010 the North American Electric Reliability Corporation (NERC) directed all utilities to review their power line system for clearance violations. The origin for this requirement stemmed from an incident in August of 2007 where a 230-kV line was knocked off-line due to a flashover between the line conductor and nearby vegetation. Upon further investigation, it was determined the site of the flashover had only 2 to 7-ft of conductor clearance where it should have been a minimum of 15-ft. Inconsistencies between actual field conditions and the original design documents is nothing new to anyone involved in design or construction of electrical transmission lines. These issues often stem from observed field changes not being reported to the office, the drawings not being updated or inadequate vegetation control the problem remains creating potential for significant clearance and safety violations.

NERC estimated there was 450,000 miles of line that would be affected by the Alert. This figure represents a significant effort and a projected cost to the industry of over \$1B. In today’s world utilities are expected to do more with less resources and complete more work at less cost. Technology has risen to the call with the development of more advanced technologies such as aerial light detection and ranging (LiDAR) to collect survey information, and software design products such as PLS-CADD. Modeling and analyzing these lines using LiDAR and PLS-CADD makes the evaluation, identification, and resolution of clearance violations more efficient and accurate.

TRADITIONAL METHODS TO IMPROVE CLEARANCE

In the past, utilities developed standard structure designs to simplify the design of their transmission lines. These standard structures were designed with significant safety factors, for certain ruling spans. Application of the standard structure and ruling span for specific transmission line was rarely optimized to their fullest extent. This conservatism left some unused “extra” capacity in the structures. There are many means and methods by which to improve clearance along a transmission line; some more popular or accepted than others. Commonly employed traditional remediation techniques often increase the loading on a structure to some degree. These remediation techniques can involve all aspects of a transmission line, from the conductor to the insulators, or even involve structure alterations and manipulation. Modification of tangent-angle structures (running-angles) and deadend structures is usually avoided due to their higher cost and outage duration required for the modification. By constraining the line remediation methods to

other than running-angles and deadends, the remediation techniques is implemented at the tangent structures adjacent to a violation to. This section elaborates on some of the more traditional remediation techniques that can be completed without manipulation of the transmission structure or tower itself.

RETENSIONING CONDUCTOR

When a transmission line is under-tensioned as compared to the design tension specified, it is possible to retension the conductor from deadend to deadend. This method can be particularly effective if there are numerous smaller clearance violations found along a deadend to deadend set of spans. The drawback of this method is it requires the line to be de-energized for an extended duration; an outage that the utility often may not want to or simply cannot take on the line.

FLOATING DEADEND

A floating deadend is generally considered a fix for a localized smaller clearance violation found in a span. A floating deadend shortens the suspension insulator string of a tangent structure to gain elevation at the attachment point of the cable, improving a spans clearance. The reduced length of the suspension insulator is compensated by adding two strain insulators deadended on the end of the shortened suspension insulator. The addition of the suspension insulators restores the electrical clearance required for the voltage class of the line. Maintaining a portion of the suspension insulator allows for the structure to still operate as a tangent structure, distributing any unbalanced tension with the swing of the remaining length of suspension insulator.

FULL STRAIN CONVERSION

The full strain conversion of a structure involves the complete removal of the suspension insulator and its replacement with strain insulators, effectively converting the tangent structure to a deadend structure. The drawback of this remediation technique is that the structure itself is often not designed to carry the loads of a deadended conductor or handle the full unbalanced load between spans.

STRUCTURE REPLACEMENT

As it implies, this method involves the replacement of existing structure with taller ones. Sometimes replacing a structure in its entirety has the added benefit of replacing an old and dilapidated structure with a brand new one. This method is good for some of the smaller wood pole structures where materials are not expensive. A variation of this method would involve installation of an intermediate structure along the span to increase the height and resulting clearance of the conductor.

WHAT IS THE NIP & TUCK METHOD?

An innovative approach to gaining additional ground clearance uses a wire retensioning technique called “Nip&Tuck” (N&T). This approach retensions a single span of conductor, reducing the sag and providing an additional amount of ground clearance. The retensioning occurs when a small amount of the conductor is removed. Once a portion of the conductor is removed (Nip), the ends are spliced back together again. The total distance of the conductor between adjacent structures is now slightly less, and therefore increases the tension and reduces the sag.

Another possibility is to use the “Tuck” method. In this method, the conductor clamp on the adjacent structure(s) is relocated a certain distance toward the area of concern (sliding the clamp). No conductor is removed. This method redistributes the ‘slack’ associated with one span to the adjacent span. Where slack is removed from one side, the conductor will be a little tighter resulting in less sag. The span on the other side of the structure will now gain the slack that was redistributed resulting in more sag on that side. Again, no conductor is actually removed, only the clamp on the insulator is repositioned. This method is best suited when the span adjacent to the problem area has additional clearance beyond what is needed. The additional sag created isn’t a problem for a span that already has some extra clearance to give away.

There are a number of concerns that need to be dealt with in using the Nip/Tuck method. Probably the foremost concerns are the increased unbalanced loads. When a piece of conductor is removed or the conductor is slid through the insulator clamp, the tension in that span increases. But in doing so, an imbalance of load is created. That imbalance load will do one of two things. The insulator string will move:

- 1) allowing a portion of the unbalanced load to be taken by the conductor in the adjacent span, and
- 2) the insulator string will move, this time the unbalanced load will be taken up by the structure.

It is important that the engineer checks that the structure integrity is not compromised.

To accomplish the design requires some state-of-the-art modeling tools and surveys. We use PLS-CADD, which is probably the method of choice for transmission line design and analysis for most transmission line engineers. With the SAPS module, a complete 3D, multi span sag analysis can be accomplished. The SAPS module has the ability to analyze the conductor as a 3D finite element model. Traditional ‘ruling span’ methodology simply does not work here. The SAPS module’s finite element capability calculates the suspension insulator movement as it determines the conductor tension.

For a more detailed look at the behavior of the conductor, through PLS-POLE the structure model can be used to account for the structure deflections as well. Of course, this level of design is very resource intensive and will severely tax most computers. Convergence to a solution can be a very time consuming process and may take several hours. Much of the analysis that we do is considered a ‘Level 1’ analysis in which only the insulator movement is considered.

For the modeling tool, we use PLS-CADD with the SAPS module. This provides the multi-span analysis program to determine the effects of the unbalanced loads on the transmission lines and the resulting load transfer to the structures. A computer model of the transmission line wire is created and SAPS is used to model its behavior under nearly any weather conditions. After identifying clearance violations, we can begin using either the “Nip” or the “Tuck” method of correction. These operations can be done individually or together on any span requiring additional clearance.

Application of the N&T method requires that the transmission system be defined with a very high degree of precision. The precision needed is most easily obtained through a properly executed LiDAR (Light Detection and Ranging) survey. This survey method, coupled with direct measurement or estimation of the conductor temperature, will define the conductor 3D location, sag, insulator string, and conductor clamp locations. In addition, it will pick up ground features, topography and vegetation. These are all

very important to know if the movement of the insulator string is going to be factored into the analysis and all of the line clearance violations identified.

CASE STUDY USING THE NIP/TUCK METHOD

In the summer of 2012, an eastern mid-coast utility retained TRC to solve several clearance issues resulting from the NERC order to check transmission line clearances. We will focus on two lines in particular; one is a 765 kV and 345 kV respectively.

765 kV line

This line is built using lattice structures with an average span of approximately 1,300 feet. Typical tower heights are about 130 feet above ground.

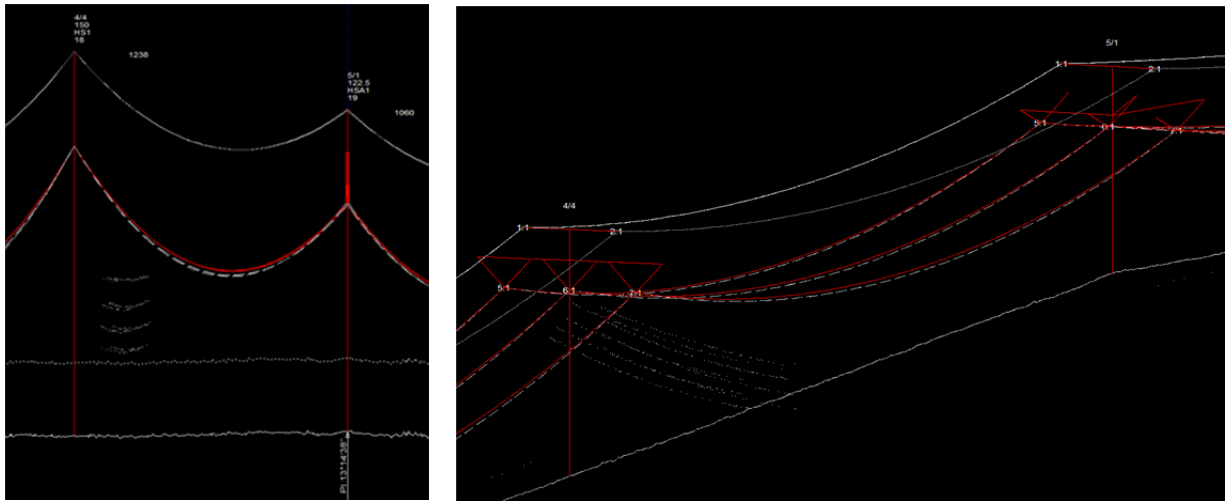


Figure 1: Method 1 (Stick Structure) Models of Lattice Towers for Nip/Tuck

The subject of this case study is a single span of the line that had a clearance violation of about 0.5 feet at the crossing of another utility's overhead shield wire. For such long spans and large sags, a violation of 0.5 feet is not a lot. The traditional methods of insulator manipulation or structure replacement to increase the conductor clearances are obviously expensive solutions and overly complicated for a violation of this magnitude. A simple 'Nip' by taking out some of the conductor in the violating span appeared to be the more cost effective solution.

Another criteria specified by the client was that the insulator strings on either side of the violation had to remain plumb. This made the solution a bit more difficult as we had to apply the 'Tuck' method to the span as well. The analysis balanced the tensions by simulating the sliding an amount of conductor from one span to the adjacent span until the insulators were essentially plumb.

The combined Nip & Tuck approach is an iterative approach; removing enough conductor allowing for a tuck from an adjacent span to balance the tensions and re-plumb the insulators while still remediating the clearance violation. The first step is to clip the insulators at the conductor attachment points enabling

SAPS then the designer graphically sags the conductor to match the survey. An amount of conductor is then 'Nipped', or removed from the span and the process repeated until all criteria has been met. In PLS-CADD the Nip is done through the 'Section Modify' menu under the 'Edit Span Specific Wire Lengths' tab. In this menu under the 'Ahead Span Unstressed Length Change (ft)' column the desired Nip and Tucks are applied. The change input in the ahead and back spans for the span in question are the effective Tucks being slid through the conductor shoe. The summation of the changes input in this column make up the total amount of conductor Nipped and removed from the line.

The process is begun by estimating an amount of conductor to be Nipped, ensuring the specified length is more than adequate to remediate the clearance violation. The Nip of the conductor changes the tension of the span resulting in a change in angle of the insulators. Using the SAPs feature the insulator swing angles are displayed by toggling the 'Label insulator swing...' option in the hidden F1 menu of PLS-CADD. The angle of insulator swing indicates the amount and direction in which the conductor needs to be Tucked to re-plumb the insulator. By adjusting the insulator string to re-plumb, there is an amount of conductor that is added back into the span with the violation. Although it is a small amount, it does have the negative effect of creating more sag in that span, the exact opposite of what we are trying to accomplish. If the Tuck of the conductor restores the violation, repeat the steps above using a larger initial Nip. This may take several iterations to develop an optimized solution.

The final step is to ensure that the increased longitudinal loads on the structures do not compromise their structural integrity. The simplest method to check the loading is to compare the existing unbalanced loads on the structure to the unbalanced loads on the structure after the Nip/Tuck method has been implemented. Again these can be easily viewed by toggling on the SAPS feature in the hidden F1 menu in PLS-CADD. This feature allows one to view the unbalanced loads for any given weather case. If the resulting unbalanced load is less than the initial unbalanced load of the existing structures, the load on the structure has been effectively reduced.

By reporting the existing conditions, we demonstrated to the client that there is some measure of an unbalanced load and insulator swing. Although in the case of the case study the imbalance and insulator swing was limited, there were spans in this line that had up to 10 degrees of existing swing, imparting a significant longitudinal load to the structure and suspension arms.. For that particular case, it was important to help the client understand the significance of the pre-existing condition of a large insulator swing, and that the swings already violated the criteria imposed upon this analysis.

There is an important item to note about the difficulty in using the Tuck method. The amount of conductor shifted from one span to the other has a total net gain of exactly 0.0 feet. It is mentioned because of the ease to which an error can occur.. Replumbing the insulators is a trial and error process, in which several different menus within PLS-CADD are accessed; one to address the conductor lengths, the other to check on insulator swings. During the course of finding the solution, it is very easy to get lost and lose track of how much sliding has occurred. Trying to retrace your steps is difficult. To assist our engineers keep track of the modifications, this analysis tracked each change in the model using a spreadsheet. This spreadsheets served three purposes:

1. To check the inputs
2. Verify that all length changes are accounted for, and
3. To serve as a summary for the client.

The table below is an excerpt of a spreadsheet providing an example of how we reported our findings to the client. For each of the 3 phases, we looked at the amount of conductor to be removed and also the before and after conditions of the two design criteria; insulator swing, and imbalance load.

Table 1: Analysis Spreadsheet for Tracking the Nip/Tuck Method

Violation Information				Wire to be Removed (ft)	Existing Structure Information					
Structure From	Structure To	Span (ft)	Extent of Clearance Violation (ft)		Structure / Ahead Span Information					
Structure From	Structure To	Span (ft)	Extent of Clearance Violation (ft)	Structure	Structure Type	Existing Imbalance (lbs)	Existing Long. Insulator Swing (deg) (Note 3)	New Imbalance (lbs)	New Long. Insulator Swing (deg)	
Str 4/4 to 5/1										
(Left Phase)										
4/3	4/4	1550			4/3	HS1	129	0.25	937	2.43
18(4/4)	5/1	1250	0.5	3	18(4/4)	HSA1	334	-1.04	-73	0.25
5/1	5/2	1060			5/1	HS1	274	0.1	83	0.07
					5/2	HS1	-120	0.74	-570	-3.13
(Middle Phase)										
4/3	4/4	1550			4/3	HS1	170	0.05	969	2.54
18(4/4)	5/1	1250	0.5	3	18(4/4)	HSA1	347	-1.12	-161	-0.05
5/1	5/2	1060			5/1	HS1	321	0.22	409	0.6
					5/2	HS1	-137	0.82	-617	-3.38
(Right Phase)										
4/3	4/4	1550			4/3	HS1	24	0.55	845	2.07
18(4/4)	5/1	1250	0.5	3	18(4/4)	HSA1	218	-0.71	-231	-0.27
5/1	5/2	1060			5/1	HS1	337	-0.38	103	0
					5/2	HS1	-58	0.35	-501	-2.75

In this case, the lattice towers, verified through an analysis of a loading tree diagram, were designed to withstand a substantial amount under the NESC Heavy Load case. The increased longitudinal loads did not present a problem.

345 kV Line

The line is built using lattice structures with an average span of about 1,300 feet and a typical tower height of 100-110 feet.

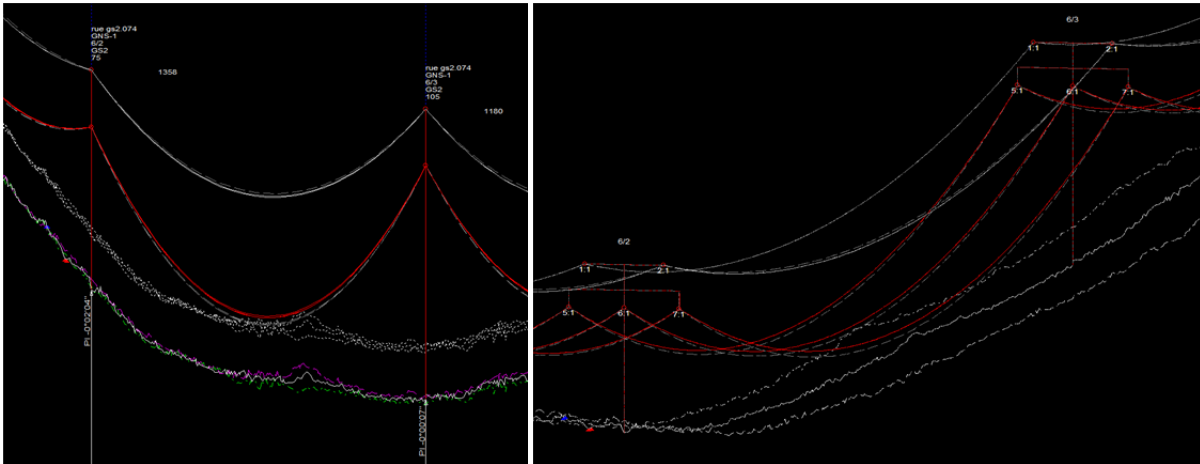


Figure 2: Method 1 (Stick Structure) Models of Lattice Towers for Nip/Tuck

The subject of this case study is a single span of the line with a clearance violation of about 1.0 to 2.5 feet. Again, this is relatively small when dealing with spans of 1,300 feet and about 50+ feet of sag. A structure replacement or any method of raising the structure can be expensive. A simple ‘Nip’ by taking out some of the conductor in the violating span proved to be the most cost effective solution.

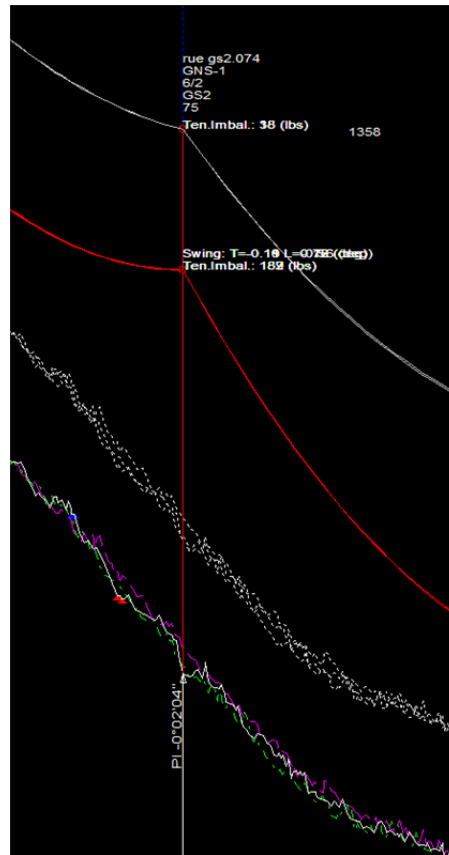


Figure 3: Structure 6/2 Sample of SAPs Insulator Swing and Tension Imbalance

The following table provides an example of how our analysis results were reported to the client, and is similar to the previous case. By removing about 3.5 feet of conductor, we were able to raise the sag of the conductor enough to maintain clearance. Again, a check of the longitudinal loads is done to ensure that the structural integrity was not compromised.

Table 2: Analysis Spreadsheet for Tracking the Nip/Tuck Method

Violation Information				Wire to be Removed (ft)	Existing Structure Information					
Structure From	Structure To	Span (ft)	Extent of Clearance Violation (ft)		Structure / Ahead Span Information					
Structure From	Structure To	Span (ft)	Extent of Clearance Violation (ft)		Structure	Structure Type	Existing Imbalance (lbs)	Existing Long. Insulator Swing (deg)	New Imbalance (lbs)	New Long. Insulator Swing (deg)
Str 6/2 to 6/3										
(Left Phase)										
6/1	6/2	830	2.5		6/1	GS2	-171	1.15	404	-2.9
6/2	6/3	1360	1	3.5	6/2	GS2	254	1.15	182	-0.56
6/3	6/4	1180	1		6/3	GS2	-63	0.34	76	-0.74
					6/4	GS2	130	1.6	-599	7.03
(Middle Phase)										
6/1	6/2	830	2.5		6/1	GS2	-183	1.24	453	-3.18
6/2	6/3	1360	1	3.5	6/2	GS2	174	2.14	139	0.72
6/3	6/4	1180	1		6/3	GS2	130	1.32	29	-0.37
					6/4	GS2	27	2.29	-630	7.18
(Right Phase)										
6/1	6/2	830	2.5		6/1	GS2	-26	0.14	534	-3.7
6/2	6/3	1360	1	3.5	6/2	GS2	36	4.03	157	0.18
6/3	6/4	1180	1		6/3	GS2	9	0.26	21	-0.27
					6/4	GS2	7	2.45	-720	7.84

Notes

- 1) These calculations are based on the assumption that the insulator strings on either side of the Nip will be placed in blocks. Insulators will be plumbed vertically after the piece of conductor is removed.
- 2) Conductor tensions are based on the NESC Heavy Loading (initial). Insulator swings are based on a 60F, no wind, final condition.

CONCLUSION

As the sophistication of technology and software increases, engineers have more options available to them to solve clearance related issues. Through the use of advanced surveys (LiDAR) and finite element modeling of multi-span systems (PLS-CADD), engineers now have the means to fix issues by using the Nip/Tuck Method. By either removing a piece of conductor, sliding the conductor clamp, or a combination of both, the sags of individual spans can be modified to provide additional clearances. The Nip and Tuck methods allow for a cost effective, local adjustment of tensions. This method works well where the amount of additional clearances to be gained is relatively small as compared to the sag. However, the methods introduce longitudinal loads on adjacent structures. So as with any changes to a transmission line’s tension, care must be taken so as to not compromise the structural integrity of the structures or line hardware.

AEP 69-kV Oil-Insulated Transmission Line Removal Project

Michelle Beckman, Bill Halliburton, Woody McOmber and David C. Slavin

Prepared for



July 2013

Prepared by

Michael Glueck

American Electric Power



**Michelle Beckman
Bill Halliburton
Woody McOmber
C. David Slavin**

Burns & McDonnell Engineering Company, Inc.



TABLE OF CONTENTS

1.0	INTRODUCTION.....	1
1.1	BACKGROUND.....	1
1.2	69-KV TRANSMISSION LINE SYSTEM DESCRIPTION.....	1
2.0	ENVIRONMENTAL BACKGROUND.....	2
2.1	LABORATORY TESTING OF THE INSULATING MINERAL OIL.....	2
2.2	ASBESTOS CONTAINING MATERIAL.....	3
2.2.1	Somastic Coating.....	3
2.2.2	ACM in Pump House.....	4
2.3	CABLE SAMPLING.....	4
2.4	PCB SOIL SAMPLING.....	4
3.0	DECOMMISSIONING AND DEMOLITION PLAN DESCRIPTION.....	4
3.1	DEMOLITION PLAN.....	4
3.2	CABLE AND FLUID REMOVAL PLAN.....	5
3.2.1	Excavation of the Buried Cable Splice Joints.....	5
3.2.2	Removal of the Insulating Mineral Oil.....	6
3.2.3	Removal of HPFF Transmission Cables.....	6
3.2.4	Cleaning of the Conduits.....	6
3.2.5	Restoring the Buried Splice Joint Locations.....	7
3.2.6	Installation of Conduit Caps.....	7
3.2.7	Stabilization of Conduits with Inert Gas.....	8
3.2.8	Removal of the Cathodic Protection System.....	8
4.0	PHASE II – FUTURE REMOVAL OF CONDUIT IN SHIP CHANNEL.....	8
4.1	CONDUIT IN THE SHIP CHANNEL.....	8
4.2	FEASIBILITY STUDY OF THE REMOVAL OF 69-KV CONDUITS.....	8
4.2.1	Feasibility Study Alternatives.....	9
4.2.2	Historical Document Review and Adjacent Pipeline Research.....	9
4.2.3	Conduit Removal Risk and Liability Assessment.....	10
4.2.4	Limited Risk Assessment Using EPA Risk Model.....	12
4.2.5	Conclusion of the Feasibility Study.....	12
5.0	SUMMARY.....	13
6.0	REFERENCES.....	14

LIST OF FIGURES

Figure 1: Route of 69-kV Underground Transmission Line System	1
Figure 2: Representation of the 69-kV Conduit Used in Ship Channel Crossing with Somastic Coating Error! Bookmark not defined.	
Figure 3: Approximate Locations Where Conduit Will Be Capped	7
Figure 4: Approximate Location on the North Side of Ship Channel Where Conduit Will Be Capped	7

LIST OF ACRONYMS AND ABBREVIATIONS

ACM	asbestos containing material
AEP	American Electric Power
Burns & McDonnell	Burns & McDonnell Engineering Company, Inc.
BOSCEM	Basic Oil Spill Cost Estimation Model
CRA	Chris Ransome & Associates Inc.
DGA	dissolved gas analysis
EPA	United States Environmental Protection Agency
gpm	gallons per minute
HPFF	high-pressure fluid-filled
kV	kilovolt
LEL	lower explosive limit
MLT	mean low tide
NPMS	National Pipeline Mapping System
OSHA	Occupational Safety and Health Administration
PCB	polychlorinated biphenyl
POCCA	Port of Corpus Christi Authority
ppm	parts per million
psi	parts per square inch
SMA	Shiner Mosley and Associates
USACE	United States Army Corps of Engineers

1.0 INTRODUCTION

1.1 BACKGROUND

American Electric Power (AEP) installed two underground oil-insulated 69-kilovolt (kV) electrical transmission lines from beside and beneath the Corpus Christi Ship Channel in the 1950s. These transmission lines were removed from service in the 1990s. In order to ensure the conduits remained intact and no oil was escaping into the ship channel, the lines remained pressurized which was a continuing maintenance issue. Therefore, AEP decided to decommission the lines in 2010 and retained Burns & McDonnell Engineering Company, Inc. (Burns & McDonnell) to provide engineering support, coordinate stakeholders, and manage the sub-consultants and subcontractors required for this project.

This decommissioning project involved the removal of cable and insulating fluid and demolition of surface structures associated with two parallel high-pressured fluid-filled (HPFF) 69-kV inactive underground transmission lines approximately 1.1-mile long (each) and an additional spare conduit installed beneath the ship channel. The two transmission lines commence at Nueces Bay Substation, travel underground along Navigation Boulevard where they turn to cross the ship channel across from Dock #4, and terminate at Avery Point Terminal, as shown below in Figure 1.

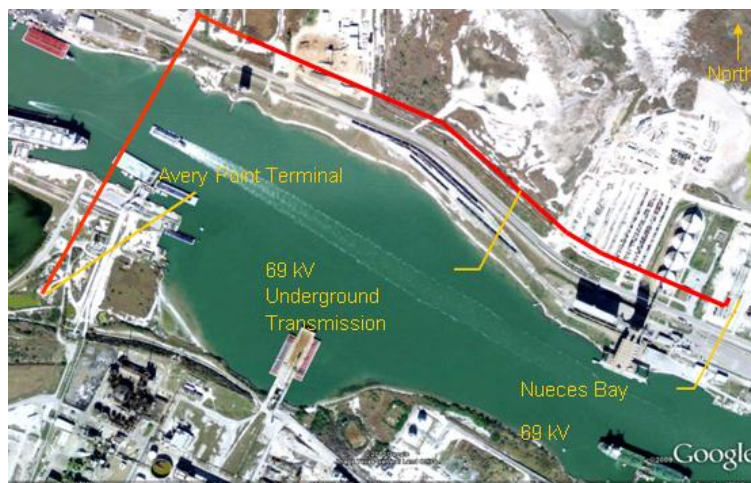


Figure 1: Route of 69-kV Underground Transmission Line System

1.2 69-KV TRANSMISSION LINE SYSTEM DESCRIPTION

Each of the transmission lines consisted of three 1.85-inch diameter copper cables, encased within a 5 9/16-inch electric-welded steel pipe (conduit) containing pressurized insulating mineral oil. The underground portion of the conduits located on either side of the ship channel was covered with an asbestos-containing somastic coating and encased in concrete. The portion of the conduits that is located under the ship channel was coated with an asbestos-containing somastic and cement mixture. The original plan was to remove the cables and conduits completely, but after much discussion, it was decided that the

majority of the steel conduit would be left in place, with the ownership of a portion of the conduit conveyed to the Port of Corpus Christi Authority (POCCA) for potential reuse. The decommissioning and demolition phase of the project (Phase I) consisted of the removal of the copper conductor cables and insulating fluid from the underground inactive conduits and demolition of surface structures associated with the system. These structures included a small pump house with a 500-gallon steel tank, a circulating pump controller, terminal stations with three pot heads on each, and all other associated debris. The second phase (Phase II) of the project (when conducted) will consist of removing the segments of conduit that cross under the Corpus Christi Ship Channel.

2.0 ENVIRONMENTAL BACKGROUND

Due to the age of the system and construction methods typically employed for these types of systems, the project team identified several environmental issues that would need to be properly managed prior to and during the decommissioning of the transmission line system. These issues included the flammability potential of the insulating mineral oil, asbestos containing material (ACM) present throughout the system, and possible polychlorinated biphenyl (PCB) contamination of the insulating mineral oil.

2.1 LABORATORY TESTING OF THE INSULATING MINERAL OIL

Based on available records, the insulating mineral oil was identified as Sun #6 dielectric mineral oil. Test results for PCB content indicated that the mineral oil did not contain PCBs, but did contain high concentrations of dissolved gases. As a result, all necessary precautions had to be taken to avoid potential safety hazards. To obtain a representative dissolved gas analysis, aliquots were collected at seven-hour intervals throughout a 48-hour period, while circulating the oil through the conduit. Below is a summary of the dissolved gas analysis (DGA) results.

1. This insulating mineral oil had not only very large concentrations of several gases, such as methane, ethane, ethylene, propane, and propylene in the pump house, but the hydrogen concentration was extraordinarily high.
2. Four hydrogen concentrations were reported to be 1,218,944 parts per million (ppm), 1,159,630 ppm, 1,755,656 ppm, and 1,029,910 ppm after circulation, with a few concentrations around 725,000 ppm. These levels of hydrogen are rare. It should be noted that whenever comparable hydrogen values were observed in a few other cases, other gases were essentially absent, unlike this case. These high concentrations of dissolved gases indicated that the cable was not fit for service.
3. Acetylene had also been observed in appreciable amounts (about 6.5 ppm), particularly in pre-circulation mode. The presence of acetylene also dictates cable abandonment, particularly in conjunction with other gases.
4. This insulating oil had shown high values of ethylene (3,251 ppm and 3,178 ppm). Moreover, the ratio of ethane/ethylene generated an additional concern.

5. The concentrations of carbon monoxide at a few points were also high, which demonstrated that the cable was past its useful life.

2.2 ASBESTOS CONTAINING MATERIAL

Based on previous sampling of materials slated for removal, ACM had been identified in the somastic coating on the conduits and in the grout and pipe coating in the Pump House at Nueces Bay Substation.

2.2.1 Somastic Coating

The entire length of the land-based 69-kV conduits is coated with somastic containing asbestos and encased in 20-by-20-inch concrete. The entire length of the 69-kV conduits that runs beneath the ship channel is coated with somastic containing asbestos and coated in a cement mix material. The somastic material had been described in the original *Okonite Company "Oilostatic" Installation Instructions*¹ manual as follows:

"The entire exterior surface of the conduit shall be coated with a primer and 7/16 inch thick layer of Somastic (a mixture of sand, asphalt, and asbestos fibers), except for the conduit ends, where approximately six (6) inches from the end of the conduit, the outside shall be free of all coating material. The approximate O.D. over the conduit and coating will be 6-7/16 inches."

A photograph illustrating the conduits beneath the ship channel showing the somastic containing asbestos and cement coating is provided as Figure 2 below.

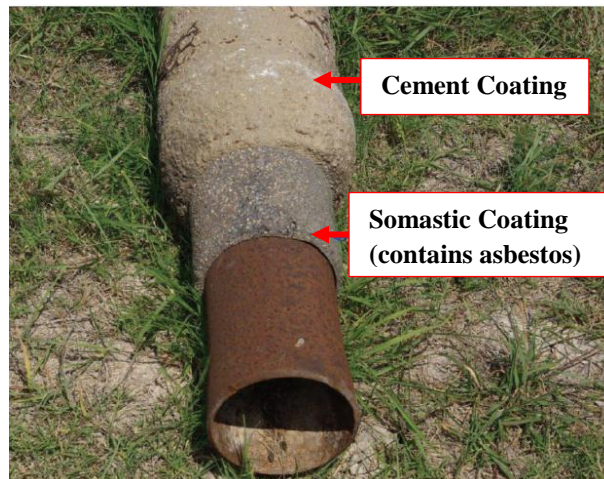


Figure 2: Conduit with Somastic Coating Beneath the Ship Channel

¹ "Oilostatic" Installation Instructions for Conduit, Cable, Pothead for Central Power and Light Company Corpus Christi, Texas. Order # 52120. Okonite FOC - 7238

2.2.2 ACM in Pump House

Before construction and demolition, the pump house had been sampled and identified as containing asbestos in the grout and pipe coating. Proper abatement procedures, including the complete and proper removal of all asbestos, were completed by a certified asbestos abatement contractor.

2.3 CABLE SAMPLING

AEP construction records, reviewed in the planning phase of the project, had indicated that the copper cable itself might be wrapped with a thin somastic asbestos-containing insulating wrap. To ensure the proper removal and transfer of the three-phase cables, each phase had to be properly sampled for asbestos at six locations along each of the underground transmission lines before removal of the conductor. Each phase of the cable was sampled on both sides of each splice joint and at the termination points at the Avery Point Terminal and Nueces Bay Substation. Due to the small amount of time allotted for construction and to ensure appropriate staging of the project with the various contractors involved, two alternative plans were developed in case the cable wrapping contained asbestos. If the cable samples had tested positive for asbestos, the cable would have been cut into small 100-foot sections by an asbestos-permitted contractor and temporarily stored in individual bins to prevent no cross contamination; work under this plan was estimated to last three weeks due to its intensive nature. If the cable samples came back negative for asbestos, each segment of the cable would then be pulled into a single large roll-off container; work under this plan was estimated to last one week. All cable wrapping samples tested negative for asbestos, so the second plan was followed as described in more detail below.

2.4 PCB SOIL SAMPLING

Two composite soil samples each were collected at the Avery Point Terminal and Nueces Bay Substation. Due to the nature of the existing pot heads installed with the transmission line in the 1950s, concern arose that there could possibly be PCB contamination in the soil near the terminal structures. Composite soil samples were collected at 6-inch and 18-inch depths. No PCBs were detected in these samples.

3.0 DECOMMISSIONING AND DEMOLITION PLAN DESCRIPTION

The decommissioning project included the removal of the cables and mineral oil contained within the underground conduits, and the demolition of associated surface structures for this electrical system.

3.1 DEMOLITION PLAN

The decommissioning and demolition of surface structures at the Nueces Bay Substation and at Avery Point Terminal consisted of:

- Pressure control house (pump house) at Nueces Bay Substation
- All equipment within the pump house (500-gallon steel tank, carbon steel piping and valves, and pump controller)
- Underground conduits up to the property boundary at the Nueces Bay Substation and the Avery Point Terminal
- Utilities disconnection and demolition
- Two cable termination point structures at the Nueces Bay Substation
- Two cable termination point structures at Avery Point Terminal
- Concrete slabs underneath cable terminations and reactors at Nueces Bay Substation

3.2 CABLE AND FLUID REMOVAL PLAN

The contractor was responsible for the removal of the transmission cables and insulating mineral oil in the cable conduits, excavation of the buried cable splices, and capping of the conduit at the Nueces Bay Substation and the Avery Point Terminal as described in the following paragraphs.

3.2.1 Excavation of the Buried Cable Splice Joints

There were four buried splice joint locations, two on each line, along the route of the underground transmission lines. The steel conduit was encased in 20-by-20-inch concrete along its entire length except for the section beneath the ship channel. The splice joints were uncovered to allow the draining of the insulating mineral oil and the pulling of the cables from the conduits. After the oil and cable were removed, the joints and surrounding land and road disturbance associated with the excavation were restored to previous conditions. Original construction records did not mention a concrete encasement, so during the initial exploratory work, there was little to no data to assist with the location of the four buried splice joint locations. The only identifier was a grounding cable which terminated outside the concrete encasement. All excavations performed around existing utilities were performed using a hydro excavator, which utilizes high-pressure water and a vacuum truck to remove earth, debris, and spoils to reduce risk of damage to existing utilities and to eliminate the need for an in-depth underground utility survey.

3.2.1.1 Roadway Restoration

The underground transmission lines ran alongside Navigation Boulevard on the north side of the ship channel. The excavations which uncovered the cable splice joints on the transmission lines cut into the road shoulder and northbound traffic lane. The road was being widened, and the construction zone encompassed the locations of the buried conduits. Following the cable and fluid removal from the conduits, the road surface was restored to its original condition, which required work schedule coordination between the POCCA and their road contractor, AEP and their transmission line removal contractors, and Burns & McDonnell.

3.2.2 Removal of the Insulating Mineral Oil

The contractor drained as much of the insulating mineral oil from the conduits as possible prior to cutting and opening the splice joints by inserting a valve in the low point of the conduit. As previously discussed, laboratory analyses for dissolved gases indicated that there were elevated concentrations of combustible gases, but no PCBs were detected in the oil. To reduce the possibility of ignition, the contractor pumped over 10,000 gallons of water into the conduits to assist with the removal of the estimated 5,000 gallons of mineral oil. The solution was pumped to a 20,000-gallon tank, which was monitored for lower explosive limit (LEL). The concern was that with such high hydrogen concentrations reported in the oil, if not diluted with water, the oil might combust when mixed with air. Also after beginning operations at the pump house of pumping water to push the oil, the viscosity of the oil made it almost impossible to push. After six hours of pumping, it was reported to the team that the oil entering the tank was only flowing at one gallon per minute (gpm), which would have taken more than two weeks to transfer all of the oil to the tank. However, after 500 gallons of oil had been removed from the conduit, the addition of the water had decreased the viscosity of the fluid and the transfer rate increased to 30 gpm. It took only three days, as originally proposed, to remove the oil and water solution from the conduits, pump the oil and water solution into the tank, and remove the water and oil from the site using disposal waste trucks.

3.2.3 Removal of HPFF Transmission Cables

The cables were pulled from the conduits by utilizing an excavator at the exposed splice locations. A trailing rope and pipe pigging device was attached to the opposite ends of the cables and pulled through the conduit to remove residual fluids. This trailing rope was used for subsequent swabbing and cleaning of the conduit following cable removal. Roll-off containers were staged for the collection of the lengths of cable as they were pulled from the conduits. Catch basins were placed under the open ends of the conduit as the cables were pulled. A vacuum truck was used to contain and remove oil that drained from the cables and conduits. Polyethylene sheets were placed on the ground between the ends of the conduits and the roll-off containers to prevent fluids from contaminating the soil. The cables were cut into lengths and placed in the containers to be collected for salvage by an AEP-approved contractor in Dallas.

3.2.4 Cleaning of the Conduits

After the fluid was drained and the cables removed, the conduits were cleaned using swabs and dry cloths. A biodegradable, water-based (non-hazardous) degreasing solvent was also used to aid in the cleaning of the conduits. The conduit was then pigged with a temporary pig launcher and catch receiver, fabricated in the field with carbon steel pipe and flanges. A series of pigs were pushed using compressed air and nitrogen at 30 pounds per square inch (psi) in each 1.1-mile run of conduit.

3.2.5 Restoring the Buried Splice Joint Locations

The conduits were re-welded and connected at the locations where the cuts in the joints were made. The weld reconnections in the conduit were restored to gas-tight conditions. The splice joints were then re-encased with 20-by-20-inch concrete. The somastic coating was not replaced.

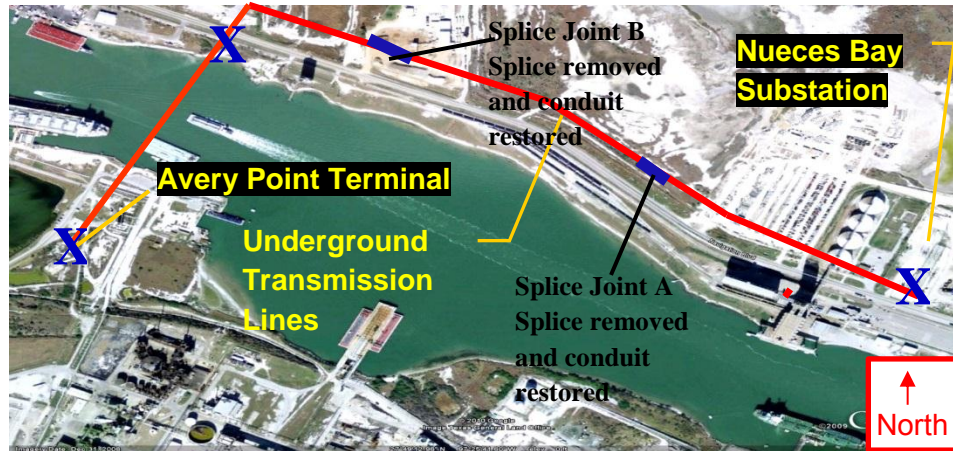


Figure 3: Approximate Locations of Splice Joints and Where Conduit Was Capped

3.2.6 Installation of Conduit Caps

The 69-kV underground conduits were capped at four locations: 1) just outside the property boundary of Nueces Bay Substation at the intersection of POCCA property; 2) where conduits enter the ship channel on the north side of the channel; and 3) just outside the property boundary of Avery Point Terminal (see figures). Welded conduit caps were placed on the ends of the conduits at the above-described locations. The welded caps were air tight to facilitate the retention of the nitrogen gas in the conduits.



Figure 4: Locations of Encased Conduits

3.2.7 Stabilization of Conduits with Inert Gas

After installation of caps on the conduits, all sections of the conduits were filled with dry nitrogen gas pressurized to at least 30 psi. Upon verification of pressure maintenance 48 hours after filling the empty conduits with gas, no further maintenance or inspection was required. The underground conduits were left in a safe and reusable manner; with the intent to deed ownership over to the POCCA.

3.2.8 Removal of the Cathodic Protection System

In preparation of Phase II, the energized, but currently deactivated, cathodic protection system was decommissioned and removed during Phase I. This system consisted of an electrical pole with a rectifier system at the north bulkhead, a buried anode underneath this rectifier and polarization cells, which connect the conduits to the grounding grids at Nueces Bay Substation and Avery Point Terminal.

4.0 PHASE II – FUTURE REMOVAL OF CONDUIT IN SHIP CHANNEL

4.1 CONDUIT IN THE SHIP CHANNEL

POCCA is in the planning phases of a project that would authorize and fund a project to deepen the inner harbor portion of the Corpus Christi Ship Channel from its existing depth of 45 feet to 52 feet to allow for larger ships and increased ship traffic. POCCA, in consultation with and under the direction of the U.S. Army Corps of Engineers (USACE), would require the removal or deepening of all pipelines of insufficient depth crossing the ship channel upon the channel's deepening. The removal of pipelines in the pipeline corridor that cross the ship channel at Dock #4 would include approximately 29 pipelines (including the three AEP conduits). Additional pipelines, as shown on the Railroad Commission of Texas's website, would also likely need to be removed or buried deeper to allow deepening of the channel. The timing and contractual structure of the channel dredging project has not been established.

Concurrently with the Phase I activities, POCCA requested that AEP evaluate the feasibility of removing the three conduits that cross the ship channel (Phase II) in preparation for the potential channel deepening project. As previously discussed, the insulating mineral oil and the copper conductors were removed and properly disposed, and the conduits were thoroughly cleaned and pressurized with nitrogen during Phase I of the project. Each of the conduits is coated with an asbestos-containing somastic and cement mixture.

4.2 FEASIBILITY STUDY OF THE REMOVAL OF 69-KV CONDUITS

AEP requested Burns & McDonnell to conduct a feasibility study to better understand the practicability, risks, liability, costs, and technical feasibility associated with the removal of the three AEP conduits beneath the ship channel. Components of this feasibility study included historical document review, summarization of discussions with potential removal contractors, commissioning of a marine survey,

summarization of the scope and liabilities associated with the project, preparation of a Limited Risk Assessment using an U.S. Environmental Protection Agency (EPA) Risk Model, assistance with the preparation of the draft AEP/POCCA Letter Agreement for Ownership Transfer, adjoining pipeline ownership research, and an overall conduit removal risk and liability assessment.

4.2.1 Feasibility Study Alternatives

The feasibility study examines the potential alternatives to AEP for final disposition of the conduit segments beneath the ship channel.

- Alternative 1 is basically considered “no-action” at the present time. Implementing this alternative would greatly reduce AEP’s liabilities and risks associated with damaging adjacent pipelines during removal. AEP would not remove their conduits until the use of the active pipelines in the immediate area was terminated, and the pipelines were cleaned and/or removed – thus minimizing the risk involved with the removal of AEP’s conduits. This alternative would have less impact to the ship channel traffic since all pipelines would be removed simultaneously. Additionally, this alternative would defer costs associated with removal to a later time which should provide for the realization of cost savings since all of the pipelines would be removed at the same time and there would be less inherent risk of damaging active pipelines. AEP has expressed an interest and desire to evaluate this option and is willing to provide its properly allocated share of the costs associated with the ultimate removal of the conduits.
- Alternative 2 examines all aspects of removing the three conduits beneath the ship channel subsequent to the completion of Phase I of the project.

4.2.2 Historical Document Review and Adjacent Pipeline Research

Several documents were key in evaluating the removal of the conduits. The 1989 pipeline survey entitled *Report on Avery Point Pipeline Survey* (Shiner Mosley and Associates ([SMA], 1989) was conducted prior to the initiation of POCCA’s most recent consideration of a dredging and ship channel deepening project in the inner harbor. The purpose of this survey was to verify that the existing pipelines within the corridor were located below -51.0 feet mean low tide (MLT) elevation and that the ship channel bottom topography was appropriate for the planned channel dredging project. Based on this survey, it was concluded that no pipelines were present above the -51.0 feet MLT elevation at the locations investigated.

POCCA informed Burns & McDonnell that eight pipelines that are adjacent to AEP’s three conduits are either abandoned or not in use (Sept. 23, 2011, email from David Krams, POCCA, Subject: AEP 69kV – Proposed Decommissioning Plan at Avery Point). POCCA also provided drawings depicting the 29 pipelines in the pipeline corridor from both the north and south manifolds; these drawings, dated October 1994, show the pipeline sizes and owners.

As additional information concerning the pipelines was necessary for contractors to submit a budgetary estimate for the conduit removal, a second marine and pipeline survey using more advanced surveying

and imaging techniques was conducted by Chris Ransome & Associates Inc. (CRA) and summarized in their report entitled *Hydrographic Survey of 69-kV Transmission Line Conduit, Port of Corpus Christi, Texas*. (CRA, 2012). The horizontal location and depth of burial of the AEP conduits and adjacent pipelines were established. In addition, the bottom topography of the pipeline corridor and the exact bottom elevation profile along the centerline of the conduits were determined. This stretch of the channel was determined to be approximately 53 feet deep with steep slopes on the channel shores. The average range of depth of burial below the bottom surface for the conduits was 2 to 4 feet, with a minimum of 0.8 feet and a maximum of 5.2 feet. Approximately 65 feet of one of the pipelines (or possibly one of the three conduits) is depicted as being exposed. The surveyors also discovered two sets of unidentifiable objects that could potentially pose a risk to construction (obstructions to the conduit removal work).

Several potential contractors were requested to provide a quote for the removal of the three conduits. Quotes were received from Orion Construction, Weeks Marine, and Russell Marine; cost estimates ranged from \$1,126,675 to \$2,525,000, and the length of the project was estimated to be 15-110 days.

AEP conducted right-of-way pipeline ownership research to provide to Burns & McDonnell for incorporation into the feasibility study. According to AEP, many companies could not provide detailed pipeline status on the pipelines they own, so ROW Services contacted the Railroad Commission of Texas to identify pipelines. ROW Services contacted some of the owners of the identified pipelines and some were verified as being active. Burns & McDonnell has contacted and/or obtained information regarding the ownership/status of the adjacent pipelines from POCCA, the Railroad Commission of Texas, the USACE, the Corpus Christi Fire Department, and the National Pipeline Mapping System (NPMS) website. After reviewing all of the information obtained, it was determined that POCCA likely had the most up-to-date ownership and pipeline status information and at least 40 pipelines in the ship channel would have to be removed or buried deeper if the channel were deepened. However, since much of the information was incomplete and contradictory, little confidence should be placed on this information. It would be prudent to assume that it is possible that additional pipelines may exist near the AEP conduits and that any adjacent pipelines may be active.

4.2.3 Conduit Removal Risk and Liability Assessment

The Burns & McDonnell project team evaluated the policies, procedures and other information provided by the potential contractors and conducted a risk assessment exercise to better understand the potential costs associated with ship channel closure, potential pipeline damage caused during removal work, and

subsequent release. The identified risks and contractor-proposed mitigation efforts are summarized as follows:

- Safety of divers associated with the project — Diver safety will be achieved by closing the channel and/or enforcing slow bell procedures when underwater diving for the project is required within the channel limits.
- Damage to adjacent pipelines — Divers will assist all underwater work to minimize the potential for damage to the adjacent pipelines owned by others. Adjacent pipeline owners will be notified of the activities in the ship channel and all parties will be aware of emergency procedures if damage to a pipeline does occur. One contractor proposed to minimize potential damage by using a hands-on diver approach to remove the AEP conduit closest to the nearest pipeline singularly.
- Airborne release of ACM — Concrete-encased conduit will remain wet or covered in plastic at all times to mitigate the release of airborne ACM.
- Stability of the north and south banks when the conduits are exposed — Further evaluation of the potential instability of the other pipelines after the removal of the overburden above the AEP conduits will be conducted.
- Interruption of ship channel traffic — Contractors will notify all mariners of the removal activities. Contractors will coordinate with the harbor master so as to minimize any impact on ship traffic.
- All risks — Risks can be minimized by the development of provisions for emergency spill response and by contractor's acceptance of responsibility for all damages.

Burns & McDonnell reviewed economic and financial studies of POCCA (Martin Associates, 2010 and POCCA, 2012) to estimate the economic impacts that could result from the closure of the ship channel. As the conduits are in the inner harbor portion of the ship channel, an area that is somewhat isolated from Nueces Bay and Corpus Christi Bay, it is highly unlikely that all port activities would be halted should the ship channel be closed due to conduit removal activities. Therefore, it is inappropriate to use the values directly from the referenced reports. As a result, Burns & McDonnell contacted Mr. Anthony Alejandro, the Director of Operations at POCCA, and Mr. Dennis DeVries, Director of Finance at POCCA, to attempt to monetize the cost to POCCA should the channel have to be shut down due to the subject activities. Burns & McDonnell did not receive a response from Mr. DeVries, but Mr. Alejandro provided much input on the consequences of a ship channel closure.

Mr. Alejandro stated POCCA makes most of their revenue based on the tariffs placed on vessels for wharfage and dockage charges, loss of revenue for POCCA results if ships are not able to move freely through the channel to load and unload their cargo. Mr. Alejandro indicated that closure for a single day would not have a severe impact, but closure for more than a day could cause problems with production for their customers. For example, if ships can't bring in feedstock, some of POCCA's customers would have to stop production. If product cannot leave the port, their customers' tanks would fill up and they

would have to stop production as well. In addition, a channel closure would directly impact the income of the pilots, tug boat companies, line handling companies, etc.

As an alternative means of estimating the impact, Burns & McDonnell used tables in the 2011 Financial Report and estimated the potential daily loss of revenues to POCCA to be \$101,169 if the inner harbor is closed. This value does not take into account reimbursements from activity interruption insurance, nor additional expenses by industries along the port that may be incurred should such a closure be required.

4.2.4 Limited Risk Assessment Using EPA Risk Model

Burns & McDonnell expanded upon information gained from the marine surveys and conversations with pipeline removal contractors to further investigate the potential financial risks and associated liabilities that pipeline removal contractors could face during the removal of AEP's three conduits from beneath the channel. Based on the historical information about the nature of the ship channel crossing, Burns & McDonnell designed three plausible scenarios in which damage to the eight adjacent pipelines would occur and thus result in a subsequent oil release: a low-risk scenario, less likely scenario, and least likely scenario. The low-risk case describes damaging and causing an oil release from the pipeline nearest (within 1.5 feet) to the AEP conduits. The less likely case describes damaging and causing an oil release from four pipelines within 8 feet of the nearest AEP subject pipeline. The least likely case describes damaging and causing an oil release from the five pipelines within 11 feet, which includes the largest diameter pipeline in the corridor (30-inch). To develop these scenarios and report on the associated financial cleanup costs for an oil spill event, Burns & McDonnell used an EPA oil spill cost model, commonly used to estimate potential cleanup and socioeconomic costs for various spill scenarios at similar site settings. This model, the EPA Basic Oil Spill Cost Estimation Model (BOSCEM), incorporates specific factors such as spill volume, oil type, cleanup techniques and effectiveness, and location-specific vulnerabilities. The resulting calculations for each scenario are \$8,259,726 for the low-risk case, \$40,298,511 for the less likely case, and \$167,464,529 for the least likely case. After reviewing this information, the decision was made to require the conduit removal contractor to carry a minimum of \$20 million (per occurrence) Sudden & Accidental Pollution liability insurance.

4.2.5 Conclusion of the Feasibility Study

In conclusion, AEP has gathered information regarding costs and risks of removing its three conduits. Costs range from \$1.1 million to \$2.2 million based on the methods utilized, but the cost of the associated risk range from \$8 million to \$167 million. The lowest contractor cost of \$1,126,675 doesn't include costs for AEP's time, permitting, oversight or additional consultation, etc. Removing AEP's conduits before the other pipelines are deactivated and cleaned involves significant risk and potential cost. If AEP removes

their conduits concurrently with the removal of the adjacent pipelines, the contractor's risk and risk to POCCA due to potential ship channel closure are significantly reduced. If this alternative is selected, the owners of the other pipelines would be intimately involved and would have ceased product flow through the pipelines, cleaned the pipelines and be in the process of removing the pipelines for disposal at the same time — all but preventing potential liability exposure to damage to or a release from these other pipelines owned by other companies. In addition, work could likely be performed more efficiently if all of the pipelines could be removed simultaneously. The three AEP conduits do not currently pose risk to the other pipelines, the public, or POCCA. Their presence in the ship channel does not impede POCCA's plans to move forward with the dredging and deepening of the ship channel any more than any of the other pipelines owned by other companies.

5.0 SUMMARY

Phase I of the project consisted of the removal of the cables and oil from the underground inactive conduits and demolition of surface structures associated with the system. Phase II of the project (when conducted) will consist of removing the segments of conduit that cross under the Corpus Christi Ship Channel. During Phase I, Burns & McDonnell was responsible for coordinating with a series of stakeholders. As a portion of the conduit was along a county road that was under construction, it was essential that cable and oil removal be coordinated and phased with ongoing road work to reduce impact to the road expansion project. Contractors with experience in conductor cable removal, cleaning and swabbing of pipelines, and demolition were utilized to ensure project success.

Numerous environmental concerns encountered during the decommissioning of the cables made this project unique, making it essential for Burns & McDonnell to take precautions to avoid potential harmful human exposures. The identified environmental concerns included the flammability of the insulating mineral oil, ACM present throughout the system, and possible PCB contamination of the oil. Phase I lasted over a year and a half, with three months of construction in the summer of 2012 and required a diverse team of interdisciplinary engineers, scientists, and construction managers. This project was completed within the projected timeline with zero Occupational Safety and Health Administration (OSHA) recordables. Burns & McDonnell also was able to save AEP a significant amount of demolition cost by meeting regularly with Port officials and drafting an agreement that benefited both parties, allowing for a majority of the conduit to be abandoned in place and deeded for future use to the POCCA.

Burns & McDonnell conducted a feasibility study to better understand the practicability, risks, liability, costs, and technical feasibility associated with the removal of AEP conduits beneath the Corpus Christi

Ship Channel (Phase II). Components of this feasibility study included historical document review, discussions with potential removal contractors, a new marine survey, summarization of the scope and liabilities associated with the project, preparation of a Limited Risk Assessment using an EPA Risk Model, assistance with the preparation of the draft AEP/POCCA Letter Agreement for Ownership Transfer, adjoining pipeline ownership research, and an overall conduit removal risk and liability assessment. AEP gathered information regarding costs and risks of removing its three conduits. Costs range from \$1.1 million to \$2.2 million based on the methods used, but the cost of the associated risk range from \$8 million to \$167 million. Removing AEP's conduits before the other pipelines are deactivated and cleaned involves significant risk and potential cost. If AEP removes its conduits concurrently with the removal of the adjacent pipelines, the contractor's risk and risk to POCCA due to potential ship channel closure are significantly reduced. If this alternative is selected, the owners of the other pipelines would be intimately involved and would have ceased product flow through the pipelines, cleaned the pipelines, and be in the process of removing the pipelines for disposal at the same time - all but preventing any potential liability exposure to damage to or a release from these other pipelines owned by other companies. In addition, work could likely be performed more efficiently if all of the pipelines could be removed simultaneously. The three AEP conduits do not pose risk to the other pipelines, the public, or POCCA. Their presence in the ship channel does not impede POCCA's plans to move forward with the dredging and deepening of the ship channel any more than any of the other pipelines.

6.0 REFERENCES

- Chris Ransome & Associates, Inc. (CRA), 2012. *Hydrographic Survey of 69-kV Transmission Line Conduit, Port of Corpus Christi, Texas*. February.
- Krams, David, 2011. *September 23, 2011 email from David Krams, POCCA, Subject: AEP 69-kV – Proposed Decommissioning Plan at Avery Point*. September 23.
- Martin Associates, 2010. *The Local and Regional Economic Impacts of the Port of Corpus Christi*. April 18, 2010
- Mullins, Henry, L., 2012. *October 16, 2012 Email from Henry L. Mullins, USACE, Subject: Corpus Christi Ship Channel Drawings (Unclassified)*. October 16.
- Port of Corpus Christi Authority (POCCA), 2012. *Port of Corpus Christi Authority of Nueces County, Texas Comprehensive Annual Financial Report for the Year Ended December 31, 2011*.
- Shiner Mosley and Associates, 1989. *Report on Avery Point Pipeline Survey*. June.

Practical Considerations and Solutions Employed in the Thermal Design and Operation of a Power Transformer

David L. Harris and John Prunte

SPX Transformer Solutions

PRACTICAL CONSIDERATIONS AND SOLUTIONS EMPLOYED IN THE THERMAL DESIGN AND OPERATION OF A POWER TRANSFORMER

David L. Harris

Customer Technical Executive
SPX Transformer Solutions, Inc.

John Prunte

Director of Technical Support
SPX Transformer Solutions, Inc.

Introduction

Presented is an analysis of the thermal characteristics of oil-filled, core form medium power transformers. The aging effects of heating on the insulation system, resulting from losses and loading, are examined and the cooling system's role in minimizing these effects is shown. How the cooling system operates and how its performance is verified by temperature rise testing will also be explained. Our intent is for this presentation to provide the necessary information and understanding as to why properly designed cooling systems are important to maintain suitable temperatures and maximize the transformer's operational life.

Losses

The transformer generates losses as a by-product of applied voltage and current flow when being utilized in the transmission system. There are several sources of losses within the transformer.

First are the no load losses, which are generated by the core when the transformer is energized. The grade of core steel and flux density are the factors considered when measuring no load loss which varies only with voltage and will remain virtually constant for variations in loading of the windings.

Load losses (the sum of I^2R), eddy, and stray losses, vary with loading changes of the transformer. I^2R losses are proportional to the square of the current carried by the transformer winding, dependent on the resistance winding material. Eddy losses are a function of the width and thickness of the winding conductors and are calculated as a percentage of the winding resistance loss. Stray losses are the losses induced in the tank, core clamp, and other magnetic steel components by the stray flux fields; magnetic shielding and increased clearances from

winding and current carrying leads can minimize the stray losses. The heat generated by these losses must be dissipated; neglecting to properly remove this heat results in accelerated aging of the cellulose insulation.

Insulation

The transformer's insulation system is a combination of oil and cellulose paper. Transformer oil is highly refined, hydrocarbon-based oil and plays an integral part in the dissipation of heat generated by the transformer. The insulation requirements include maintaining dielectric strength from switching transients, lightning strikes, and maintaining mechanical strength against short circuit forces.

Cellulose paper insulation is a specially processed and thermally upgraded material that, once oil impregnated, allows continuous voltage withstand without dielectric failure. The useful life of a transformer is based upon the ability of the insulating paper to maintain its dielectric strength and prevent failure. Over time, heat, oxygen, and moisture cause the insulating paper to deteriorate and lose its tensile strength.

Tensile Strength:

The tensile strength of the insulating paper allows the transformer to withstand the physical effects of a short circuit and maintain dielectric integrity. Oftentimes people misunderstand the terms "end-of-life" and "loss-of-life" as referring to the life of the transformer. This is incorrect since the terms actually apply to the loss of insulation life. Originally the end-of-life of the insulation was considered to be 50% of the original tensile strength; now, this is generally accepted to be 20%.

Degree of Polymerization:

The degree of polymerization of the insulating material represents the average number of glucose units in the cellulose polymer chain. These values can range from 800 to 1600 units with the most probable value being approximately 1200 for new transformers. As the paper undergoes aging, these polymer chains degrade and break down (into shorter chains) as a result of being subjected to a severe fault, such as overheating or arcing, and exposed to moisture, oxygen, and heat from loading. As shorter length chains are formed, the average degree of polymerization is lowered. Thus, this method allows one to assess the condition of the cellulose insulation within the transformer. Since these values do represent averages, cellulose samples under evaluation should be compared to fresh samples of the same origin.

New Kraft paper will have a degree of polymerization around 1100 to 1200. After factory drying tests, this value will drop to approximately 1000 and then decreases exponentially with time. A tentative value of 200 is used to indicate the end of the cellulose's useful life. For partial rewinding of failed coils, a typical minimum value of 300 is generally used.

This is an intrusive test which does require a paper sample, and the acquisition of this

sample requires the unit be taken out of service. Please note that the sample should be representative of the highest hot spot temperature where the degree of polymerization would be lowest, and the area from which the sample was removed will need to be reinsulated before returning the transformer to service.

Rated Loading

Loading is defined in terms of the nameplate rating of the transformer. The nameplate ratings define the operational parameters around which the transformer has been designed. Typically, medium power transformers are rated for loading at temperature rises of 55 and/or 65 degrees C and are also defined in cooling terms of ONAN, or self-cooling, and two stages of ONAF, or forced air cooling.

Increased loading capability using forced air cooling is typically 33.3% of the self-cooled rating for the first stage and an additional 33% of the self-cooled rating for the second stage. For example, a transformer rated at 12 MVA ONAN and a 65 degree C rise is defined as being capable of supplying a 12 MVA load with an average winding and top oil temperature rise limit of 65 degrees C by self cooling alone. The first stage of ONAF cooling will supply 16 MVA (12×1.333) of load at an average winding and top oil temperature rise limit of 65 degrees C and 20 MVA (12×1.667) of load with an average winding and top oil temperature rise limit of 65 degrees C with the first and second stage of forced cooling in operation.

Thermal Design

The primary factors that influence the thermal design of the transformer include the losses generated from operation of the transformer under load, the circulation of oil in the windings and radiators, the effective surface area provided by the radiators, and the volume of air across the radiator fins by the fans. All of the above factors affect the following:

- average oil temperature
- winding temperature gradient
- hot spot winding temperature gradient

As noted earlier, losses occur due to heating of the core and windings and must be removed to prevent the windings from reaching temperatures that can cause accelerated aging of the cellulose insulation. Losses are the result of winding current density controlled by the winding conductor area and core steel material area controlling flux density in the core. With loss evaluation specified, the conductor and core steel quantities are normally designed to the established limits per the design practice of the manufacturer, unless some other design or customer parameter necessitates the use of more of these materials. This results in a higher loss design since the materials are being minimized to reduce the overall material costs of the transformer. Applying an evaluation of the losses will require that the manufacturer minimize the combination of the cost of losses generated and the cost of materials; thus, the higher the loss evaluation, the more

conductor and core steel will likely be used to reduce the generated losses and their associated cost.

The differential between the average conductor temperature of the winding and the average oil temperature in the transformer tank is defined as the gradient. The gradient is directly related to the amount of conductor surface area exposed to the surrounding oil. A higher gradient means that winding current density is higher, and less surface area is exposed to the oil, meaning more heat is retained by the windings. This requires more external cooling to lower the average oil temperature so that when the gradient temperature is added, the average winding rise meets the temperature rise guarantee. With a lower gradient, less cooling is needed since the winding is able to release the heat generated by losses to the surrounding oil, thereby allowing a higher average oil rise while still meeting the guaranteed temperature rise. Increasing the amount of conductor surface area exposed to oil to allow more heat to migrate out of the windings can be accomplished in several different ways:

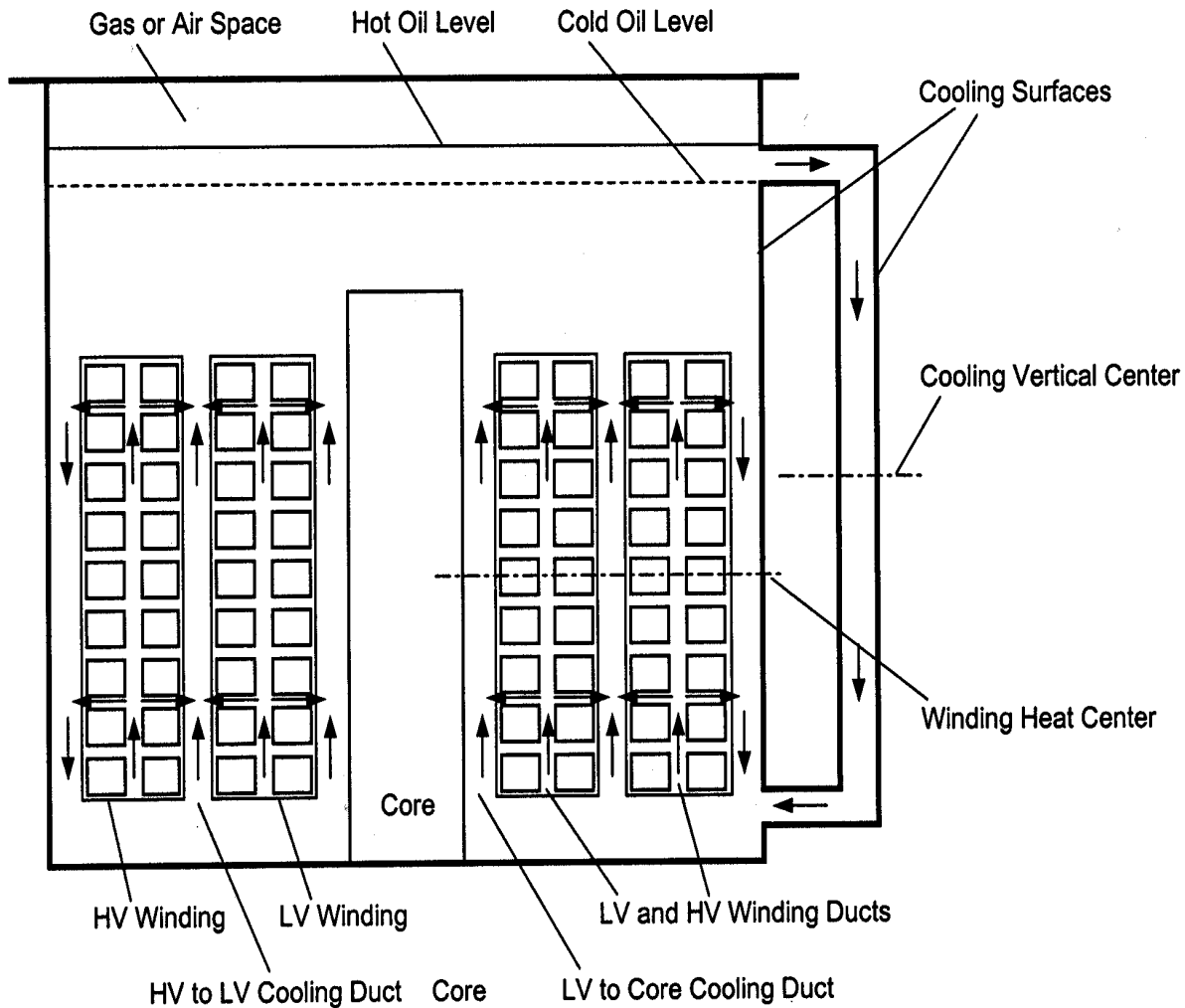
- Turns can be redistributed to increase the number of disc sections
- Cooling ducts can be inserted in the radial build of the winding
- Number of radial spacers and/or the width of the radial spacers can be reduced

Transfer of the heat produced by losses in the windings and core steel is critical to the performance and life of a transformer. This heat transfer can be accomplished using various transfer mechanisms, such as thermal conduction, thermal convection, and thermal radiation.

Thermal conduction is the direct transfer of kinetic energy of particles between two systems. When an object—in this case, core and windings—are at a different temperature than the liquid surrounding it—mineral oil—heat flows so that the liquid reaches the same temperature as the windings and core, at which point they are in thermal equilibrium. Such spontaneous heat transfer always occurs from a region of high temperature to another region of lower temperature, as described by the second law of thermodynamics.

Thermal convection occurs when bulk flow of a fluid, such as mineral oil, transfers heat from the windings to the radiators through a process often called "natural convection". All convective processes also move heat partly by diffusion. Another form of convection is forced convection by use of a pump, fan, or other mechanical means.

Thermal radiation occurs when the mineral oil is transferred to the radiator fins where the heat is transferred by radiation to the surrounding ambient air which is at a lower temperature. As the oil absorbs heat from the windings, it loses density and rises up through the windings, collecting even more heat along the way, until it finally reaches the top of the windings. This pool of oil over the top of the windings migrates to the tank and radiator surfaces, where it cools off and becomes denser, returning it to the bottom of the tank and windings where the process is repeated.



Arrows represent the typical flow patterns of oil circulation in the windings and tank

Figure 3
Typical Transformer Oil Circulation Pattern

The two most commonly used oil circulation systems are **natural circulation**, or thermo siphon, which relies on the change in the density of the oil due to temperature variation to produce oil flow, or **forced oil flow**, which circulates the oil by using pumps in the external coolers.

The thermo siphon process is dependent on the location of the heat center of the windings in relation to the vertical center of the external cooling. This relationship, called the “thermal head”, becomes more efficient as the vertical center of the external cooling is raised above the heat center of the winding. By using pumps to circulate the oil, a constant volume of oil flow is maintained, independent of the transformer load and heat exchange rates required for natural circulation. This consistency in oil flow volume comes at an increased cost in equipment, power consumption, and maintenance, thus, oil pumps would normally be specified only when higher efficiency is required due to space limitations or special loading conditions.

Radiators are used as a means to dramatically increase the amount of oil surface area exposed to the surrounding environment for a given space, greatly improving the efficiency of the heat exchange from the oil to the surrounding environment. Radiators are normally made of thin parallel vertical plates stacked horizontally, and heat is transferred from the oil to the surrounding environment by natural air convection or fans along the exposed plate surface. Again, as dictated by space limitations or loading conditions, heat exchangers (coolers) with higher efficiencies can be employed which use various combinations of pumps, fans, and cooling mediums, such as water, at a significantly higher cost.

Fans are a relatively inexpensive means to increase the rate of heat convection of the radiators. The volume of air a fan can move through a radiator is dependent upon the geometry and diameter of the fan blades and the operating speed of the fan motor, with higher speed and larger diameter making for a greater volume of air movement. The fan speed and blade characteristics also determine the level of noise produced by the fan, with lower speed and smaller diameter being associated with lower noise. The guaranteed sound level can become a limiting factor in transformer loading, since low sound requirements require the fan speed to be reduced and, therefore, a reduction in air volume per fan. Thus, more fans and the space required for mounting them must be available in order to achieve the nameplate MVA rating at the guaranteed sound level.

Temperature Rise Test

A temperature rise test is normally performed at the minimum and maximum nameplate ratings to verify that the thermal design of the transformer will supply the nameplate load ratings within the guaranteed temperature rise limits. A simulated load is applied to the transformer—since the energy requirements would be excessive for actual loading—by circulating sufficient current at rated frequency to one set of terminals to produce the maximum total losses for the connection and loading condition being tested and shorting the terminals not under test. The top oil temperature is stabilized at the total maximum loss and the top oil, bottom oil, and average

ambient temperatures are measured and recorded. The current is then reduced to the rated value for the connection being tested and held for one hour, then the oil temperatures are again measured, the applied current is shut off, and the average winding temperatures are measured and corrected to the time of shutdown. The temperature rise results are used to calculate the hottest spot temperature rise of the windings and to verify that the temperature rise guarantees were not exceeded.

Normally, the reported hottest spot temperature rise is a calculated result and not a directly measured value. Even with fiber optic temperature probes that allow a temperature sensor to be placed in direct contact with the coil and have the ability to locate the hottest spot by finite element analysis, the process to locate and install fiber optic probes in transformer windings on a routine basis remains cumbersome and costly. Difficulties occur in trying to ensure the probe-sensing tip has proper contact with the heat source and is not damaged due to handling during the manufacturing process, especially since repairing or replacing a malfunctioning fiber optic probe in a winding requires an almost total disassembly of the transformer. Due to these difficulties, calculation methods are currently the preferred way of reporting the hottest spot temperature rise; a relatively accurate estimate can be provided with the computation tools available without any additional equipment installed in or on the transformer.

Applying Loads At and Beyond the Nameplate Rating

Guidelines for loading oil filled transformers beyond the nameplate rating are given in IEEE Guide C57.91. Listed below are additional factors that can identify greater operational risks, other than the aging and mechanical deterioration of the insulation system, and should be considered when a transformer is loaded beyond the maximum nameplate rating. The risks associated with transformer overloading are as follows:

- Evolution of free gas in oil due to winding and conductor lead insulation heating by load and eddy currents as well as insulation in contact with structural metallic parts at elevated temperatures due to stray flux. This free gas may jeopardize the dielectric strength and integrity of the insulation.
- Reduced mechanical strength of the conductor and structural insulation due to high operating temperatures, especially if a transient resulting in a peak mechanical force were to occur at this time.
- Permanent deformation as a result of thermal expansion of the conductors, insulation, or structural parts that could contribute to mechanical or dielectric failure.
- Gasket leaks and loss of oil in the bushings from pressure build-up, when operated above rated current, resulting in the failure of the bushing.
- A build-up of oil decomposition products on de-energized switch contacts due to localized heating at the contact point when overloaded. This increased contact resistance could result in a thermal runaway condition, in extreme cases, resulting in contact arcing and severe gas evolution.
- An excessively high top oil temperature could result in the loss of oil through the pressure relief device if the hot oil expansion is greater than the tank capacity. This loss of oil could

also present a problem if the oil level drops upon cooling to where electrical parts are exposed.

- Elevated bushing temperatures.
- Elevated gasket temperatures and aging of the gaskets.
- Internal auxiliary equipment, such as reactors and current transformers, may also be subjected to the same risks listed above.

The effects associated with these risks vary between each transformer and must be analyzed on a case-by-case basis. Since the temperature rise test is performed in the maximum loss tap position, the results calculated from this data will provide a somewhat conservative prediction of loading capability when the transformer is operated at other than the maximum loss tap position.

Ambient temperature is also an important factor in determining the loading capability of a transformer. Winding hot spot, top oil, and average winding gradients are added directly to the ambient temperature to determine the operating temperatures of the transformer. IEEE uses a standard 24 hour average ambient temperature of 30 degrees C as the basis for determining transformer ratings. The ambient temperature used should be the average for a 24 hour period, with the associated maximum temperature for the 24 hour period no higher than 10 degrees C above the average ambient temperature. The transformer installation also needs to be taken into account as sound walls, buildings, or indoor applications result in the re-circulation of ambient air, requiring adequate ventilation and appropriate control of the ambient temperature. In order to determine this, use the average 24 hour ambient temperature for loading for normal life expectancy and the maximum 24 hour ambient temperature for short time loading with a moderate loss of life.

Theoretical Life of a Transformer:

The theoretical life of a transformer is based on the thermal aging of the cellulose insulation, at continuous loading at maximum rating, 80°C winding hot spot temperature, and maximum ambient temperature of 40°C. The initial measurement was based on the reduction of the cellulose insulation tensile strength by 50% which resulted in a theoretical life of 65,000 hours, or 7.42 years. The basis for tensile strength was later reduced to 25%, resulting in a theoretical life of 15.42 years.

Degree of polymerization is based on the structure of polymer chains of glucose units with the most probable initial value being about 1200. As the paper insulation undergoes aging, these polymer chains degrade into smaller units. If the paper is subjected to a severe fault, such as overheating or arcing, the polymers will also be degraded. As shorter length chains are formed, the average degree of polymerization is lowered. Thus, this method allows one to assess the condition of the cellulose insulation within the unit. Using a reduction of the degree of polymerization to 200 would result in a theoretical life of 150,000 hours, or 17.21 years. Further interpretation of the IEEE Transformers Committee members, as stated in IEEE C57.91-1981, stated that the functional life of a distribution transformer was 180,000 hours, or 20.55 years.

The introduction of natural ester fluids to replace mineral oil may result in a reduction of the aging of the cellulose insulation and increased life of the transformer.

The calculations of theoretical life are based on a continuous loading of the transformer at the maximum rating with a maximum ambient temperature; however, power transformers are usually loaded well below their maximum nameplate rating, resulting in longer lives. Also, each reduction of transformer hot spot temperature by 6 to 8 degrees can result in doubling the theoretical life of the transformer as shown in table 5 below.

Figure 3 from IEEE Standard C57.12.00-2010 IEEE Standard for Liquid-Immersed Distribution, Power and Regulating Transformers shows the insulation life expectancy variation relative to hottest spot temperature.

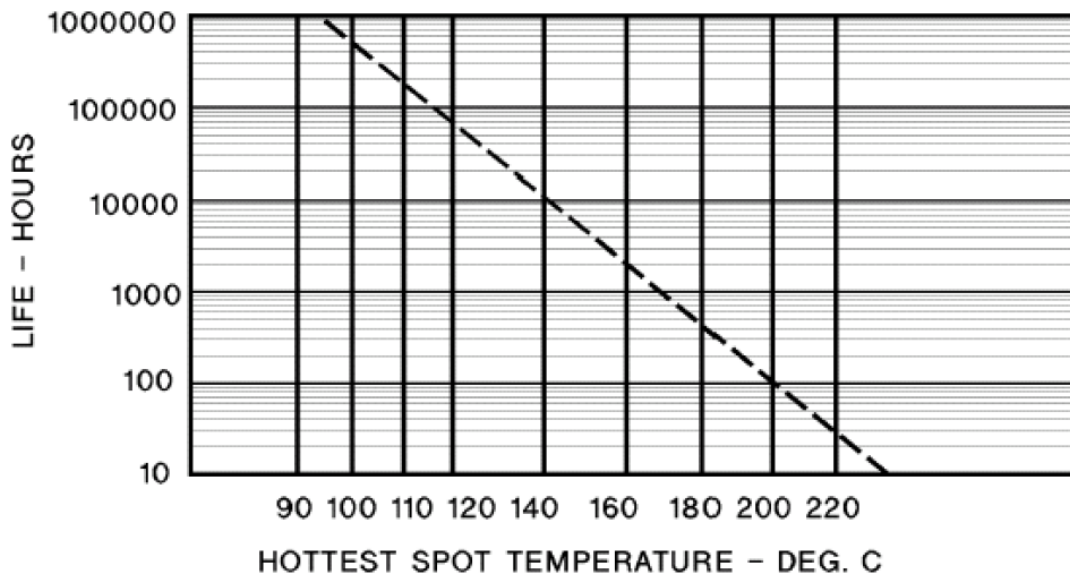


Figure 3—Minimum life expectancy curve for liquid-immersed distribution, power, and regulating transformers rated in accordance with Clause 5, at 65 °C average winding rise, 80 °C hottest-spot rise

Additionally, ensuring the radiators and cooling fans are operating properly to perform the cooling required to control the transformer hot spot temperature will help achieve optimum insulation aging.

The only variable in the equation for transformer life is hot spot temperature (HST), as shown in the following equation: $Life = \exp\left(\frac{15000}{HST + 273} - 27.604\right)$

Hartford Steam Boiler provides insurance for many utilities to cover catastrophic transformer failures. The charts below are based on their data resulting from insurance claims for substation transformers and generator step-up transformers.

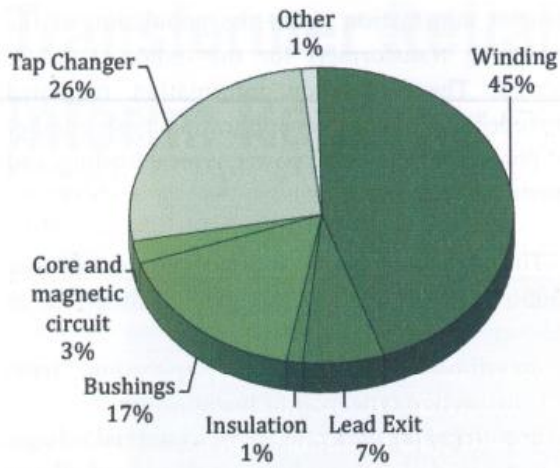


Figure 1: Failure locations of Substation Transformers (>100kV) (based on 364 failures)

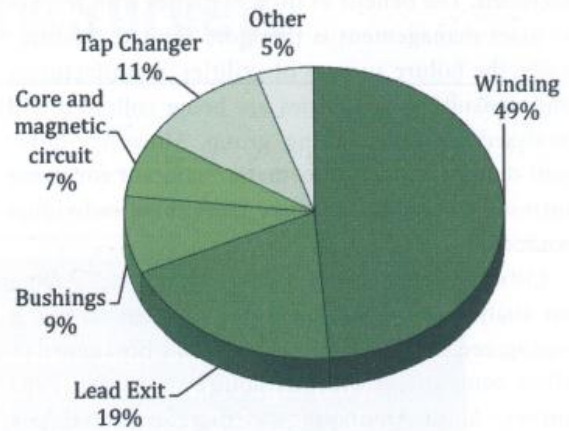


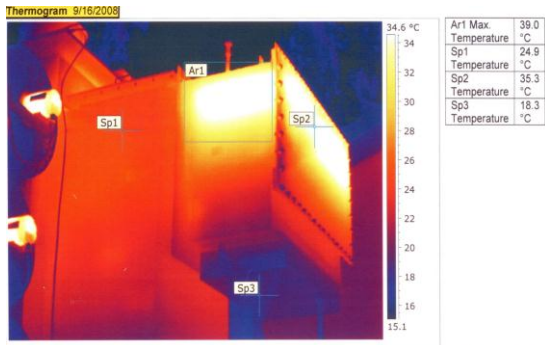
Figure 2: Failure Locations in Generator Step-Up Transformers (>100 kV) (based on 82 failures)

Tap Changers, both de-energized (DETC) and on-load tap changers (LTC), can experience contact coking issues resulting in failures of the tap changer, and many times can also result in catastrophic failure of the transformer if the transformer is not removed from service and the contacts and/or insulating liquid is not maintained to resolve the coking issues.

Tap Changer contacts:



Infrared scanning of the transformer can be used to monitor LTCs and other components of the transformer to detect changes in the operating temperature and early detection of changes in operating temperatures.



Infrared scanning of the cooling system (radiators and fans) can also be used to ensure that all equipment is functioning properly and provide designed temperature levels of the windings and other transformer accessories.

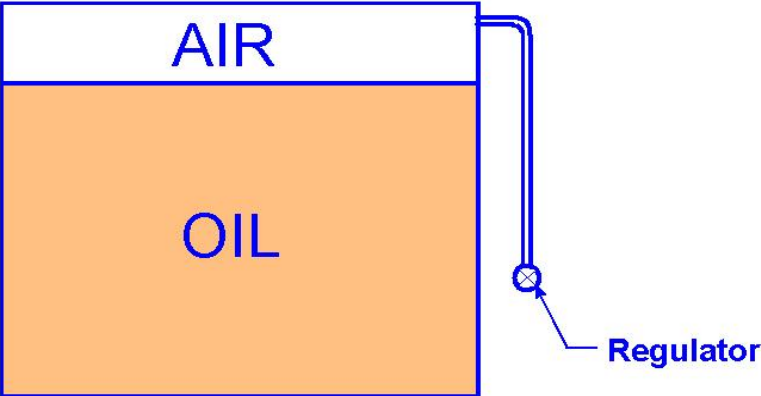
Transformer bushings are the link connecting windings in a liquid filled transformer with the transmission and distribution lines of the substation. A bushing failure can result in contamination of the transformer’s internals, resulting in extensive damage to the transformer.



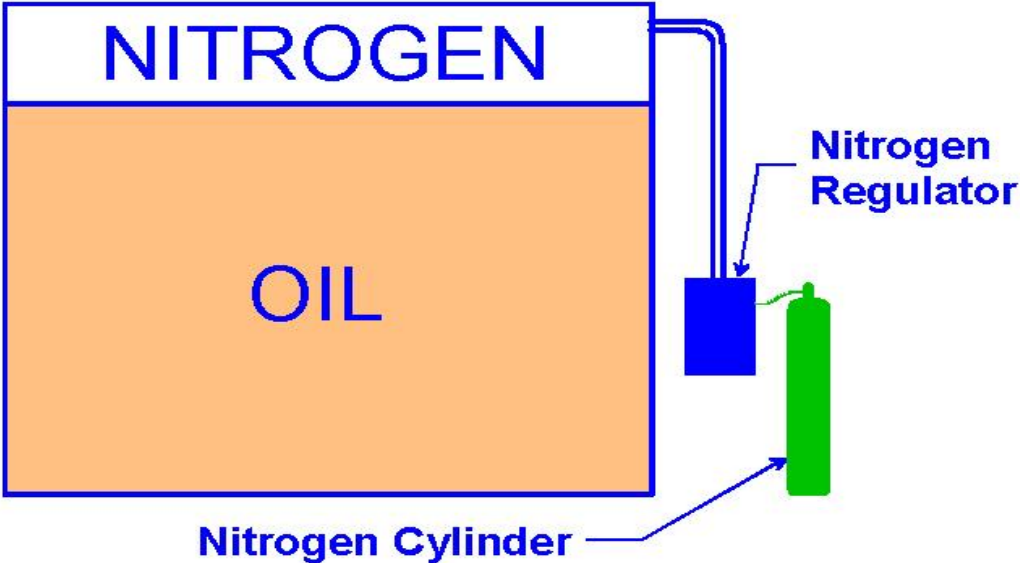
Gaskets provide a seal for manholes, bushings, and accessories installed externally on the transformer with internal connections. As gaskets age, they lose their durability and this loss of integrity can result in oil leaks. In the event of emergency overload operation, aged bushings could develop oil leaks due to the higher temperature and pressure resulting from the overload operation.

The oil preservation system is critical for maintaining the integrity of the transformer against oxygen and moisture.

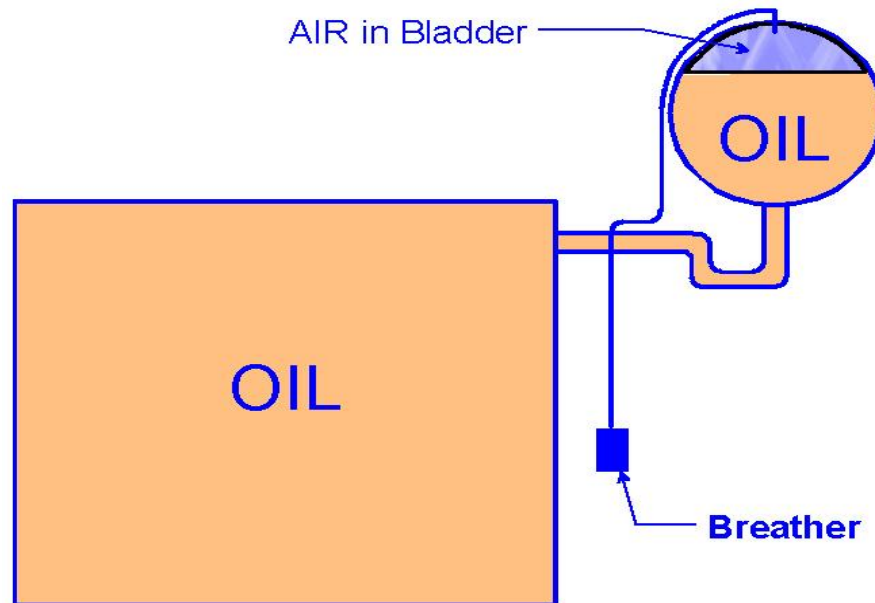
Sealed Tank routinely filled with nitrogen when placed in service.



Inert gas oil preservation system designed to continuously maintain the nitrogen blanket above the oil.



Conservator oil preservation



The four factors that affect the aging of the transformer most are as follows:

- Time
- Temperature
- Moisture
- Oxygen

Controlling any of these parameters, individually or in combination, can significantly retard the aging process of insulating oil and paper. The role of the oil preservation system is to limit the entry of moisture and oxygen into the transformer liquid (mineral oil or natural ester fluid) and provide optimum control of the cellulose aging process.

Conclusion

The key to maximizing operational life of a transformer centers on proper care of the insulation system. In addition to minimizing exposure to moisture and oxygen by routine maintenance of the oil, a thermal design that is well coordinated to the loading requirements of the transformer helps reduce the effects of temperature on the insulation and slows down the degradation of the insulation system. Presently, this is best accomplished by using loading guide calculations found in IEEE Guide C57.91.

Optimization of the Power Transformer Dry-out Process in the Field—Application of Advanced Diagnostic Technologies

Diego M. Robalino, Ph.D. and Peter Werelius, Ph.D.

Optimization of the Power Transformer Dry-out Process in the Field

Application of Advanced Diagnostic Technologies

Diego M. Robalino, Ph.D.
Senior Applications Engineer
Megger North America

Peter Werelius, Ph.D.
Application & Product Specialist
Megger Sweden

Abstract: Utilities in North America face the continuous and growing demand for power from customers. Utilities primary focus is on providing an efficient, secure and reliable energy supply to the entire industrial, commercial and domestic population. Power and distribution transformers — maybe the most important components of the energy system — are impacted by the normal and unidirectional aging process. Due to load demand, there are few opportunities to take transformers out-of-service for testing and/or maintenance. Therefore, the risk of failure must be minimized by applying technical methods capable of reducing time and materials spent during the testing and maintenance of high voltage apparatus.

Field dry-out of power transformers is nothing new to power system operators; the procedure and the expectations of the different types of processes are well known (as are the limitations of each specific system). At the beginning of the manufacturing process, strict control is implemented in the quality of materials used for the construction and assembly of transformers. Special attention is given to the solid insulation components in order to minimize exposure to an environment where they might get contaminated (especially with moisture). After assembly completion of the active part of the transformer, the windings and core are subjected to different dry-out processes to remove moisture from the cellulosic material without affecting the life expectancy parameters (defined by the degree of polymerization and tensile strength of the cellulose). Throughout the life of the transformer and due to the normal aging effect, several byproducts will evolve within the insulation system, and field operators will encounter the challenge of re-conditioning the insulation system of the transformer, removing as much as possible these aging byproducts on-line or off-line.

While a variety of methods are available for field dry-out, identifying the real problem inside the transformer and selecting the correct (or appropriate) process should be the first decision. Today, advanced condition assessment is performed in the field using dielectric frequency response (DFR) instruments capable of discriminating moisture in the solid insulation from dielectric oil conductivity. The dry-out process must later be evaluated, and the remaining moisture in the insulating system requires an accurate estimate before the transformer is put back into service. In this work, thanks to the support of a local utility and the implementation of safe procedures for field dry-out processes, a power transformer is continuously monitored using DFR; analysis and validation is carried out comparing cold trap water volume.

In this document, DFR field application is demonstrated to optimize the dry-out process, providing immediate condition assessment of the insulation spectrum variation throughout the process, determining the efficiency of the process and minimizing the risk of overstressing the mechanical structure of the solid insulation.

I. INTRODUCTION

There are several factors affecting the condition of power transformers. These factors accelerate the aging process of the insulation system and therefore, reduce the reliability of the operation increasing the risk of failure. Electrical, thermal, mechanical and chemical stresses are actively and continuously deteriorating the mechanical and dielectric properties of the insulation materials.

Moisture is a formidable enemy. The presence of moisture in the oil and paper insulation of oil-immersed power and distribution transformers is inevitable. Sources of moisture vary and can be linked to factors such as manufacturing process controls, time of exposure to the atmosphere and leaks, as a byproduct of the aging process based on specific thermal and load profiles and the type of construction of the transformer itself. Nevertheless, the best way to assure dryness of a new unit is confirming the effectiveness of the dry-out process on the factory floor. The importance of this critical stage during the manufacturing process is part of this study and has been incorporated to illustrate the benefit of a controlled system during thermal dry-out of the active part before assembly.

Throughout the service life of the transformer, the moisture concentration tends to increase, and field operators should monitor these changes in the dielectric characteristics of the solid or liquid insulation. It is important to understand how the dielectric characteristics of the oil-paper insulation can provide field operators with the necessary information to implement preventive or corrective actions that may extend the life of the unit, minimize the risk of failure and increase the reliability of operation. The insulation system of most power transformers consists of oil and cellulose. Both these materials change their dielectric properties over the transformer's life span. When measured at a fixed frequency only, the property changes in different materials cannot be discerned.

Dielectric response techniques have been studied and evaluated by several researchers and industry experts. Time domain and frequency domain testing technologies are available for data acquisition; analysis of the dielectric response in order to determine the percentage moisture concentration in the solid insulation is performed in the frequency domain.

The application of Frequency Domain Spectroscopy (FDS) during transformer dry-out processes is described throughout this document.

II. FREQUENCY DOMAIN SPECTROSCOPY (FDS)

A. Fundamentals of FDS

FDS is a generalized advanced application of the well-known capacitance and dissipation factor ($\tan\delta$) or power factor measurements usually performed at or close to power frequency (50/60Hz). FDS is commonly used to determine the condition of the insulation system in high voltage electrical equipment. FDS provides several measurements performed at different frequencies rather than a single measurement at a single fixed frequency.

The measurement principle can be described as follows: a digital signal processing unit generates a sinusoidal test signal at a specific frequency. This signal is amplified with an internal amplifier and then applied to the selected capacitance of the unit under test (UUT). The applied voltage and the current through the specimen are measured with high accuracy using a voltage divider and an electrometer. As a result, the complex impedance, "Z," is obtained as a function of frequency including its values close to power frequency as well. The diagram of the measurement set-up applied on a two-winding transformer is shown in figure 1.

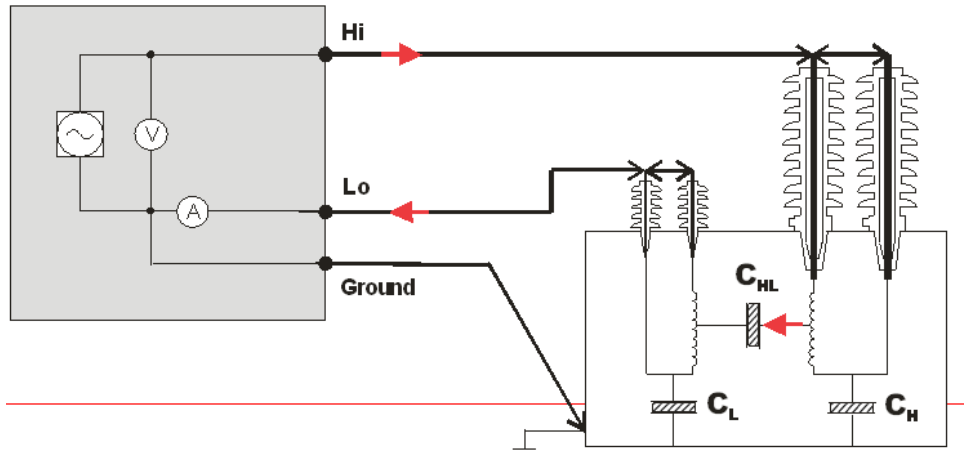


Figure 1. FDS measurements set-up for a two-winding transformer.

From the complex impedance value, the relevant parameters such as dissipation factor and capacitance are derived. Moreover, if the geometrical capacitance of test object is known or it is estimated by a dedicated modeling software, then the complex permittivity can be obtained at different frequencies $\hat{\epsilon}(\omega)$. Likewise, from the real and imaginary components of the complex permittivity, dissipation factor can easily be calculated as

$$\tan \delta(\omega) = \frac{\epsilon''(\omega)}{\epsilon'(\omega)} \quad (1)$$

One of the great advantages of FDS over the time domain method is that FDS is relatively insensitive to interferences. State-of-the-art technology implemented an efficient filtering system capable of minimizing the corruptive effect of AC and DC noise in substations reducing the influence of line frequency and its harmonic components.

By measuring capacitance and dielectric losses over a frequency spectrum, normally between 1 kHz and 1 mHz (rather than at a fixed frequency), plentiful data regarding the status of the insulating material can be obtained. The data on dielectric responses makes possible to conduct in-depth analysis of each component of the insulation system, and as a result, determining the percentage moisture concentration in the solid insulation (%mc), the conductivity of the liquid insulation (σ), the presence of contaminants and the thermal behavior of the 60Hz power factor value for that unique tested insulation. A typical dielectric response of an oil/paper system is shown in figure 2.

FDS signal is normally fixed to 200V_p. Several references investigating oil/paper systems, such as power transformers, bushings, mass impregnated high and medium voltage cables [1][2][3], have shown that this type of insulation behaves linearly. Therefore, the power factor or dissipation factor measured at line frequency is independent of the applied voltage under ideal conditions. As a matter of fact, low voltage is often sufficient for $\tan \delta$ measurements in the field and factory.

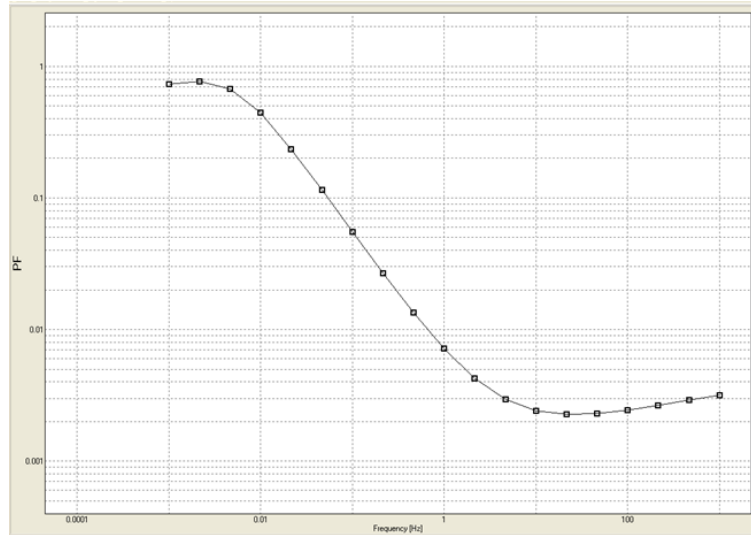


Figure 2 Typical dielectric response of an oil-paper insulation system

B. Dielectric properties of the liquid insulation

Transformer oil is a non-polar liquid with a capacitance that changes very little with frequency. The relative permittivity, ϵ_r , of oil is usually in a range 2.1-2.3. The dielectric loss of oil is mainly governed by its DC conductivity (σ_{DC}) and varies considerably with the quality of the oil [3], [4]. As a result, measured dissipation factor, as a function of frequency, will slope downward in a straight line as shown in figure 3.

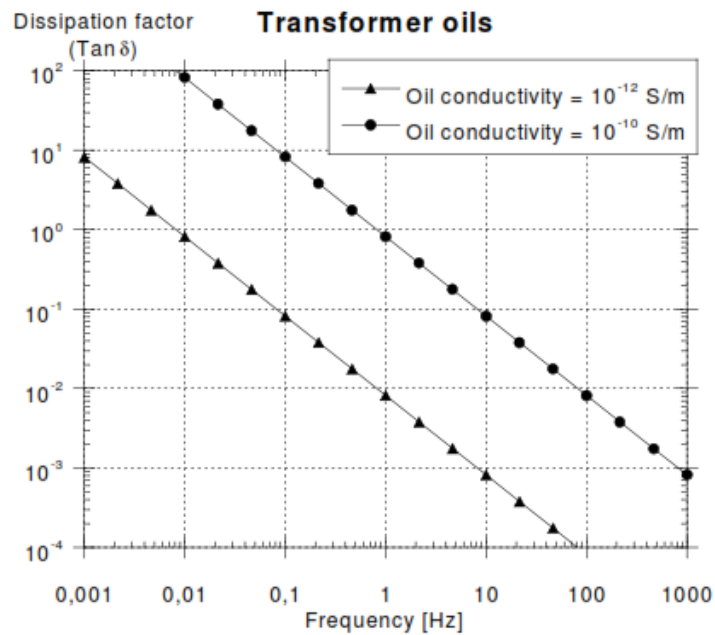


Figure 3 Typical frequency response of transformer mineral oil with different conductivity values

C. Dielectric properties of the solid insulation

Oil impregnated cellulose paper encountered in power, distribution and instrument transformers, as well as bushings and PILC cable, has a complex structure characterized by frequency dependence in both capacitance and loss factor. The qualitative analysis of cellulosic insulation (paper, pressboard, and wooden blocks) is expressed in terms of its moisture content, which increases due to ageing and exposure to atmosphere. Changes in moisture content in paper are detectable using FDS as shown in figure 4.

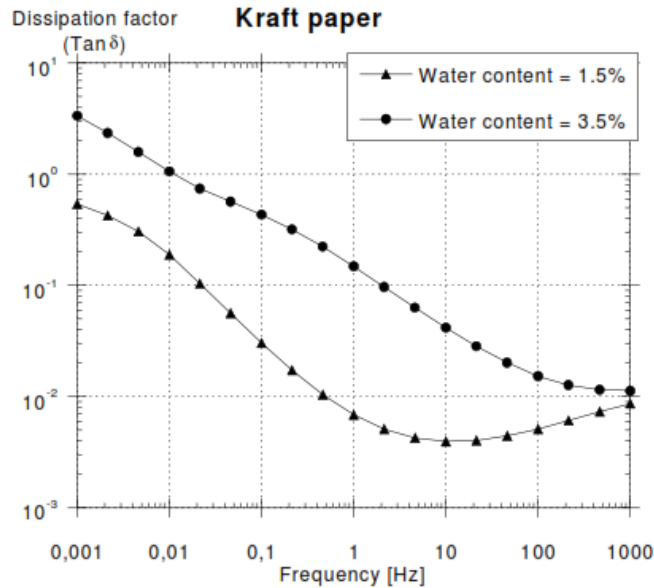


Figure 4 Frequency response of cellulosic insulation with different % m.c.

D. The XY model application in the Dielectric Response

FDS measurements on oil-immersed transformers used the “XY-model” to analytically represent the inter-winding insulation system inside a transformer. The insulation structure is represented by the relative amount of spacers (sticks) and barriers (pressboard cylinders) in the cooling duct as shown in figure 5. Parameter “X” is defined as the ratio of the sum of all barriers in the duct, lumped together, and divided by the duct width. The spacer coverage “Y” is defined as the total width of all the spacers divided by the total length of the periphery of the duct.

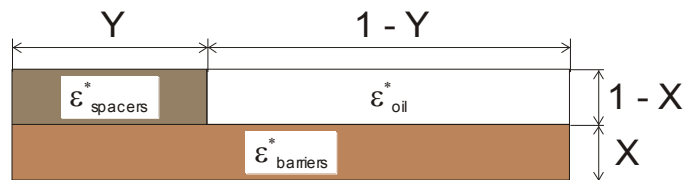


Figure 5 Sketch diagram of the XY model

The permittivities of oil, ϵ^*_{oil} , spacers, $\epsilon^*_{spacers}$ and barriers, $\epsilon^*_{barriers}$, are complex functions dependent on both frequency and temperature variables.

The total dielectric response of the XY model can be calculated by four capacitors in series and parallel with each other as shown in figure 6. Dividing the geometry capacitor, the total permittivity could be obtained. The widely applied method is that the capacitors are in series in X direction and in parallel in Y direction. [5]

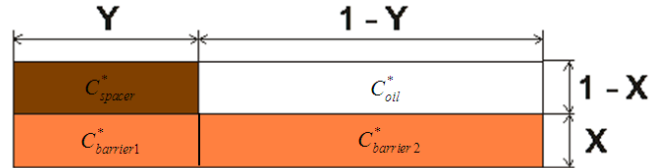


Figure 6 Capacitor model of the XY model

As a result of the use of the capacitor model in the permittivity environment, the complex permittivity of the oil/paper inter-winding insulation can be expressed mathematically as a function of frequency and temperature as presented in eq. 2.

$$\epsilon(\omega, T)_1 = \frac{Y}{\frac{1-X}{\epsilon_{spacer}} + \frac{X}{\epsilon_{barrier1}}} + \frac{1-Y}{\frac{1-X}{\epsilon_{oil}} + \frac{X}{\epsilon_{barrier2}}} \quad (2)$$

The finite element method simulation carried out in [6], shows that the capacitor model neglects the electric field distortion due to the discontinuous effect. Results of simulations show that the error varies with geometry, relative permittivities of the two materials and the oil conductivity. Additionally, the error magnitude varies with frequency. The approach proposed in [6] is to modify the capacitor model considering not only the capacitors to be in series in X direction and parallel in Y direction, but also representing the capacitors in parallel in Y direction and in series in X direction, from where eq. 3 is given by:

$$\epsilon(\omega, T)_2 = \frac{1}{\frac{X}{Y\epsilon_{sticks} + (1-Y)\epsilon_{barrier}} + \frac{1-X}{Y\epsilon_{spacer} + (1-Y)\epsilon_{oil}}} \quad (3)$$

The true value lies between two permittivities described by equation 1 and equation 2, and can be expressed by a through factor “K”:

$$\epsilon_{eq} = (1-K)\epsilon_1 + K\epsilon_2 \quad (4)$$

The XY model is a simple modeling tool developed to describe the ratio of the solid and liquid insulation in a power transformer. FEM simulation used to duplicate the errors of the XY model allowed the alternative to develop an improved capacitive model for the inter-winding insulation system of transformers as presented in eq. 4.

As of now, the FDS technique has been applied as an advanced diagnostics tool that evaluates the insulation condition when high power factor values are encountered during routine testing procedures. DFR is shown in this document to be a simple tool to be used for factory quality assurance/quality control (QA/QC) of the dry-out process as well as an effective tool to monitor the dry-out process and its effectiveness in the field.

III. POWER TRANSFORMER DRY-OUT PROCESS

A. Importance of the dry-out process

Dry-out is an essential step to remove moisture from the insulation during the transformer manufacturing process [7]. A reliable test methodology to measure the dry-out rate of the solid insulation used in transformers is essential for manufacturers and field operators. The test method should be non-destructive and non-invasive to avoid damage of the surface insulation due to mechanical or electrical stresses during the test. A well-monitored dry-out process will provide data that can be used as an indicator of the initial condition of the transformer at the beginning of its service life. Later on, field dry-out can be compared and data analyzed to identify the effectiveness of the dry-out method.

Several techniques are used on the manufacturing floor to dry-out the active part of a transformer. In most cases, the manufacturer will infer the value of moisture concentration in the solid insulation by means of measurements performed on the liquid or gaseous medium. A Best Practice for a new transformer should be to perform a dissipation factor test and dew point test during factory acceptance test and as part of the field commissioning routine. Generally, the insulation dissipation factor of a newly delivered power transformer should not exceed 0.5% at 20°C top-oil temperature.

After the thermal dry-out in the oven, the active part of the transformer is tanked, fastened, secured and other accessories are assembled. At this point, without insulating liquid present, the moisture analysis is performed based on the dew point test measuring relative humidity, temperature and pressure of the gas [8]. The resulting data is the moisture content for the surface insulation. However, manufacturers should not only be concerned with surface moisture concentration but also, and importantly, with “bulk” moisture concentration under two different conditions: without oil (air/paper) and immersed in oil (oil/paper).

Reader should keep in mind that these numbers apply to transformers with Kraft paper thermally or non-thermally upgraded immersed in mineral oil. Newly developed technologies using natural or synthetic ester oils will provide higher values and clarification will be needed from the manufacturer of the transformer as to what power factor number will be acceptable. In lieu with these new oil technologies, the dielectric response could be used to estimate moisture in the insulation if the modeling system allows modification of the relative permittivity value of the liquid insulation to approximately 3.2 – 3.4. It is important to note that a single dissipation factor value obtained at line frequency might not be sufficient to evaluate the condition of the complex insulation system.

B. Factory Dry-out

A very good estimation of moisture concentration has been achieved in vertical ovens where the dry-out process for the active part of distribution transformers is exclusively thermal (see figure 7). The time specified to keep the unit inside the oven is mainly established based on average estimation and not on a known percentage value of moisture concentration at the beginning of the process.



Figure 7 Core-winding modules set for thermal dry-out in the factory

Before the thermal process of the core-winding modules (the active part of the transformer), the dielectric response can be obtained to determine the initial condition prior to dry-out in the form of moisture concentration. An example of a dielectric response of a distribution transformer is shown in figure 8.

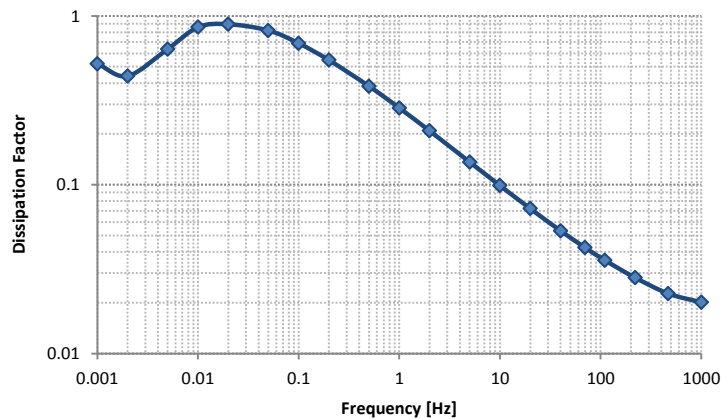


Figure 8 Dielectric Response of the active part of a distribution transformer before dry-out

During the process, the FDS method was used to apply a low voltage sinusoidal signal in 15-minute intervals while the temperature of the insulation system continuously increased, trying to reach equilibrium at approximately 120°C. The variation of the response throughout the entire dry-out process was obtained and finally a 4-day trending chart was obtained showing the moisture reduction on the active part of the distribution transformer under a thermal effect. The chart is presented in figure 9.

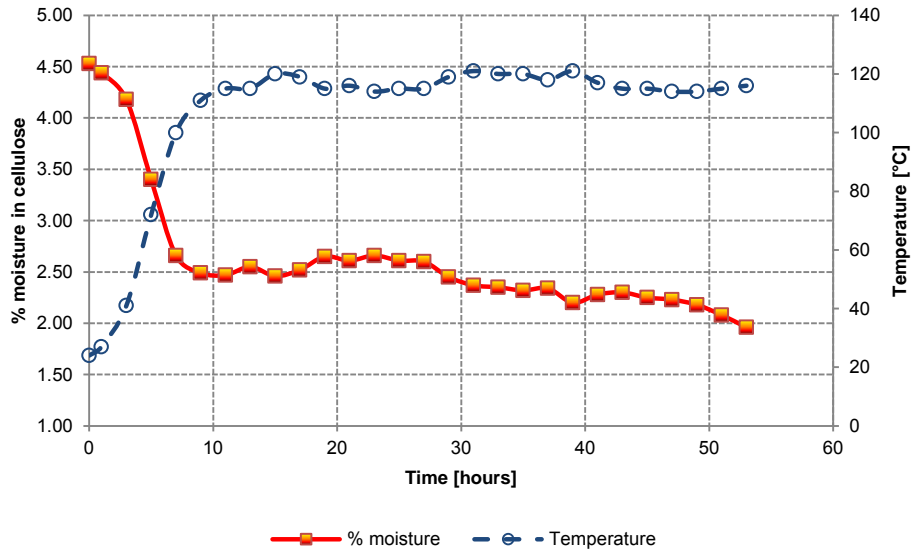


Figure 9 Moisture reduction under thermal effect on active part of a distribution transformer

As it can be clearly observed in figure 9, this is not the end of the dry-out process. The unit now is removed from the oven and fixed inside the tank. After thermal dry-out, the sealed unit gets under vacuum for approximately 12 additional hours. This transition time from the oven to the vacuum process allows exposure of the insulation to the ambient and possible re-adsorption of water from the air at the solid insulation surfaces.

C. Field Dry-out

There is a variety of mechanisms and equipment used for field dry-out of power and distribution transformers. The efficiency of the mechanism is correlated to the velocity of the process. Figure 10 shows a chart summarizing different mechanisms and their processing velocity [9].

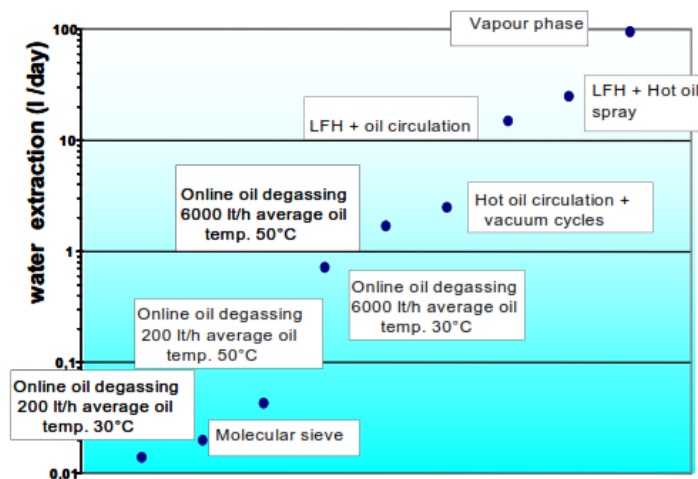


Figure 10 Field dry-out mechanisms. Drying velocity from 3% down to 1.5% moisture [9].

Upon confirmation with the FDS method that the insulating system of a power or distribution transformer is wet, the combination of heat and vacuum is a typical and quite efficient approach to minimize the amount of moisture in the cellulose. Nonetheless, this stage has been mistaken many times and technicians in the field have tried to reduce the moisture in the cellulose by reduction of moisture in the liquid insulation. A typical setup for an off-line dry-out system including heat and vacuum is presented in figure 11.

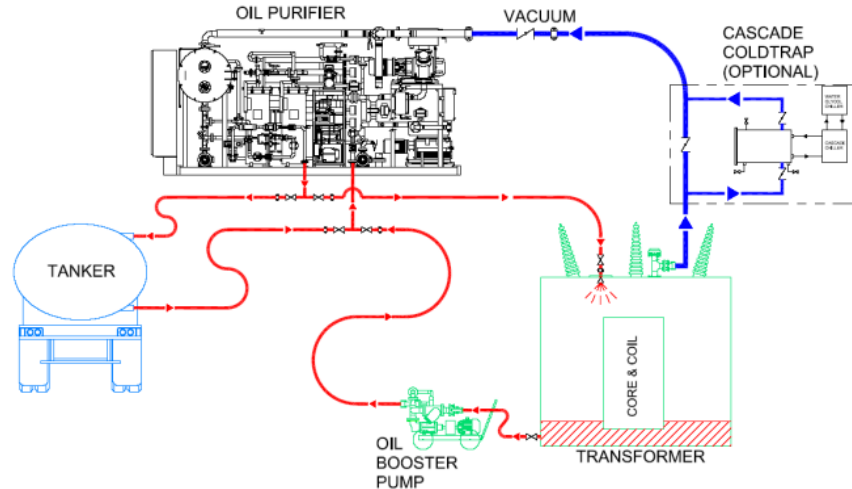


Figure 11 Typical setup for field off-line dry-out process

For the hot oil spray method, the oil level can usually be reduced to less than 10% of the total oil volume. Heated oil at temperatures around 60°C is pumped into the transformer and the process continues until oil returning to processor at a temperature greater or equal to 50°C. If using flooded hot oil circulation, then pump the oil out when the temperature is achieved and apply vacuum.

D. FDS monitoring during field dry-out

In order to validate the benefit of the FDS technology, a local utility investigated the application of FDS during field dry-out on an old 5MVA transformer, nominal voltage 69/12.5kV, Dyn1 which was removed from operation due to a high dissipation factor value (0.9% @ 20°C) encountered during a routine testing procedure.

The high dissipation factor value indicated the existence of a problem in the insulation system; however, it did not indicate whether the problem was in the solid or in the liquid insulation. As a result the utility conducted FDS diagnostics to identify the source of the problem. The dielectric response of this unit is presented in figure 12. The analysis of the dielectric response confirmed a 3.5% moisture concentration in the cellulose; and, $1.5 \cdot 10^{-12}$ S/m conductivity of the liquid insulation. The engineering team, together with the field operations team, decided to take this unit temporarily off-line for dry-out process with heat and vacuum.

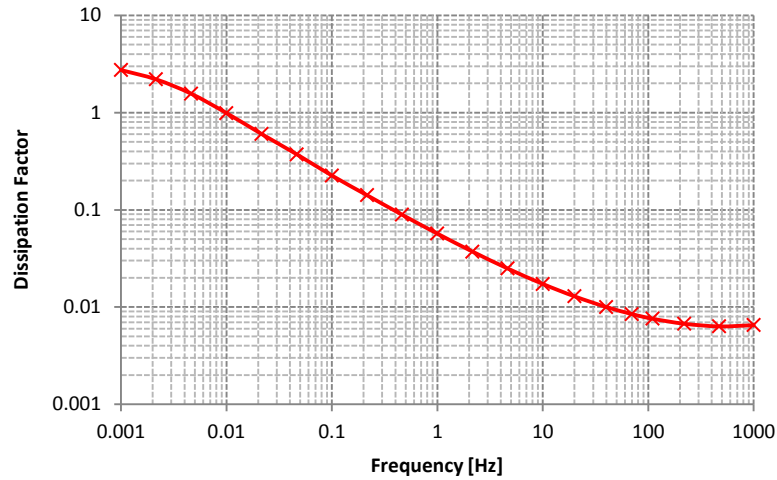


Figure 12 Dielectric response of a 5MVA transformer in the field with moisture content of 3.5% before dry-out process

The FDS dielectric response was obtained in measurement intervals of six (6) hours. It was decided to reduce the voltage during the test and the voltage was finally set to $15V_{rms}$. The first 24 hours sequence of measurements is presented in figure 13.

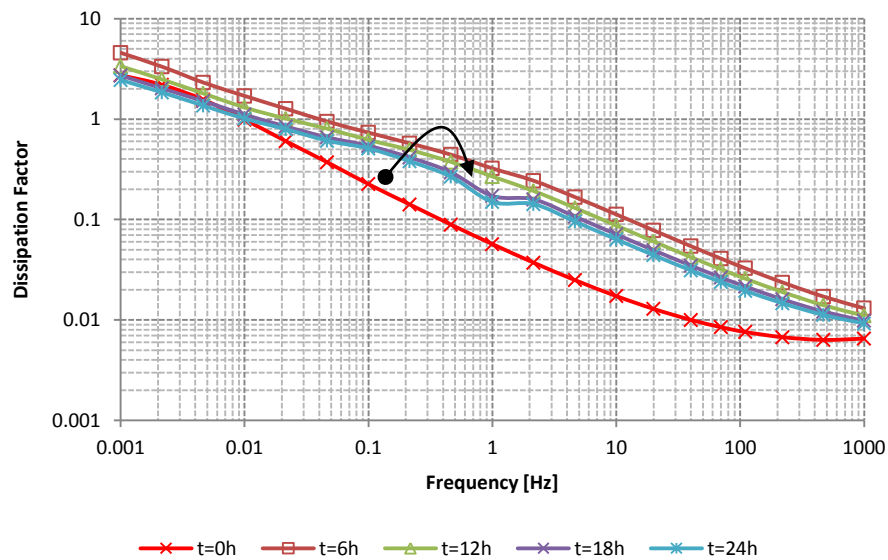


Figure 13 Dielectric response of the 5MVA transformer put under vacuum dry-out for 24 hours.

A fast change of the shape of the dielectric response is clearly observed in the first six (6) hours of vacuum process, between $t=0h$ and $t=6h$, after bringing the temperature up to $\sim 65^{\circ}C$. The following measurements describe a similar shape of the response obtained after six (6) hours of vacuum. The data shows continuous decay of dissipation factor values together with the entire dielectric spectrum. The model for vacuum assumes constant conductivity value of $1 \cdot 10^{-17}$ S/m and relative permittivity of the surrounding medium equal to unity.

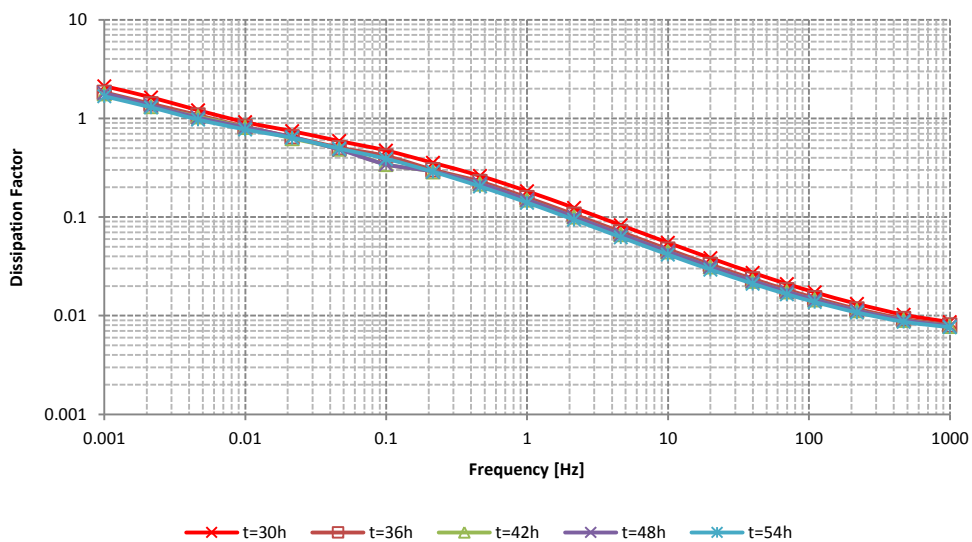


Figure 14 Dielectric Response of a 5 MVA transformer during vacuum dry-out. Interval from 30 to 54h

During the next 30h of the vacuum process (see figure 14), the data reveals the process is not being efficient, and that there is no improvement in the condition of the solid insulation. This is a clear indication for operators to re-heat the core and windings and initiate a new vacuum cycle.

The moisture content in this unit was finally left at 2.6%. In order to validate the results, the unit was re-tested after two weeks of operation. The FDS results indicated a total of 2.6% moisture concentration in the cellulose ratifying the readings performed during dry-out and under vacuum.

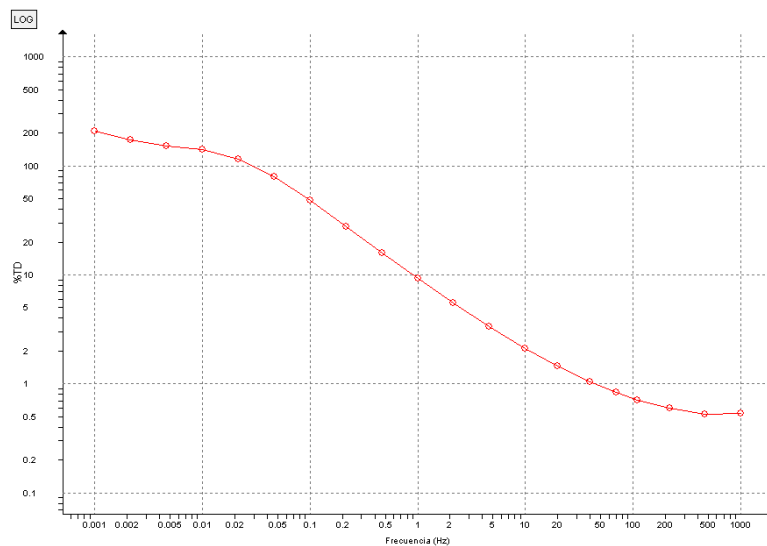


Figure 15 Dielectric response obtained after 2 weeks of operation after dry-out

IV. DISCUSSION AND CONCLUSIONS

It has been clearly demonstrated that FDS can easily be applied at the factory as a Quality Assurance/Quality Control (QA/QC) test that monitors the level of dryness of the active part of power and distribution transformers in the thermal dry-out process. FDS provides manufacturers with the ability to determine the correct level of dryness, and as a result, optimizes energy resources looking at the velocity of the dry-out process based on a reference dielectric response.

The surface of cellulose insulation is not a good indicator for the moisture inside the solid insulation. Ideally, side samples should be taken and tested by Karl Fisher titration, damaging the integrity of the surface insulation. Although taking side samples may not be feasible for all manufacturers as it is very time consuming, especially if it has to be sent to a laboratory. Moreover, a manufacturer may have to wait for results and the manufacturer is not able to take immediate decisions during the dry-out process. Therefore, laboratory analysis is not practical.

The application of the FDS method in the field to estimate the percentage moisture concentration in cellulose during dry-out process is relevant. The process described in this document clearly shows the point where the process reduces efficiency and slows down the moisture extraction. This finding alone provides guidelines to the operator to improve the process, i.e., continue as is, or stop the process declaring completion of the dry-out activity.

Special attention will be required when the dry-out process is applied to old transformers. The tensile strength of the solid insulation can be compromised if continuous vacuum is applied.

V. REFERENCES

- [1] U. Gäfvert, G. Frimpong, and J. Fuhr, "Modeling of Dielectric Measurements on Power Transformers", paper 15-103, CIGRE session 1998.
- [2] A. C. Gjaerde, L. Lundgaard, and E. Ildstad, "Effect of Temperature and Moisture on the Dielectric Properties of Oil-Impregnated Cellulose", paper 1060-1, Proc. of the ISH, 1995.
- [3] V. Der Hauhanessian, Measurement and Analysis of Dielectric Response in Oil-Paper Insulation Systems. Doctoral Thesis, Swiss Federal Institute of Technology Zurich, Diss. ETH. No. 12832, Zurich, 1998.
- [4] U. Gäfvert, L. Adeen, M. Tapper, P. Ghasemi, B. Jönsson, "Dielectric Spectroscopy in Time and Frequency Domain Applied to Diagnostics of Power Transformers", Proc. Of the ICPADM, Xi'an, China, 2000.
- [5] S.M. Gubanski, J. Blennow, B. Holmgren, M. Koch, A. Kuechler, R. Kutzner, J. Lapworth, D. Linhjell, S. Tenbohlen, P. Werelius, "Dielectric Response Diagnoses for Transformer Windings," CIGRE WG D1.01 (TF 14), Brochure 414, 2010
- [6] Cheng, J. ; Werelius, P. ; Ohlen, M. "FEM analysis of the transformer insulation XY model," Proceedings of the Transmission & Distribution conference, 2012
- [7] Ernst, W., Kau Ho, Levin, A. "Dry-out properties of insulating paper in distribution transformers", Proceedings of the Conference on Electrical Insulation and Dielectric Phenomena (CEIDP), 2012
- [8] Valery G. Davydov, "Moisture Related Phenomena in Transformers and Reactors: Need for Development of a New Reference Document," Proceeding TechCon North America 2012.
- [9] P. Koestinger, E. Aronsen, P. Boss, G. Rindlisbacher, "Practical Experience with the drying of Power transformers in the field, applying LFH Technology," CIGRE, Session 2004, A2-205.

VI. BIOGRAPHY

Diego Robalino currently works for Megger North America as a senior applications engineer, where he specializes in the diagnosis of complex electrical testing procedures. While doing research in power system optimization with a focus on aging equipment at Tennessee Technological University, Robalino received his electrical engineering Ph.D. from that institution. With an international background spanning the distance from South America to Eastern Europe, he's garnered additional education experience in project management and electric drives/automation. Dr. Robalino has many years of management responsibility in the power systems, oil and gas, and research arenas managing the design, construction and commissioning of electrical and electro-mechanical projects. He is an active member of IEEE and ASTM with multidisciplinary engineering interests that lead him to author technical papers and articles related to insulation diagnostics and condition assessment of HV components.

Peter Werelius was born in Stockholm, Sweden, in 1966. He received a Master of Science and Doctorate degrees in Electrical Engineering both from KTH (Royal Institute of Technology) in Stockholm, Sweden. He started his professional career starting up a spin-off company, WaBtech, in 1996, manufacturing FDS/DFR (Frequency Domain Spectroscopy/Dielectric Frequency Response) test equipment. From 1999, he continued the work on the FDS/DFR application, now within Programma Electric and later within GE Energy Services after GE acquired Programma in 2002. In 2005, he together with others founded Pax Diagnostics. In 2008 Pax Diagnostics was acquired by Megger and Dr. Werelius is now working as product manager and technical specialist in transformer testing. Peter Werelius has published a number of papers/articles mainly related to FDS/DFR measurement techniques and application. He is member of IEEE and Cigré and actively participates in working groups and task forces.

Analyzing the Phenomena of Wind-Induced Vibrations on Unloaded Davit Arms

Erik A. Ruggeri, P.E.

**ANALYZING THE PHENOMENA OF WIND-INDUCED
VIBRATIONS
ON
UNLOADED DAVIT ARMS**

Erik A. Ruggeri, P.E.

**TRANSMISSION AND SUBSTATION DESIGN AND OPERATION SYMPOSIUM 2013
Dallas, Texas**

INTRODUCTION

The issue of unloaded davit arms vibrating and fatiguing to failure has been prevalent in our industry for decades. At extra high voltages davit arms are fairly long slender structures with relatively high flexibility and low structural damping, they are susceptible to wind-induced vibrations. This is particularly true at larger voltages where clearances require longer davit arms than lower voltages (138 kV and less).

Davit arms represent a bluff structure. A bluff structure is one in which the flow separates from large sections of the structure's surface. The area of re-circulation downstream of a bluff structure is called the wake. In most conditions, the wake of a bluff structure will be unsteady and will shed vortices. Under the right circumstances (dependent on wind speed and Reynold's number), the shedding vortices create an oscillating pressure differential. This differential leads to motion in the across-wind direction. If a resonant frequency of the bluff structure lies within the spectrum of vortex shedding frequencies, and there is not sufficient damping, large across-wind amplitudes are probable, resulting in fatigue damage and potential failure at the arm's weld.

This type of failure is typically caused by excessive alternating stress levels at the weld due to either the 'along-wind' response or to the 'across-wind' response. The former is known as static drag load and is typically not detrimental to the arm. The across-wind response is due to a phenomenon called vortex-shedding.

Historically, this type of failure is of greatest concern when double circuit poles are installed but only one circuit is installed. However, we have seen arm failures in the short interim between installation and wire stringing. In order to avoid vibration and fatigue issues on the unloaded arms, pole vendors recommend installing weights at the arm's tip. Some recommend 100lbs – 150 lbs while others recommend approximately 10% of the arm's mass. Over the last year and a half, we have been analyzing this phenomenon in order to determine a more scientifically based damping methodology than the general 'rule of thumb'.

INVESTIGATION

We performed a dynamic analysis on the arms provided by two different vendors in order to determine their resonant frequencies and the effects of vortex shedding - both with and without additional mass. As part of such an analysis, the arm is modeled using finite elements in the software program STAAD-Pro™. This program is capable of determining the fundamental (or natural) frequencies of the arm. Each of these frequencies can be correlated to a wind speed by the equation:

$$V_i = \eta_i * D/S$$

Where η_i is the i^{th} natural frequency, D is the mean diameter, and S is the Strouhl number. 'V_i' are then the critical wind speeds for vortex shedding.

The arm models were first analyzed in order to determine their natural frequencies and to obtain an understanding of which arms are more prone to vortex shedding. Table 1 summarizes the arms' first two natural frequencies and the corresponding wind speed.

Table 1A: Arm Modal Frequencies-Vendor A

Arm Type	1 st Natural Frequency, η_1	2 nd Natural Frequency, η_2	Excitation Wind Speed for 1 st mode	Excitation Wind Speed for 2 nd mode
Tangent Static Arm	7.0 Hz	33.2 Hz	17.8 mph	85.0 mph
Tangent Phase Arm (Middle)	12.3 Hz	61.9 Hz	39.5 mph	184.0 mph

Table 1B: Arm Modal Frequencies – Vendor B

Arm Type	1 st Natural Frequency, η_1	2 nd Natural Frequency, η_2	Excitation Wind Speed for 1 st mode	Excitation Wind Speed for 2 nd mode
Tangent Static Arm	9.6 Hz	45.4 Hz	31.0 mph	145.1 mph
Tangent Phase Arm (Middle)	12.0 Hz	49.2 Hz	38.4 mph	156.6 mph

If the critical wind speed for excitation is likely to occur on site, then the corresponding dynamic loads and stresses should be calculated. As evident in the table, the first mode is that which contributes to vortex shedding; the 2nd mode and higher modes exceed the 50-year return period wind speed. Although one vendor's arm has a significantly lower wind speed for the 1st excitation mode, each vendor's arm will likely see that first excitation wind speed at some point and for some period of time.

Once the natural frequency was determined in STAAD, the model was subjected to dynamic loading at that frequency by performing a time history load analysis. Based upon the critical wind speed (1st mode excitation speed) shown in Table 1, harmonic loading was applied to the arm in the form of a sinusoidal forcing function as follows:

$$F(z,t) = 1/2C_L * \rho * u(z)^2 * D(z) * \cos(\eta_i t + \zeta(t))$$

Where C_L is the lift coefficient, $u(z)$ and $D(z)$ are the wind velocity and diameter at height (z) , respectively. $\zeta(t)$ is a randomly varying process to account for turbulence. In a dynamic analysis, this load is inputted as a forcing function applied at the modal frequency. With an accurate F.E. model geometry and user-input damping ratio, the software solved the equation for forced harmonic motion and computed the structure's response. The second order differential equation for driven harmonic oscillators is as follows:

$$\ddot{x} + 2\beta\eta\dot{x} + \eta^2x = F(t)/m$$

In this equation, β is the damping ratio and η is the natural frequency. The damping is the sum of the inherent structural damping (β_s) and the aerodynamic damping (β_a). The aerodynamic damping can be a negative value by a phenomenon known as ‘negative aerodynamic damping’ wherein the motion-induced forces are in phase with the velocity component of the structure. If the sum ($\beta_s + \beta_a$) is less than zero, this increases amplitude and the associated stress ranges on the shaft.

The corresponding support reactions were calculated within STAAD-Pro and used to determine the approximate stress range at the weld.

In order to simulate a 50 lb or 100 lb weight added to the end of the arm, a concentrated mass was applied, effective in the vertical direction only. The natural frequency of this system was calculated, and the corresponding forcing function was applied.

Although the damping ratio will change with the addition of weights, the amount it will change cannot be quantified. Therefore, the models maintained the .03 ratio for all cases. This value should err on the conservative side due to its influence on the stress levels at the base.

The results are tabulated in Table 2 for the shield wire from both suppliers. We focused on the static wire arms that have lower excitation wind speeds and are more prone to vibration. Figure 1 below that is an image from the F.E. model showing the stress contours for the unweighted vibration.

Table 2: Arm Specifications and Calculated Stresses

Arm Type	Length	Weight	Base/Tip O.D.	Thickness	Dynamic Stress Range-undamped	Dynamic Stress Range-50 lb damper	Dynamic Stress Range-100 lb damper
Static Arm Vendor A-Octagon	20'-9"	800 lbs	12"/6"	5/16"	12.4 ksi	2.9 ksi	1.6 ksi
Static Arm Vendor B-Hexagon	20'-7"	756 lbs	15"/7.5"	3/16"	39 ksi	7.8 ksi	4.2 ksi

The two arms have different dynamic responses. While the dynamic stresses are lower in Arm ‘A’, the excitation wind speed is also much lower – 16 mph vs 31 mph. Depending on the area and exposure, arm ‘B’ may be less likely to vibrate.

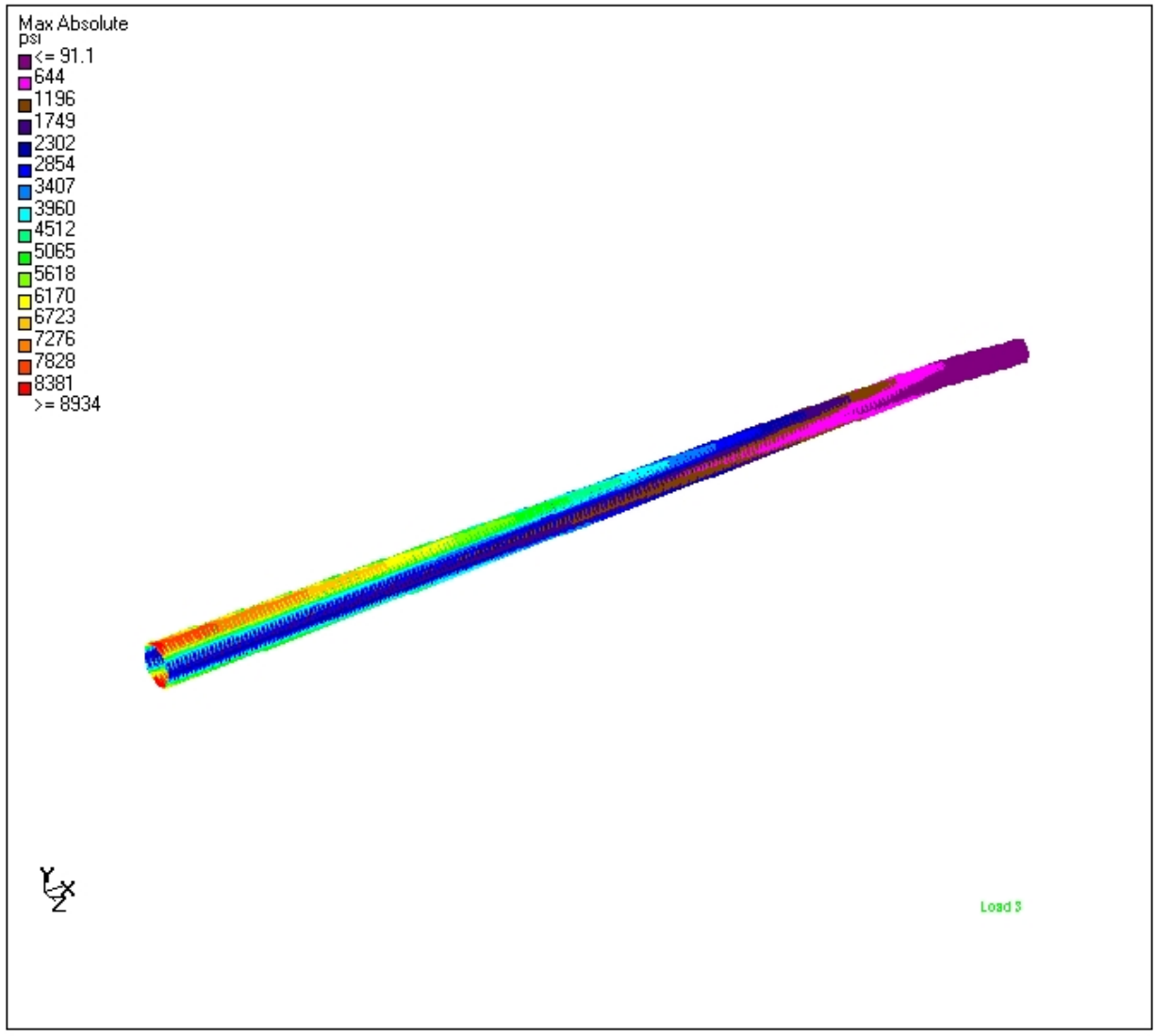


Figure 1 – Tangent Arm STAAD Model

The calculated stresses can then be compared to allowable values in order to determine if additional damping is required. For fatigue loading, the AISC Manual of Steel Construction (Appendix K) specifies the stress limits, dependent on the number of load cycles and the material/weld configurations. For a complete joint penetration (CJP) weld, the threshold stress range, F_{th} (for indefinite life) is 10 ksi.

Further, the European standard, ECCS-#43, “Recommendations for Fatigue Design of Steel Structures” is more restrictive in setting allowable fatigue stress values. That standard limits the stress ranges somewhere between 7 – 8 ksi.

The graph below is a S-N diagram generated from laboratory tests of three shield wire arms. The stress range is more restrictive than either aforementioned standard.

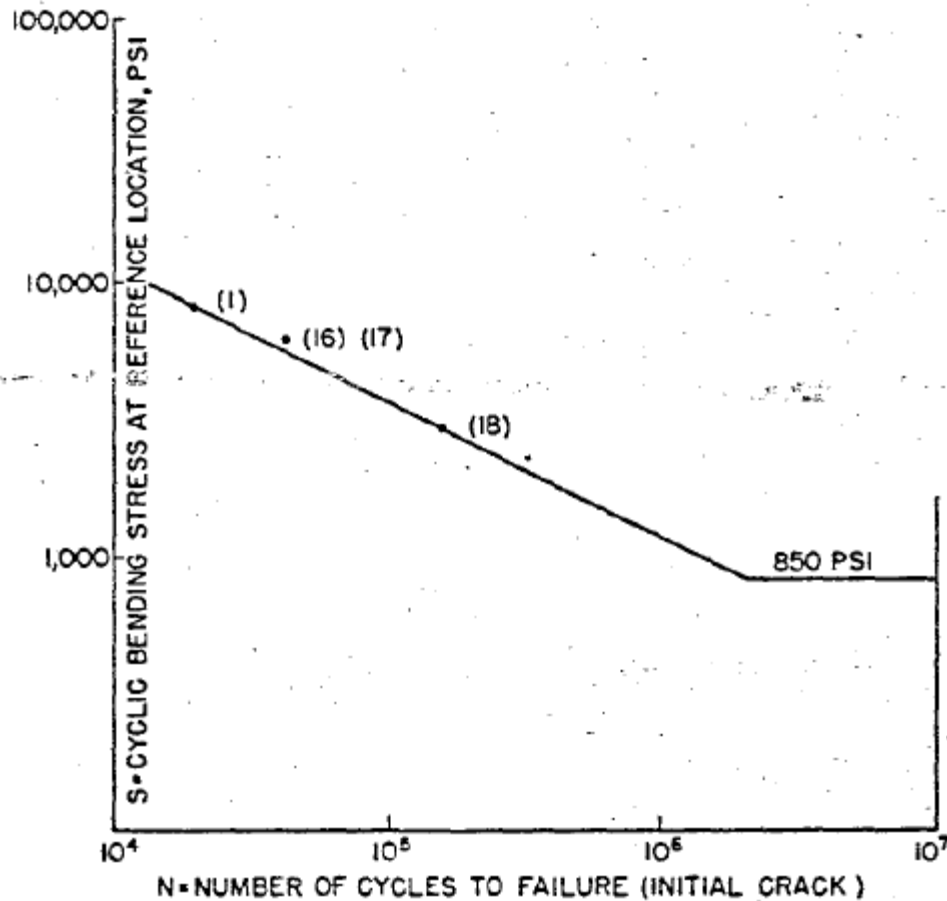


Fig. 5 Minimum Value S-N Diagram for Tests of Three Ground Wire Arms at Three Different Stress Levels.

This S-N diagram is for fatigue crack initiation rather than member failure.

The stress ranges in this initial analysis were relatively high in comparison to standards and available stress-life diagrams. However, we recognized that this theoretical approach is very rudimentary and the arm model is stiffer than it is in reality. Field work to better capture the harmonic frequencies and damping characteristics helped refine the results.

FIELD STUDIES

In order to validate the modal behavior and the responses of the computer models, the utility subcontracted ESI Engineering, INC to perform field measurements. ESI used modal impact hammers and accelerometers to measure the natural frequencies and damping of the vacant shield wire and phase arms on the tangent poles. They then ran these data through a Fast Fourier Transform in order to graphically determine the modal frequencies.

The first field study was conducted in the fall of 2011 on structures supplied by Vendor A. Figure 2 shows the results that were obtained, and Table 3 below that compares the field results to those obtained in the F.E. model.

Top Shield Davit Arm		Mode 1	
		Frequency, Hz	% Critical Damping
0 lb		4.125	4.8
50 lbs		3.625	6.8
100 lbs		3.500	6.5
Middle Conductor Davit Arm		Mode 1	
		Frequency, Hz	% Critical Damping
0 lb		5.500	3.7
50 lbs		5.125	3.3
100 lbs		4.625	10.9

Figure 2 – Measured Values of Modal Frequencies and Damping

Table 3: Measured vs. Calculated 1st Natural Frequencies-Vendor A

Tangent Static Arm Measured	Tangent Static Arm Calculated	Mid. Phase Arm Measured	Mid. Phase Arm Calculated
4.13 Hz	6.97 Hz	5.50 Hz	12.3 Hz

The values in the F.E. model are higher for two reasons: First, the natural frequencies and mode shapes are direct functions of the stiffness and mass distribution in the model which are not constant along the length of the arm. Second, the computer model assumes the base of the arm is rigidly fixed. In reality, there is some flexibility due to the arm-to-pole connection and the flexibility of the structure itself.

In the STAAD model, we adjusted the rigidity of the supports (using spring constants) in order to obtain a first modal frequency close to that measured in the field. With this level of fixity, we then compared the measured modal frequencies with weights added to those calculated in the F.E. model. The results were within a few per cent and are shown in Table 4.

Table 4: Measured vs. Modeled Natural Frequencies with Spring Supports-Vendor A

Arm Type	1st Modal frequency, 50 lb Damper-Measured	1st Modal frequency, 50 lb Damper-Modeled	1st Modal frequency, 100 lb Damper-Measured	1st Modal frequency, 100 lb Damper-Modeled
Tangent Static Arm	3.63 Hz	3.63 Hz	3.50 Hz	3.28 Hz
Tangent Phase Arm (Middle)	5.13 Hz	5.29 Hz	4.63 Hz	4.93 Hz

These lower frequencies correspond to a much lower first mode excitation wind speed (~9 mph for the static arm and 16 mph for the middle phase arm).

The measured damping ratios for the first mode were lower than the 3% value assumed and applied thus far. However, the damping did not always increase with the addition of weight. Field technicians noted that the way the weights were attached (hooks and shackles) “introduced non-linear effects when the arm was impacted by the hammer, similar to a slack rope condition”. Due to the inconsistencies in the damping, and the influence of the damping on the stresses at the arm’s base, we re-analyzed the stresses from Table 2 with the damping values for the 2nd mode which is 1.9%. The results for this analysis are shown in Table 5.

Table 5: Arm Specifications and Modified Stresses-Vendor A

Arm Type	Length	Weight	Base/Tip O.D.	Dynamic Stress-undamped	Dynamic Stress-50 lb damper	Dynamic Stress-100 lb damper
Tangent Static Arm	20'-9"	800 lbs	12"/6"	8 ksi	1.6 ksi	08 ksi

As expected, the stress values increase with the reduction in damping, and the undamped condition stress ranges exceed both AISC and ECCS suggested values for fatigue consideration.

In May of 2012, ESI mobilized to test the other vendor’s tangent pole arms (static and middle phase). In pre-mobilization discussions, we decided to bolt weights at the end of the arm to mitigate the slack rope condition discovered during the first field tests. The decision was made with the understanding that wind-induced motion will not have the initial acceleration of an impact hammer and thus will not induce rattling of the mass’s hardware.

We also decided to measure the effects of damping by securing the static phase arm to the middle-phase arm with cables. Figure 3 lists the results that we received.

Top Shield Davit Arm	Mode 1	
	Frequency, Hz	% Critical Damping
0 lb	6.375	2.3
50 lbs	6.000	1.8
100 lbs	5.000	2.0
Cable - 7.00" Gap	8.250	2.4
Cable - 6.75" Gap	8.250	1.4
Cable - 6.00" Gap	8.250	1.3
Middle Conductor Davit Arm	Mode 1	
	Frequency, Hz	% Critical Damping
0 lb	8.750	1.3
50 lbs	8.375	1.6
100 lbs	8.125	2.2
Cable - 6.00" Gap	8.250	1.8

Figure 3 – Measured Values of Modal Frequencies and Damping

While the trend in modal frequencies is similar for the same reasons, the damping ratios looked more accurate with the modifications to the test set-up. It is interesting to note that the effect of securing the arms caused the static wire arm to adopt a modal frequency close to that of the phase arm to which it is secured. These rows are noted as ‘Cable – x’ Gap’. Also of interest is that the percentage of critical damping decreases as the interconnecting cable is tightened.

Table 6: 1st Natural Frequencies -Measured vs. Calculated : Vendor B

Tangent Static Arm Measured	Tangent Static Arm Calculated	Mid. Phase Arm Measured	Mid. Phase Arm Calculated
6.38 Hz	9.6 Hz	8.75 Hz	12.04 Hz

Again, the field-measured frequencies correspond to lower excitation wind speeds: 21 mph for the static arm and 28 mph for the phase arm. The same procedure was applied to the F.E. model; the supports were changed from a fixed condition to spring constants in order to match the measured modal frequencies, and the dynamic forcing function was applied at these adjusted frequencies. The modified natural frequencies again correspond to a reduction in the excitation wind speed. Table 7 shows the calculated stresses based on the adjustments made as a result of the field measurements.

Table 7: Arm Specifications and Modified Stresses-Vendor A&B

Arm Type	Length	Weight	Base/Tip O.D.	Dynamic Stress Range-undamped	Dynamic Stress Range-50 lb damper	Dynamic Stress-100 lb damper
Vendor A	20'-9"	800 lbs	12"/6"	8.0 ksi	1.6 ksi	0.8 ksi
Vendor B	20'-9"	756 lbs	15"/7.5"	34.7 ksi	9.6 ksi	4.1 ksi

In order to comply with ECCS fatigue stress recommendations, 50 lbs of weight are required on the static arms. However, the stresses noted above likely err on the non-conservative side. They did not take into account residual stresses from the welding and the galvanization process.

CONCLUSION

Although this is not a widespread problem in our industry, it is common enough to merit further investigation. This study shows the comparative benefit of tuned mass damping. The question that arises is whether this is the best damping method. Utilities have said that the weights they purchase cost around \$3/lb which is not insignificant on large projects.

Another technique for attenuating resonant vibrations is particle mass damping. Multiple auxiliary masses are placed in the arm and vibrational energy is removed through friction and momentum exchange of these particles. The advantage is the simplicity, long life, and they are effective through a wide range of frequencies. The disadvantage is that experimental work is required to determine what type of jelly beans to use, as it were. Small aggregate or a chain within the arm could work.

Either way, laboratory experimentation in a low-speed wind tunnel would be invaluable in refining these finite element models and obtaining a better understanding of the stress levels and fatigue characteristics.

As noted and referenced earlier, in 1979, the IEEE published a paper titled, "Evaluation of Service Life of Steel Poles under Dynamic Loading." A team performed laboratory and field investigations on davit arms after several arm failures on a Detroit Edison 345 kV line in 1971. As a result of this study, they recommended the following:

- 1.) Do not install drain or weep holes near the base of the arm due to the stress concentration factors associated with these discontinuities.
- 2.) Design with thicker connection plates. They observed that, during vibratory loading, deformation of this plate caused local deformation of the arm plate adjacent to the weld.
- 3.) Eliminate galvanizing the arm in favor of a protective paint coating. The residual stresses associated with this process are particularly large at the plate corners. Doing so increases the fatigue life by a factor of three.

The method that suppliers use to design and fabricate arms has not changed in over 40 years and therefore is unlikely to change. When a project involves unloaded arms or arms that may vibrate due to galloping conductors, we, as engineers, would be well advised to consider specifications that include dynamic loading criteria and preventative measures that can be built into the design and fabrication process.

Axial and Lateral Capacity of Tapered Helical Piles for Transmission Pole Structures

Mark H. Fairbairn, P.E., Lee Goen, P.E., Jason Herron, EIT, and Gary L. Seider, P.E.

Axial and Lateral Capacity of Tapered Helical Piles for Transmission Pole Structures

by

Mark H. Fairbairn, P.E., M.ASCE, Senior Civil/Structural Engineer, Thomas and Betts, W8020 150TH Avenue, Hager City, WI 54014, USA mark.fairbairn@tnb.com

Lee Goen, P.E. CHANCE[®]/Hubbell Power Systems, Inc., 210 North Allen Street, Centralia, MO 65240, jlgoen@hubbell.com

Jason Herron, EIT, CHANCE[®] / Hubbell Power Systems, Inc., 210 North Allen Street, Centralia, MO 65240 jwherron@hubbell.com

Gary L. Seider, P.E., CHANCE[®] / Hubbell Power Systems, Inc., 210 North Allen Street, Centralia, MO 65240 glseider@hubbell.com

ABSTRACT: The foundations for most transmission line structures constructed in North America today are drilled shafts. However, drilled shafts are not always a suitable foundation choice. This paper details one example where helical piles were used as the foundation at select tower locations on the XCEL Energy Stinson-Bayfront Line 3315 32.1 Mile Re-Build 115 kV transmission line project. The structures were steel H-Frames, made by Thomas & Betts Meyer. The tangent structures were specified as direct embedded, and the running angle and dead-end structures were either helical piles or drilled shafts. The line is located in a remote area of northwest Wisconsin near Duluth, MN. Helical piles were used at tower locations with poor road access, and in areas considered environmentally sensitive where large vehicles would destroy the landscape and vegetation. Xcel, Hubbell / CHANCE, and Thomas & Betts teamed together to design this project. Xcel Energy produced the load and design drawings, Thomas & Betts designed the H-Frame Pole structures and the pile transition connections, and Hubbell / CHANCE designed the helical pile foundations. Prior to line construction, full-scale load tests of the helical pile / connection were performed at the Thomas and Betts Structure Test Facility located in Hager City, Wisconsin. The running angle and dead-end pile and transition systems were successfully loaded and tested to values that meet or exceed the ultimate design structure groundline reactions. These results are presented. The piles, tested together in a multi-pile group, were subjected to a combination of axial tension, compression, and lateral shear. In addition, four full-scale load tests were conducted on the line right-of-way at the actual tower locations. The tests consisted of pile penetration tests, axial tension, and lateral shear tests. These test results are compared to the theoretical capacity of the piles based on site soil type and strength. The results of the tests allowed the helical pile design to be adjusted prior to start of construction to provide the contractor with minimum depth and installation torque requirements.

INTRODUCTION

In 2012 Xcel Energy undertook to re-build existing Line 3315, an 115kv wood H-Frame power transmission line located in Northern Wisconsin, north of U.S. Highway 2 and south of Lake Superior. The new structures were to be steel H-frame structures. Xcel decided to consider the use of helical foundations to replace some of the reinforced concrete drilled shaft foundations on the line. The helical foundations were to be used at sites that were remote, difficult to access or a considerable

distance from existing concrete plants. The tangent structures on the line were to be direct burial structures and would require neither concrete foundations nor helical foundations.

DESIGN OF PILE TRANSITION AND PILES

On March 22, 2012 a meeting was held between representatives of XCEL Energy, Thomas and Betts and Hubbell/Chance to discuss the use of helical foundations, the transition of the piles to the structures and the design requirements and constraints. A total of 22 structures were identified by XCEL Energy as candidates to use the helical foundations. This total was made up of 7 dead-end structures and 15 running-angle structures. For these structures the overturning moments exceeded the soil capacity needed to allow the use of direct burial. In addition site access to some structures was limited.

XCEL Energy stated several requirements and desires for any proposed helical foundation system. First, the use of helical piles would allow the use of lower impact vehicles for construction. Second, the foundation would be capable of supporting the loading without the need for guying. Third there would be an installation time savings. XCEL Energy would provide the Load and Design Drawings, Thomas and Betts would design the structures and transition connection to the piles, and Chance/Hubbell would size and design the helical piles.

During the discussion the need for adjustment in the transition was expressed. While the installation of the helical pile can be somewhat controlled it was recognized that variation in placement should be expected. For this project a tolerance in any direction of plus or minus 3” was deemed acceptable. The design of the transition would need to mate or match up with the piles and have suitable adjustability to allow for the tolerance. A desire to connect the system without the need for field welding was also expressed and a bolted connection was agreed upon.

Prior to start of construction on the line, it was decided to conduct full-scale load tests on the helical piles and connections. This was done at the Thomas & Betts Test Facility in Hager City, Wisconsin. In addition, it was proposed to perform axial and lateral tests the helical piles on the line right-of-way at select structure sites to further confirm the design.

Initial Layout and Load Requirements for Helical Piles

After considering several possible helical pile configurations, two layout schemes of piles were established. For the deadend structures a four pile layout was initially submitted but two additional piles were subsequently added to optimize pile loading and match expected soil conditions. These two piles were added along the longitudinal axis to help carry the deadend loading. For the running angle four potential three-pile layouts were considered. These layouts were developed to take advantage of the structure loading to optimize the foundation. Pile forces based on the layouts were provided to Hubbell/Chance based on the expected maximum forces expected in the field. Figure 1 shows the basic layout specified for the test structures.

Design of Helical-to-Pile Transition

Designs for the transitions were developed which allow for the placement tolerance. Adjustability is provided in all directions. The top of the transition includes a flange plate which will attach the structure to the foundation. This connection allows the foundation and transition to be

assembled and the structures added at a later date. The transition attaches to the helical pile using a pile cap assembly which slides over the pile and is connected by 1 ½” diameter pins. The connection requires field drilling of holes but does not require field welding.

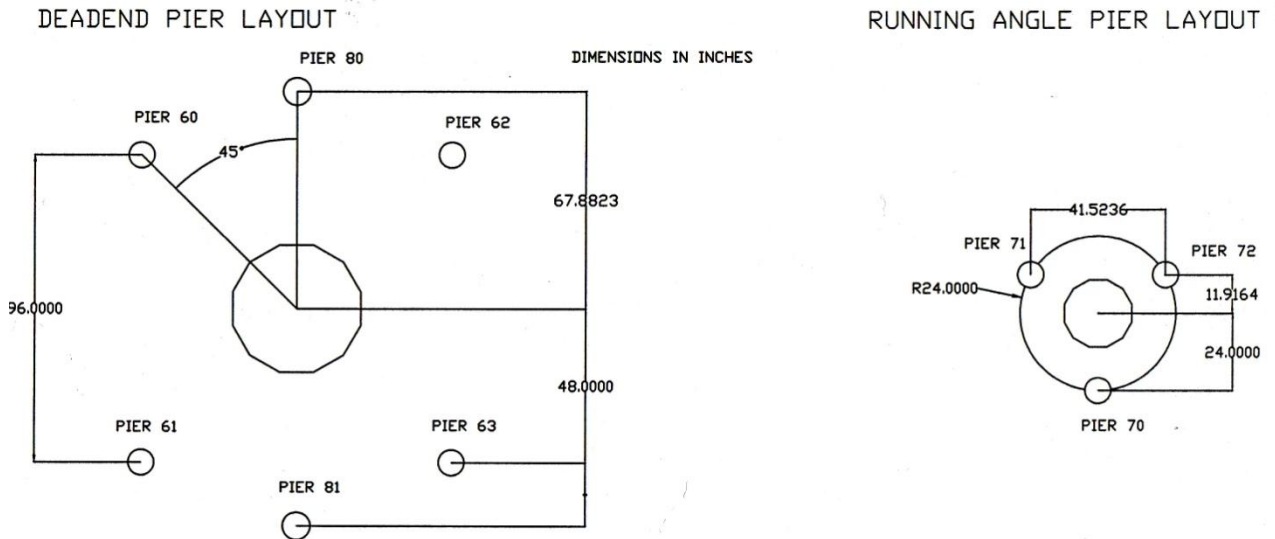


Figure 1. Location of Piles

INSTALLATION AND FULL SCALE TEST OF POLE-TO-HELICAL TRANSITION AND HELICAL PILE FOUNDATION

The Thomas and Betts Hager City, WI facility includes a full scale test stand capable of testing transmission structures. The main test foundation is conventional concrete but a field adjacent was adjacent, available, and utilized for installing and testing the pile/transition systems. A method to test each system was developed using a short pole to apply the proper forces to the foundation system. The testing focused on the transition and helical foundation system and not the entire H-frame structure.

Test loads were developed to match the design forces. Axial loading was created and applied using screw anchors and vectoring. The loads in the piles based on the applied test loading given in Table 1. These forces are given in KIPS. For the axial forces a positive value denotes tension. Shear Y is left to right and shear Z top to bottom.

Deadend	(kips)					
		Case 1			Case 2	
Pier	Vertical	Shear Y	Shear Z	Vertical	Shear Y	Shear Z
60	101.69	-7.97	-8.18	79.22	-7.15	-7.41
61	-47.74	3.54	-3.99	-67.87	4.41	-4.82
62	43.30	3.54	-3.99	41.89	4.41	-4.82
63	-106.12	-7.97	8.18	-105.2	-7.15	-7.41
80	103.34	-0.12	-11.83	90.93	-0.07	-11.89
81	-107.76	-0.12	-11.83	-116.86	-0.07	-11.89

Running Angle						
		Case 3			Case 4	
Pier	Vertical	Shear Y	Shear Z	Vertical	Shear Y	Shear Z
70	-121.67	-11.22	0.0	-90.46	2.96	-4.41
71	60.01	-3.14	-4.67	91.28	10.58	0.0
72	60.01	-3.14	4.67	-90.46	2.96	4.41

Table 1. Forces in Helical Piles

Installation of Piles and Transition System at the Hager City Test Facility

In late July 2012 the locations of the helical piles were established and marked by a surveyor at the test stand. Locations and offsets were noted by markers and flag. Two weeks later on August 14 and 15th the line construction crew and representatives of XCEL Energy, Hubbell Chance and Thomas and Betts began the process of installing the nine helical piles. In addition five guy screw anchors were installed to facilitate vectoring of the test loading.

Using a jig developed by the contractor to aid in locating the piles the helical piles were placed and installed. See figures 6 and 7 for typical installation equipment. The next step was to level and cut off the top to approximately 2 feet above ground. This was accomplished by using a laser to mark each pile and then cutting with a torch. Following leveling a pile cap is placed over the pile. This cap is the bottom of the transition system and will be connected to the pile shaft by pins. Each cap was predrilled and these holes were used to locate and drill the helical piles as shown in Figure 2. Figures 3 and 4 show the completed foundation systems.

Total time to install the piles and transition was 3.25 hours for the running angle and 6.25 hours for the deadend. Improvement of these times is expected with experience. In addition, use of two crews likely is desired, one to install the piles and a second to assemble the transition. Table 2 below shows a breakdown of the installation tasks

Structure Type	Running Angle	DeadEnd
Overturning Moment (ft-kips)	350	2435
Installation of Piles (minutes)	60	105
Level and Cut Piles	45	60
Assemble/Install Transition	45	90
Drill holes in piles, insert pins	45	90
Total Minutes (Hours)	195 (3.25)	375 (6.25)

Table 2. Installation Time

Comparison of Design versus Actual Location of Piles

The setting criteria for the helical piles were established as +/- 3" in any direction. Any offset vertically is handled by leveling and cutting of the pile. The transition handles the horizontal offset. Table 3 compares the design versus actual dimensions. Note the values are within criteria

	Pier	Design T	Design L	Actual T	Actual L	Difference T	Difference L	Resultant.
Deadend	60	-48.0	-48.0	-50.06	-49.69	-2.06	-1.69	2.66
(inches)	61	-48.0	48.0	-47.47	48.28	0.53	0.28	0.6
	62	48.0	-48.00	49.44	49.78	1.44	-1.78	2.29
	63	48.0	48.0	48.56	47.13	0.56	-0.88	1.04
	80	0.0	-67.88	0.13	-67.53	0.13	0.35	0.37
	81	0.0	67.88	1.25	70.25	1.25	2.37	2.68
Running Angle	70	0.0	24.0	0.25	21.81	0.25	-2.19	2.2
(inches)	71	-20.76	-12.0	-21.31	-11.72	-0.55	0.28	0.62
	72	20.76	-12.0	22.19	-13.31	1.43	-1.31	1.94

Table 3. Setting Dimensions.



Figure 2 Drilling Transition.



Figure 3 Running Angle Transition



Figure 4. Deadend Transition

Test of Deadend and Running Angle Structures

On August 22 and 23, 2012 two load conditions were tested for the deadend structure. The first load condition was for a full tangent deadend condition. Tangent deadend would consider wires only on one side of the structure and loading in the longitudinal direction. Figure 5 shows a close-up of the foundation at 100% of the Case 1 loading. The second load condition applied some of the loads at 30 degrees to the longitudinal direction which simulated a structure turning a line angle. For this condition additional dead load was applied utilizing the guy anchors. On August 22nd a problem developed in the guy anchor between 50% and 75% of case 2. The anchor which was used to apply vertical and horizontal loads to the test pole began to fail at well below design capacity. The test was halted and modifications were made to the anchor. The structure deflected 29.5” at the top of the pole and 1.4” at the flange plate at 100% of case 1. The maximum pile movement was 1.08” up, 0.48” down, and 1.6” laterally under full loading.

The running angle was tested on August 22nd and 23rd. The maximum deflections were 14.03” at the pole top, 2.28” at the flange, 0.75” up in the piles, 0.25” down in the piles and 0.96” laterally.



Figure 5. Deadend Load Case 1 100%



Figure 6. Running Angle Case 4 100%

Conclusions: The helical pile and transition systems for both the running angle and deadend structure applications were successfully installed and tested to 100% of the ultimate loading. In addition, the system was capable of adjustment for tolerances.

LINE RIGHT-OF-WAY TESTS

Two tests were conducted at two structure sites on the right-of-way (ROW). The test sites were chosen to represent the hardest conditions found (on the line ROW,) per the geotechnical report and the loosest or poorest soil conditions on the ROW. The hardest conditions were to evaluate the capability of the equipment and the helical foundation to be installed at the site. The poorest site was chosen to determine that the capacity of the helical foundation was adequate to withstand the load in the worst soils on the job.

The load tests conducted were a vertical axial tension test to 120 kips to evaluate the axial capacity of the helical foundation. A lateral test load of 14.4 kips was also applied to evaluate the performance of the helical foundation under lateral load. Structure 189 was selected as the poorest soil condition and Structure 242 as the hardest soil condition. Structure 242 was the first site visited and installation began with the lead section and length that was recommended based on theoretical design methods.

Structure 242: Soils at structure 242 consisted of approximately 7 feet of stiff to hard silty sandy clay that graded to 11 feet of dense silty sand, which in turn transitioned to weathered sandstone. A three-helix lead section made of 2.25 inch round corner solid square bar, (CHANCE® Type SS225), with three helix plates (8", 10", 12"), was installed near the edge of the ROW at Structure 242. Figure 7 shows a three-helix lead section ready for installation at Structure 242. Installation torque was monitored and recorded at 1 foot intervals. Once the square shaft lead section was installed, 8 inch nominal pipe shaft extensions, (CHANCE Type RS8625), were attached to the lead section via a transition coupler. The pipe shafts were used to extend the helix bearing plates down to competent load bearing strata, and transmit the axial load down to the helix plates, which in turn transfer the axial load to the soil. The 8" nominal pipe shafts also resisted the horizontal shear load induced by lateral loads on the structure. The choice to use 8 inch pipe was con



Figure 7. Three-Lead Helix.



Figure 8. Eight Inch Diameter Pipe Extension.

The torque rating (23000 ft-lb) of the Type SS225 - 2.25" square bar lead section, was the controlling factor regarding the amount of torque that could be applied to the helical foundation. It was anticipated that once a few feet of the 8 inch diameter pipe extension had penetrated the soil, that the applied torque could be increased above the rating of the SS225 shaft because of the effort required to displace the sand around the pipe and the friction between the sand and the pipe shaft. Figure 8 below shows the 8 inch diameter pipe extension being connected to the 2.25" square shaft lead section.

The first installation started to encounter rock and cobble after about 9 to 10 feet of penetration. At that point, the installation torque reached 23,000 ft-lb, but there was not adequate pipe length in the soil to resist the lateral loads. It was decided to take the torque beyond 23,000 ft-lb and a target of 30,000 ft lbs was agreed upon. At 11 feet 30,000 ft-lb of torque was recorded and a torsion failure of the SS225 lead section shaft occurred. The extension was removed it was obvious that the SS225 had fractured under excessive torsion load. The pile was abandoned since it was not possible to recover the lead section. A boulder pile was observed on the ROW that was the result of clearing an adjacent field or from the excavation of a pipeline near structure 242. It was assumed boulders were causing the installation problems.

With the failure of the lead section, it was decided to modify the helices on the lead section to aid penetration into the rock laden soil. The installation was attempted again at a location a few feet down the line. The leading edge of the helix plates were modified by cutting back the straight edge to a curved edged using an acetylene torch. See the field modified three-helix lead section in Figure 9 below. This second attempt to install at structure 242 was initially pre-drilled to 10 feet using a continuous flight auger, and then the lead section and extension were installed to a depth of 14 feet when high installation torque was again encountered. This was not deep enough to develop the required lateral capacity, so this second attempt was also abandoned.



Figure 9. Modified Helices.



Figure 10. Pre-Augering.

A third installation was pre-drilled to a depth of 17 feet, the length of the available auger. See Figure 10 for an example of pre-augering. The helical foundation installation was attempted again and after reaching 17 feet with a torque reading of 16,000 ft-lb an obstruction was encountered and the helical foundation would not penetrate further. It was decided to conduct a tension load test on this helical foundation. The pipe shaft extension was cut off to an appropriate length above grade and field modifications were made to the pipe shaft to attach a cap on top of the helical foundation for the

tension test. See Figure 11 for an example of a tension test termination set-up on a pipe shaft helical foundation. A test beam was set on wooden cribbing for support. A hollow ram hydraulic jack was placed on top of the beam and a thread bar was used to transfer load from the jack to the foundation. See Figure 11 below showing the test beam set on the cribbing with the hydraulic jack in place. The test was performed using the general procedures of ASTM D-3689 Standard Test Methods for Deep Foundations Under Static Axial Tension Load. Unfortunately, the resulting load-deflection relationship was found to be unacceptable due to excessive pile movement. This was attributed to the necessity to pre-auger the full length of the helical pile in order to install it. The soil was subsequently disturbed to the point that it would not bear the required tension load. Location 242 proved to be too difficult for the installation of helical piles. The presence of the boulders and cobbles was thought to be the likely reason for the installation related problems.



Figure 11. Termination Set-up.

Because of the difficulty to install the helical foundations and the unsatisfactory load test results, it was decided to abandon this site as a candidate for helical piles and to review the other locations planned to use the helical foundations. After consultation with Xcel project staff that was present on site, it was decided to eliminate sites which exhibited similar soil conditions as structure 242 as reported in the boring logs. As a result, five tower sites were removed from the list where the helical foundations were scheduled to be used. The lesson learned was the sites with dense silty sand and weathered sandstone were not good candidates for helical foundations.

Structure 189: Soils at structure 189 consisted of approximately 14 feet of loose to medium-dense poorly graded sand (glacial outwash) that graded to 30+ feet of medium-dense fine- to medium-grained sand. This site was selected to represent the loosest soil conditions that were on the ROW. Upon

arriving at the structure site, a test location was selected and the recommended lead section with 4-helix plates (8", 10", 12", 14") on Type SS225 lead section was installed followed by an RS8625 10 ft. pipe shaft extension. This foundation was installed without incident to approximately 20 feet with the installation torque reaching approximately 23,000 ft-lb at termination depth. Figure 12 shows the four-helix lead section used at structure location 189. The photo was taken after the installation and tests were completed.



Figure 12. Four-helix Section.

The test at this site was not to determine the installability of the helical foundations, but rather to determine if the required axial tension and lateral capacities could be developed by the helical foundations in the loose sand. It was assumed that the compression capacity of the helical foundations would equal or exceed the tension capacity.

With the foundation installed, the test frame was set up to apply the tension test. The load was applied and deflections read and recorded. The test was again performed using the general procedures of ASTM D-3689 Standard Test Methods for Deep Foundations Under Static Axial Tension Load. The maximum axial tension test load was 120 kip. The data was compiled in the field and the load - deflection readings were considered acceptable. Figure 13 below shows the resulting graph of the load and deflection data.

Upon completion of the tension test, it was agreed that the helical foundation used for the tension test could be used for the lateral load test. Therefore, the test set up was modified to apply a lateral load to the helical foundation. The lateral load was applied incrementally by extending the ram of a hydraulic jack against the side of the helical foundation at a point just above grade. The reaction of the jack was resisted by the track-hoe excavator used for the helical pile installation. Deflection of the pile at or near the ground line was measured at each load increment with a single or multiple dial indicators attached to a simple cross beam arrangement. The maximum lateral test load was 14.4 kip. The data was compiled in the field. The results of the lateral test were considered acceptable. See Figure 14 showing the resulting graph of the load and deflection data for the lateral load test.

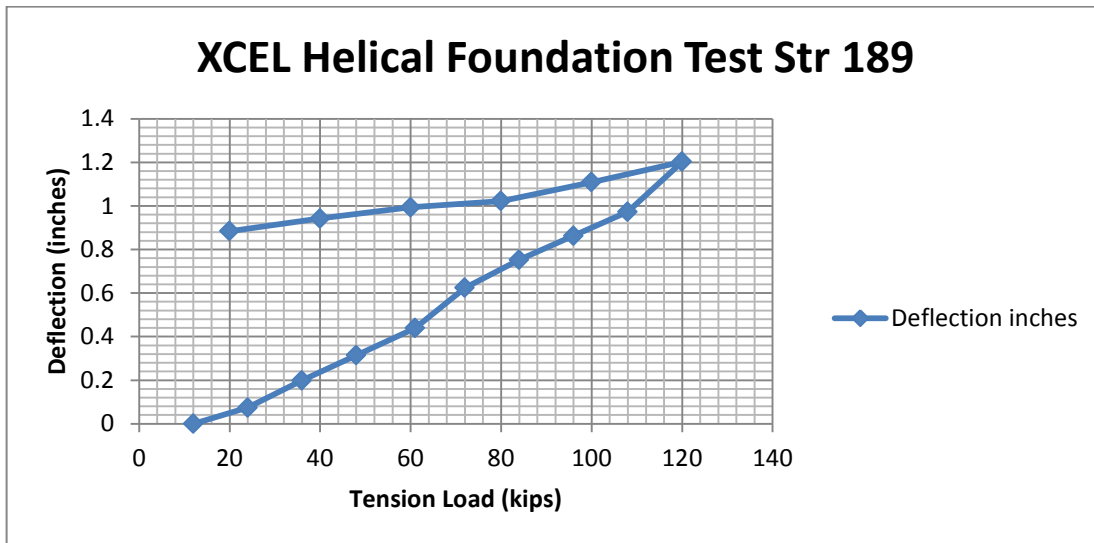


Figure 13. Axial Deflection versus Tension.

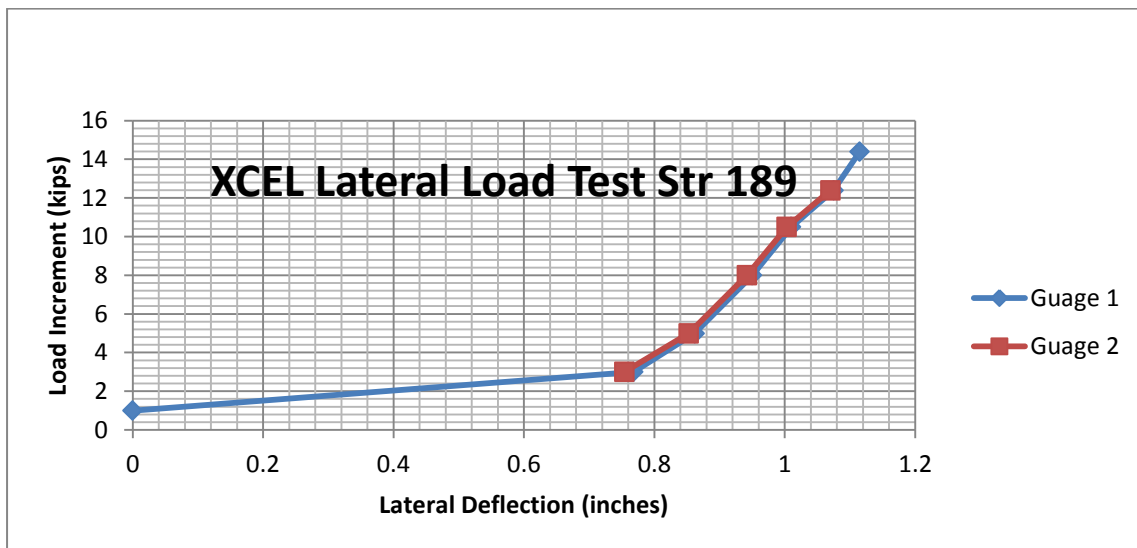


Figure 14. Lateral Deflection versus Lateral Load.

Conclusions: The test efforts at structure 189 were successful and demonstrated that the tapered helical piles selected for this project would provide acceptable results. In addition, the tests at Structure 242 verified the soil conditions that would be difficult for the installation of tapered helical pipe shaft foundations. Experience during the on-site testing aided in identification and elimination of 5 structure sites with similar conditions from the original list of 22 structures where helical foundations were intended for use. The tests conducted at structure 189 confirmed that the helical foundation was adequate to resist the required structure loads even in the poorest soil conditions on the job. Thereby, it was determined that the helical foundations were adequate for use at the other identified structure locations where the installation could be accomplished.

Engineering and Constructing High Quality Drilled Shafts

Calvin Stripling, P.E.

Engineering and Constructing High Quality Drilled Shafts

Calvin Stripling, P.E.

Associate Civil Engineer

Burns & McDonnell

Engineering and Constructing High Quality Drilled Shafts

A high quality drilled shaft has the following properties: Concrete throughout the shaft that meets specified requirements; reinforcing steel in the correct location with correct concrete to steel bond; good load transfer from the shaft concrete to the *in situ* geomaterial [Brown 2004]; and correct concrete cover over the reinforcing steel.

High quality drilled shafts, that is, shafts with the attributes listed above, result when proper attention is given to the following items: Reinforcing steel congestion; hole stability during excavation and concrete placement; fluid properties of the concrete during placement; effect of the drilling fluid on the bond between the concrete and *in situ* geomaterial; amount of suspended sediment in the drilling fluid; plumbness tolerance of the drilled shaft versus the specified concrete cover.

Reinforcing Steel Congestion

Drilled shafts in the electric utility industry are routinely designed for very large moment and shear loads requiring a large amount of reinforcing steel and often resulting in congested reinforcing. Congested reinforcing usually causes fluid concrete in the excavation to trap accumulated sediment and other material between the fluid concrete and the excavation wall or within the fluid concrete itself. Tremie-placed concrete does not, as previously thought, rise uniformly in a drilled shaft scouring the side walls of the shaft as it rises. Instead, it has been observed that there is a differential in the concrete level between the inner and outer portion of the reinforcing cage [Mullins 2005]. The more congested the reinforcing steel is the more the differential in the concrete level inside and outside the cage. When the rising column of concrete is higher inside the cage than outside the cage there is a natural tendency for any accumulated sediment on top of the concrete to slough off toward the side. Even a small accumulation outside the cage can be detrimental to the bond in the bearing formation [Brown 2004]. If the rebar is very congested, the difference in the fluid concrete level inside the cage and outside the cage can be as much as several feet

and it has been observed that the fluid concrete will actually spill over the hoop steel to fill the annular space outside the cage trapping within the concrete in the annulus whatever is on the top of the rising column of concrete.

Although the minimum clear spacing is dependent upon other properties of the fluid concrete mix, the maximum aggregate size is a very important consideration in the clear spacing. The 1999 FHWA Drilled Shaft Manual [O'Neil 1999] recommended a clear space between bars at least 5 times the diameter of the largest aggregate used in the shaft concrete. Research has shown that 5 times the diameter of the largest aggregate is probably not enough clear space and that the clear space between bars should be 8 to 10 times the diameter of the largest aggregate used [Deese 2004]. The 2010 FHWA Drilled Shaft Manual [Brown 2010] recommends a clear distance between reinforcing bars of 8 times the diameter of the largest aggregate used unless concrete placement in a dry shaft can be assured in which case the recommended clear distance is 5 times the diameter of the largest aggregate used.

Hole Stability During Excavation and Concrete Placement

To avoid defects in the shaft, hole stability must be maintained during excavation and concrete placement. For holes drilled with slurry it is absolutely necessary that positive pressure be maintained against the sides of the hole at all times. Groundwater seepage can result in sidewall cave-ins or sloughing. Cave-ins or sloughing during concrete placement will result in defects in the concrete. Even if cave-ins or sloughing do not occur, the geomaterial in the sidewalls of the shaft can soften or loosen altering its properties for the worse. Temporary casing, of course, can be used for excavation stability but casing is not without its problems since what can occur is bottom seepage with bottom softening from the fluid pressures and stress relief from the hole. Even if a temporary casing is sealed into impervious stratum, seepage around the base of the casing can result in a large void outside of the base of the casing with resulting concrete loss when concrete is placed. This, in turn, can result in less concrete head within the

casing than groundwater head outside the casing. When this occurs water can flow into the casing and dilute the concrete.

Fluid Properties of the Concrete During Placement

Concrete used in drilled shaft construction must be able to flow easily wherever it needs to go in the hole without any external help such as vibrating or rodding [Brown 2004]. The ability of concrete to flow where it is required to be, its workability, is generally measured by the slump of the concrete, making slump arguably the most important property of the fluid concrete used in drilled shafts. Although the slump test is not a good measure of the workability of a concrete mix, it is the field test most commonly used to measure workability. The concrete mix should be designed to remain workable from the first concrete placed in the drilled shaft until the last concrete is placed including removal of any temporary casing. The terminology “remain workable” means that the slump loss over the placement time (the time of the first introduction of water to the final concrete placement including removal any temporary casings) should be less than 2 inches. Poor concrete workability can produce several problems in drilled shafts. When concrete is placed by tremie the oldest concrete is at the top of the rising column of concrete and if it becomes stiff from loss of workability (loss of slump) the new concrete under it can break through and trap the trash and contaminated concrete on top of the column. Concrete placement without a tremie also requires concrete with proper workability throughout the time of placement so that the concrete will flow through the reinforcing steel, displace water, and produce the appropriate lateral stress against the *in situ* geomaterial so that a good bond is produced with the geomaterial. When casing is used, if concrete workability is reduced by the time the casing is pulled, not only will it be difficult to pull the casing but the fluid concrete will have a tendency to arch inside the casing and be lifted with it, creating a neck in the drilled shaft. Even if necking is avoided stiff fluid concrete is unlikely to create a good bond with the geomaterial it was intended to bond with.

In order for concrete to create a proper bond with the *in situ* geomaterial in which the shaft is placed the concrete should behave hydrostatically, that is, exert equal pressure in all directions like water does. As determined in research by research [Bernal 1983] concrete with a slump of 4 to 5 inches acts hydrostatically only to depth of about 15 feet. This same research shows that for fluid concrete to behave hydrostatically to a depth of 30 feet or more the fluid concrete must have a slump in the range of 7 to 9 inches. The slump may need to be greater than 7 to 9 inches for shafts larger than 8 feet in diameter [Brown 2007].

Time of placement is the time from the introduction of water into the first batch of concrete to the last concrete placement, including the removal of any temporary casing. Typical drilled shaft specifications, including many state DOT specifications, require that concrete maintain a slump of at least 4 inches over the time of placement. Maintenance of a four-inch slump over the time of placement is probably not adequate for most drilled shafts. When 8-inch slump fluid concrete is placed in an excavation containing 4-inch slump fluid concrete the materials are so different due to the difference in slump that poor results are likely to occur ranging from a lack of homogenous concrete throughout the shaft to the poor workability problem with tremie-placed concrete mentioned previously.

Drilling Slurry and the Properties of the Drilled Shaft

Drilling slurry, if used properly, can be effective in controlling excavation stability. Polymer slurry has been found to allow significantly more side shear to develop than Bentonite slurry. This is true most significantly for granular soils where filter cake develops due to loss of fluid into the granular geomaterial. In cohesive geomaterial the difference in side shear is much less significant. In either case, where Bentonite slurry is used the bond quality is improved by minimizing the exposure time of the geomaterial to the slurry. Currently, polymer slurry is used almost exclusively for electrical utility structure foundation installations. It is well known that polymer slurry does not effectively suspend sand particles and the popular misconception is that allowing the slurry to settle for 30 minutes to 2 hours or

more, depending upon shaft size, solves all sediment problems. While the amount of sand in suspension is a concern, a greater concern is the amount of silt-sized and fine sand particles that can settle out during concrete placement. Although polymer slurries do not effectively suspend sand particles which settle out rapidly, silt-sized particles (finer than a #200 sieve) and fine sand particles can remain in suspension for long periods. The larger diameter and deeper shafts routinely used today require much longer concrete placement times providing the silt and fine sand sediment more time to settle out of suspension. Because of the possible head differential across the top of the rising concrete column as described earlier sediment settling out of suspension may become entrapped and included in the rising concrete at the top of the column. It has been reported that a contractor installing a shaft on the east coast was forced to overpour shafts more than 6 feet to remove the silt-contaminated concrete [Brown 2004]. Experiences with polymer slurry in silty fine sands indicate that engineers and contractors should exercise caution in its use in such situations [Brown 2004].

Plumbness Tolerance and Concrete Cover

Concrete cover over the reinforcing cage is important to prevent corrosion of the reinforcing steel. Plumbness tolerances of drilled shaft excavations and thus the shafts themselves are usually specified as a percentage of shaft embedment length and less often as a percentage of shaft diameter. The relationship of the plumbness tolerance and the specified concrete cover is important to assure there is sufficient concrete covering the rebar cage for the full length of the shaft. An example of the interaction between plumbness tolerance and concrete cover may be seen in a situation where a common tolerance of 1.5% of the shaft length is specified along with the commonly specified 3 inches of concrete cover. Assuming the shaft is at the maximum allowable out-of-plumbness, the specified 3 inches of cover will be reduced to 0 inches of cover before the excavation has reached a depth of 17 feet.

Some allowable tolerances for shaft vertical plumbness are:

1. ACI 336.1: 1.5% of length (Section 3.1.3).

2. ACI 117: 2% of length (Section 3.1.3).
3. TxDOT: 0.83% of length (Item 413.3).
4. OkDOT: 1% of length (Item 516.04).
5. LaDOT: 1.5% of length (LaDOT Drilled Shaft Inspection Manual).
6. FHWA: 1.5% of length for soil, 2.0% of length for rock.

As for the other side of the issue, specifying concrete cover, the 2010 FHWA Drilled Shaft Manual [Brown 2010] recommends the following:

1. Shaft diameter less than or equal to 3 feet – 3 inches of concrete cover.
2. Shaft diameter greater than 3 feet and less than 5 feet – 4 inches of concrete cover.
3. Shaft diameter 5 feet and greater – 6 inches of concrete cover.

The writer has seen this recommendation routinely violated with shafts of 6 feet and larger specified with only 3 inches of concrete cover.

Conclusion

The construction of high quality drilled shafts requires that everyone involved have an incentive to produce a quality product. The contractor cannot be concerned only with completing the shaft and the engineer can't get so caught up in the arrangement of the rebar for the load to be carried that the constructability aspects are overlooked.

- The designing engineer must be knowledgeable about drilled shaft constructability issues and should produce a design that is easily constructed.
- The contractor should be conscientious with a genuine desire to produce a quality product and should have well-trained workers who have the proper equipment to do the job.
- Inspectors should be well-trained and knowledgeable about drilled shaft construction, which aspects of the shaft design that are critical, and the geological conditions at the construction site.

- The project should include provisions for measuring quality inspection techniques such as non-destructive testing, load testing, and test installations.

END NOTES

Bernal 1983

U.S. Department of Transportation. Federal Highway Administration. Study of the Lateral Pressure of Concrete as Related to the Design of Drilled Shafts. FHWA/TX-84/45+308 – 1F. Juan B. Bernal and Lyman C. Reese. Austin, Texas: Center for Transportation Research, University of Texas at Austin, 1983.

Brown 2004

Brown, Dan A. "Recipe for Success with Drilled Shaft Concrete." *Foundation Drilling*, Nov. 2004: 16-24.

Brown 2007

Brown, Dan A., and Anton Schindler. "High Performance Concrete and Drilled Shaft Construction." *Geotechnical Special Publication No. 158. Contemporary Issues in Deep Foundations*, 2007.

Brown 2010

U.S. Department of Transportation. Federal Highway Administration. *Drilled Shafts: Construction Procedures and LRFD Design Methods*. FHWA-NHI-10-016. Dan A. Brown Ph.D., P.E., John P. Turner Ph.D., P.E., and Raymond J. Castelli P.E., May 2010.

Deese 2004

Deese, Gregory G. "Slurry Sand Content and Concrete Interaction in Drilled Shaft Construction." Thesis. University of South Florida, 2004.

Mullins 2005

Mullins, Gray Ph. D., P.E. and Alaa K. Ashmawy Ph.D., P.E. Factors Affecting Anomaly Formation In Drilled Shafts - Final Report. Report to Florida Department of Transportation. University of South Florida, 2005.

O'Neill 1999

U.S. Department of Transportation. Federal Highway Administration. *Drilled Shafts: Construction Procedures and Design Methods*. FHWA-IF-99-025. Michael W. O'Neill Ph.D., P.E. and Lyman C. Reese Ph.D., P.E., August 1999.

The 46th ANNUAL TSDOS



TRANSMISSION AND SUBSTATION DESIGN AND OPERATION SYMPOSIUM

Thank you to our 2013 sponsors!

TITLE SPONSORS

